MODELLING AND ON-LINE IMPLEMENTATION OF ADVANCED CONTROL STRATEGIES FOR BIOHYDROGEN PRODUCTION IN MICROBIAL ELECTROLYSIS CELL REACTOR SYSTEM

AZWAR BIN MUHAMMAD YAHYA

FACULTY OF ENGINEERING
UNIVERSITY OF MALAYA
KUALA LUMPUR

2017

MODELLING AND ON-LINE IMPLEMENTATION OF ADVANCED CONTROL STRATEGIES FOR BIOHYDROGEN PRODUCTION IN MICROBIAL ELECTROLYSIS CELL REACTOR SYSTEM

AZWAR BIN MUHAMMAD YAHYA

THESIS SUBMITTED IN FULFILMENT OF THE REQUIREMENTS FOR THE DEGREE OF DOCTOR OF PHILOSOPHY

FACULTY OF ENGINEERING
UNIVERSITY OF MALAYA
KUALA LUMPUR

2017

UNIVERSITY OF MALAYA

ORIGINAL LITERARY WORK DECLARATION

Name of Candidate: AZWAR BIN MUHAMMAD YAHYA

Matric No: KHA090060

Name of Degree: Doctor of Philosophy (PhD)

Title of Thesis:

Modelling and on-line implementation of advanced controlstrategies for biohydrogen production in microbial electrolysis cell reactor system

Field of Study: Process System Engineering and Control

I do solemnly and sincerely declare that:

(1) I am the sole author/writer of this Work;
(2) This Work is original;
(3) Any use of any work in which copyright exists was done by way of fair dealing and for permitted purposes and any excerpt or extract from, or reference to or reproduction of any copyright work has been disclosed expressly and sufficiently and the title of the Work and its authorship have been acknowledged in this Work;
(4) I do not have any actual knowledge nor do I ought reasonably to know that the making of this work constitutes an infringement of any copyright work;
(5) I hereby assign all and every rights in the copyright to this Work to the University ofMalaya ("UM"), who henceforth shall be owner of the copyright in this Work and that any reproduction or use in any form or by any means whatsoever is prohibited without the written consent of UM having been first had and obtained;
(6) I am fully aware that if in the course of making this Work I have infringed any copyright whether intentionally or otherwise, I may be subject to legal action or any other action as may be determined by UM.

Candidate's Signature Date:

Subscribed and solemnly declared before,

Witness's Signature Date:

Name:

Designation:

ABSTRACT

One free energy source that is sustainable and renewable is the hydrogen gas. The most interesting fact about this gas is when used on vehicles or fuel cells, it is more efficient than the conventional internal combustion engines. When these compounds react with air, the by-product is just water. Because of these advantages, the hydrogen gas is known as a low-carbon energy source. This is one solution for modern society, so that the dependence on fossil fuels can be minimized. Other advantage of the hydrogen gas is that it can be produced from various surrounding sources such as water, natural gas, biomass and organic waste. When viewed in terms of the economy, the selection of hydrogen fuel as a source of alternative energy is very appropriate.

There are several alternative technologies for the production of biohydrogen process namely biophotolysis, photofermentation, dark fermentation and microbial electrolysis cells (MEC). However, MEC is known to be an attractive alternative technology that is environmentally friendly and can be used for hydrogen production. It involves a bio-electrochemical process using microorganisms as catalysts. MEC process has advantages compared with other processes because the microorganisms are capable of oxidizing all organic substrates to produce hydrogen gas which cannot be extracted by microorganisms through the photo or dark fermentation process. Microorganisms in the reactor are able to catalyze the oxidation or reduction reaction at the anode and cathode electrodes, respectively. By increasing the cathode potential in the MEC reactor, it is possible to continuously produce hydrogen electron exchange assisted by the bacteria. This method greatly decreases the amount of energy needed to produce hydrogen from organic matter compared to hydrogen production from water via electrolysis.

Hydrogen production process in the MEC is a highly nonlinear and complex due to the microbial interactions. Its complexity makes MEC system difficult to operate and control under optimal conditions. However, these problems can be alleviated using an

integrated process system engineering approach, which involves process modeling, optimization and control complementing each other. Artificial Neural Networks (ANN) is one of the most effective and powerful technique to be used to model such complex processes and unknown systems. ANN is able to cope with non-linear process between input and output variables without the requirement of explicit mathematical representation. In the process control system, ANN has been widely used when conventional control techniques failed to give good performance.

In this work, various schemes including ANN for controlling the current and voltage of MEC were studied i.e. Direct Inverse Neural Network, Hybrid PID-Neural Network and Internal Model-based Control schemes. A comparative study has been carried out under optimal condition for the production of hydrogen gas where the controller output are based on the correlation of optimal current and voltage to the MEC system. Various simulation studies involving multiple set-point changes and disturbances rejection have been evaluated and the performances of both controllers are discussed. On-line model validation of MEC system and closed loop control for online system are also presented in this work.

ABSTRAK

Satu sumber tenaga bebas yang berkekalan dan boleh diperbaharui adalah gas hidrogen. Fakta yang paling menarik tentang gas ini adalah apabila digunakan pada kenderaan atau sel-sel bahan api, ia adalah lebih cekap dari pembakaran dalaman enjin konvensional. Apabila bahan inibertindak balas dengan udara, produk sampingan hanyalah air. Oleh kerana kelebihan ini, gas hidrogen dikenali sebagai sumber tenaga yang mengandungi karbon yang rendah. Ini adalah salah satu penyelesaian bagi masyarakat moden, supaya pergantungan kepada bahan api fosildapat dikurangkan. Kelebihan laingas hidrogen adalah dapat dihasilkan daripada pelbagai sumberalam lainseperti air,gas asli, biomas dan sisa organik. Dari perspektif ekonomi, pemilihan bahan api hidrogen sebagai sumber tenaga alternatif adalah sangat bersesuaian.

Terdapat beberapa teknologi alternatif bagi pengeluaran proses hidrogen iaitu biophotolysis, foto fermentasi, fermentasi gelap dan sel mikrob elektrolisis (MEC). Walau bagaimanapun, MEC dikenali sebagai teknologi alternatif yang sangat menarik dan mesra alam serta boleh digunakan untuk pengeluaran bio-hidrogen. Ia melibatkan proses bio-elektrokimia menggunakan mikroorganisma sebagai pemangkin. Proses MEC mempunyai kelebihan berbanding dengan proses lain kerana mikroorganisma mampu mengoksidakan semua substrat organik untuk menghasilkan gas hidrogen yang tidak boleh diekstrak oleh mikroorganisma melalui foto atau proses fermentasi gelap. Mikroorganisma dalam reaktor dapat menjadi pemangkin kepada pengoksidaan atau tindak balas penurunan pada anod dan katod elektrod. Dengan meningkatkan potensi katod secara elektrokimia dalam MEC, penukaran hidrogen elektron dengan bantuan bakteria dapat dihasilkan secara berterusan. Kaedah ini dapat mengurangkan jumlah tenaga yang diperlukan bagi penghasilan hidrogen daripada bahan organik berbanding penghasilan hidrogen melalui elektrolisis daripada air.

Proses pengeluaran hidrogen dalam MEC adalah sangat tidak linear dan sangat kompleks disebabkan interaksi mikrob. Kerumitan ini membuatkan sistem MEC sukar untuk dikendalikan dan dikawal di bawah keadaan yang optimum. Walau bagaimanapun, masalah-masalah ini boleh diatasi dengan menggunakan pendekatan kejuruteraan sistem proses yang bersepadu, iaitu melibatkan pemodelan proses, pengoptimuman dan kawalan yang melengkapi satu sama lain. Rangkaian Neural Buatan (ANN) adalah salah satu teknik yang paling berkesan dan berkuasa yang akan digunakan untuk pemodelan proses kompleks dan sistem yang tidak diketahui tersebut. ANN mampu untuk mengendalikan proses bukan linear di antara pembolehubah masukan dan keluaran tanpa memerlukan perwakilan matematik yang jelas. Dalam sistem kawalan proses, ANN telah digunakan secara meluas kerana kegagalan teknik kawalan konvensional memberikan prestasi yang baik.

Dalam penyelidikan ini, pelbagai skim termasuk ANN untuk mengawal voltan semasa dan MEC telah dikaji iaitu songsangan neural network langsung, rangkaian hibrid PID-neural dan skim berasaskan model kawalan dalaman. Satu kajian perbandingan telah dijalankan di bawah keadaan optimum untuk pengeluaran gas bio-hidrogen di mana keluaran pengawal adalah berdasarkan korelasise masa arus dan voltan optimum untuk sistem MEC. Kajian simulasi melibatkan pelbagai perubahan set-titik dan penolakan gangguan telah dinilai dan prestasi kedua-dua kawalan dibincangkan. Pengesahan model secara atas talian sistem MEC, dan kawalan gelung tertutup bagi sistem atas talian turut dipersembahkan dalam kajian ini.

ACKNOWLEDGEMENTS

In the Name of Allah, the Beneficial and the Merciful.

All praises belong to Allah SWT the Rabb of the universe, the owner of guidance, instructions and light of science. May the special mercies of Allah and peace be on our master Muhammad SAW who is the seal of all Ambiyaa. May Allah mercy and peace be on his family, all his companions and all those coming until the Day of Qiyaamah who follows him dutifully.

I would like to express my special appreciation and thanks to my adviser and supervisor Professor Ir. Dr. Mohamed Azlan Hussain for his support and guidance in carrying out of my PhD research work. I wish to express great respect and sincere thanks to Ir. Dr. Ahmad Khairi Abdul Wahab, my co-supervisor, who has been a tremendous mentor to me, support, guidance, constructive comment and encouragement. Indeed, I sure will not ever have finished my research work without their inspiration.

I also wish to sincerely thank to all lectures and lab staff at Depatment of Chemical Engineering. I am indebted to postgraduate classmates especially Mohd Fauzi bin Zanil, M.Eng.Sc., Faisal Abnisa and Jakir Khan, M.Eng.Sc. of Department of Chemical Engineering. I would like to thank and apologies to all my friends that I could not mention personally one by one. I am grateful to "University Malaya Research Grant (UMRGRP006H-13ICT)" Program for the financial support provided during my postgraduate study.

Finally, words of love and my deepest appreciation, affection to my wife, Rahmah Kurniasih and my beloved children, M. Fathurrahman Al-Munzir, Saidati Nur Fathiah, M. Ammar Nur Syafiq, Annisa Naila Nur Lathifah, M. Alby Luthfy Dhiaurrahman, for their endless love and understanding, through the duration of my studies. Last but definitely not the least, I would like to thank my great family, and my parents, brothers Safzani and young sister Zahara for their blessing and support.

TABLE OF CONTENTS

LIST OF FIGURES

LIST OF TABLES

LIST OF SYMBOLS AND ABBREVIATIONS

Abbreviations and Acronyms

VFAs	Volatile fatty acids
ATP	Adenosine triphosphate
GTP	Guanosine triphosphate
PNS	Purple Non-Sulfur
PSB	Purple Sulfur Bacteria
SRT	solidsretentiontime
AnSBR	Anaerobic sequencing batch reactor
FBR	Fluidized bed bioreactor
CSTR	Continuously stirred reactor
BESs	Bio-electrochemical systems
MFC	Microbial Fuel Cells
MEC	Microbial Electrolysis Cells
CEM	Cation exchange membrane
NHE	Normalhydrogenelectrode
HER	Evaluationhydrogenreaction
ARB	Respiration anode bacteria
VSS	Volatile suspended solids
POME	Palm oil mill effluent
RSM	Response surface method
PID	Proportional integral derivative
ANN	Artificial neural networks
DINN	Direct inverse neural network
IMC	Internal model control
HNN	Hybrid neural network

PID-ZN	PID Ziegler-Nichols tuning method
RMSE	Root-mean-squared-error
ISE	Integral Square Error
IAE	Integral Absolute Error
ITAE	Integral Time Absolute Error
GRNN	General Regression neural network
NTU	Nephelometric Turbidity Units
AC	Voltage alternating current
DC	Direct current
DAQ	Data Acquisition
P&ID	Process and Instrumentation Diagram

Nomenclature

S	Substrate concentration (mg-SL^{-1})
x_a	Concentration of anodophilic microorganisms
x_m	Concentration of acetoclastic microorganism
x_h	Concentration of hydrogenotrophic microorganisms
Q_{H_2}	Hydrogen production rate (mLd^{-1})
$q_{m,a}$	Maximum reaction rate of the anodophilic microorganism [mg-Amg-x^{-1}d^{-1}]
$q_{m,m}$	Maximum reaction rate of the acetoclastic methanogenic microorganism [mg-Amg-x^{-1}d^{-1}]
$K_{S,a}$	Half-rate (Monod) constant of the anodophilic microorganism [mg-AL^{-1}]
$K_{S,m}$	Half-rate (Monod) constant of the acetoclastic methanogenic microorganism [mg-AL^{-1}]
K_M	Mediator half-rate constant [mg-ML^{-1}]

$K_{d,a}$	Microbial decay rates of the anodophilic microorganism [d^{-1}]
$K_{d,m}$	Microbial decay rates of the acetoclastic methanogenic microorganism [d^{-1}]
$K_{d,h}$	Microbial decay rates of the hydrogenotrophic microorganism [d^{-1}]
K_h	Half-rate constant [mgL^{-1}]
Y_M	Oxidized mediator yield [mg-Mmg-A^{-1}]
Y_{H_2}	Dimensionless cathode efficiency [dimensionless]
Y_h	Half-rate constant [mgL^{-1}]
V_r	Anodic compartment volume [L]
m	Number of electrons transferred per mol of H_2 [mol-e^- mol-H_2^{-1}]
F	Faraday constant [Ad mol-e^{-1}]
R	Ideal gas constant [ml-H_2 atm K^{-1}mol-H_2^{-1}]
T	MEC temperature [K]
P	Anode compartment pressure [atm]
E_a	Electrode potentials [V]
R_e	External resistance [Ω]
R_{in}	Internal resistance [Ω]
I_M	MEC current [A]
E_C	Counter-electromotive force for the MEC [V]
M_T	Total mediator weight percentage [mg-Mmg-x^{-1}]
M_r	Reduced mediator fraction for each electricigenic microorganism (mg-Mmg-x^{-1})
M_o	Oxidized mediator fraction for each electricigenic microorganism (mg-Mmg-x^{-1})
A_s ,A	Anode surface area [m^2]

Greek letters

$\mu_{m,a}$	Maximum growth rate of the anodophilic microorganism [d^{-1}]
$\mu_{m,h}$	Maximum growth rate of the hydrogenotrophic microorganism [d^{-1}]
$\mu_{m,m}$	Maximum growth rate of the acetoclastic methanogenic microorganism [d^{-1}]
β	Reduction or oxidation transfer coefficient [dimensionless]
i_0	Exchange current density in reference conditions [A m^{2-1}]
γ	Mediator molar mass [mg-M mol_{med}^{-1}]
α_1	Dimensionless biofilm retention constant for layers 1
α_2	Dimensionless biofilm retention constant for layers 2
μ_h	Hydrogen growth rate [d^{-1}]
η_{ol}	Ohmic losses due to resistance to the flow of ion in the electrolyte & electrode [V]
η_c	Concentration loss due to mass transfer limitation [V]
η_a	Activation loss due to activation energies and electrochemical reactions [V]

CHAPTER 1: INTRODUCTION

1.1 Background

One of the great challenges in the coming decade is how to get new renewable energy sources that are environmentally friendly and to replace high dependency on fossil fuels. Until recently, almost all of the energy needed is derived from the conversion of fossil energy sources, such as for power generation, industrial and transportation equipment that uses fossil fuels as a source of energy. Fossil fuels are source of non-renewable energy and also have seriously negative impacts on the environment, e.g. soil, water, air, and climate. The use of fossil fuels cause excessive global climate change because of the emissions of greenhouse pollutants and the formation of compounds *COx* , *NOx*, *SOx*, *CxHy*, ash, and other organic compounds that are released into the atmosphere as a result of combustion (Argun et al., 2008; Kotay & Das, 2008).

Based on the above considerations, in recent years various studies have been conducted to obtain a sustainable source of energy that can replace fossil fuels and which do not have a negative impact on the environment. Hydrogen is one alternative fuel substitute for fossil fuels and is considered as an "energy carrier" with a promising future. It has a high energy content of 122 kJ/g, that is 2.75 times greater than those of hydrocarbon fuels (Mohan, Babu, et al., 2007).

Hydrogen plays a very important role and contribution in the global era that is based on clean renewable energy supplies and sustainably which will provide major contributions to the world economic growth. Hydrogen fuel is environmentally friendly, clean and is the most abundant element in the universe in its ionic form. Hydrogen gas is also colorless, tasteless, odorless, light and non-toxic. When it is used as fuel, it will not produce pollution to the air but it produces only water as its end-product when it burns

(Hallenbeck & Benemann, 2002). Hydrogen gas which is produced by biological processes becomes very interesting and promising because they can be operated at ambient temperature and pressure with minimal energy consumption, and become more environmentally friendly (Hallenbeck et al., 1978).

Electrochemical systems represent a novel alternative for energy recovery from organic waste and biomass residue, where microorganisms can be employed to catalyze electrochemical oxidation-reduction reactions. Microbial Electrolysis Cell (*MEC*) is among such bioelectrochemical systems. Performance of *MEC* largely depends on anaerobic biofilm occupied by anodophilic (electrogenic) microorganisms, which transfer electrons to the anode during their metabolism activities (Bond et al., 2002). Though anodic compartments in all electrochemical systems are similar, the cathode reactions differ. MEC require a small additional input of electrical energy provided by an external power supply to facilitate the reaction of hydrogen formation on the cathode (René A Rozendal et al., 2006).

In the MEC, a small amount of electricity is applied to the anode chamber to suppress the production of methane and furthermore oxygen is kept out of the cathode chamber to assist bacterial oxidation of organic matter present in wastewater to produce hydrogen gas. MEC has tremendous potential in the future and the development of this technique is still in its infancy. Information about the anode materials and microorganisms, efficient and scalable designs are required for the successful applications of the microbial electrolysis process (Hu et al., 2008).

This thesis describes the mathematical model and development of advanced control of MEC for hydrogen production from wastewater in fed-batch reactor. The model is based on material balances with the integration of bio-electrochemical reactions describing the steady-state behaviour of biomass growth, consumption of substrates, hydrogen production and power current characteristics. The model predicts the concentration of

anodophilic, acetoclastic methanogenic and hydrogenotrophic methanogenic microorganisms. Cathodic reactions in MEC are represented by two distinctive electrochemical balances, while the same set of equations are used to describe anodic compartment balances. This study can also be used to improve the basic and current knowledge about the performance of the microbial electrolysis cells and electrochemical fed-batch reactor process in producing hydrogen gas as an alternate fuel.

1.2 Problem statement

MEC is a novel and promising renewable energy technology that can produce H_2 and can also serve for wastewater treatment. At the moment, there are many studies of MEC involving simulation reported in the literature. The MECs present many technological challenges that need to be overcome before commercial application. For instance, the nonlinear and highly complex process in hydrogen production is due to the microbial interaction. Furthermore, the process also depends on the microbial activity which shows irregular correlation between current and voltage.

Another important and interesting phenomenon of the MEC system is the competition between anodophilic and methanogenic microorganisms to consume the substrate in the anode compartment. Competition among these microbial populations has profound effects on the performance of the MEC bioreactor. An initial study of this system used a model involving competition among anodophilic, methanogenic acetoclastic and hydrogenotrophic methanogenic microorganisms in the biofilm as reported by (Pinto et al., 2010).

Process control is required in the MEC plant so that the process can continue to operate consistently and hence allowing the production rate of hydrogen gas to be continuously produced optimally. *MEC* current and voltage are two important variables that need to be controlled and observed at all times because it is directly related to the production rate of

hydrogen gas. The main difficulty encountered in controlling MEC system is how to determine the amount of applied voltage and *MEC* current accurately because the condition of the process is very highly uncertain and nonlinear. Another problem encountered in the control of the MEC system is the unknown composition of microbes in the reactor. The effect of internal and external disturbances, time delay and noise effects are other problem that cannot be ignored, making it difficult to control the system using conventional control approaches. Therefore, these technical problems can be solved using a process system engineering approaches; process modelling, optimization, and control.

There are some advanced solutions that can be applied to enhance the control performance of *MEC* reactor and eliminate the nonlinear barrier in the optimal control. Neural network (*NN*) is an effective technique and a powerful tool to be used in modelling and control of complex processes and unknown systems. *NNs* are able to cope with non-linear process between input and output variables without the requirement of explicit mathematical correlation. In the literature, several studies and investigations on the modeling of biohydrogen production using ANN approach is reported. For example, El-Shafie (2014), use *ANNs* to successfully predict hydrogen yield with the following input: initial medium *pH*, initial glucose concentration and reaction temperature. A model was trained, tested and validated to predict the hydrogen production profile. However, none of these studies in the literature involve neural network based controller for bio-hydrogen gas production in the *MEC*.

In this thesis, *MEC* mathematical model will be developed and improved, it will also be validated by experimental studies, and to design an advanced controller for its control system. A comparative study between inverse neural network, hybrid *PID*-neural network and Internal Model-based Control (*IMC*) system and control *PID* will also be discussed. The performance and assessment of these *PID* and neural network controller for tuning

and rejection of the load disturbances and noise will be studied. The requirements for a good controller for optimal H_2 gas production are also highlighted in this work, where better control system for optimum bio-hydrogen gas production can be achieved.

1.3 Objectives of research

The overall goal of this thesis is to focus mainly on developing a microbial electrolysis cell (*MEC*) mathematical model and the implementation of the controller for the advanced control system.

The main objectives of this study are outlined as follows:

(1) To study the effect and optimize of the operating and kinetics parameters on the performance hydrogen production process in *MEC* fed-batch reactor.

(2) To design of *PID* controller algorithm, adaptive-PID controller and advanced control strategy to optimize the hydrogen production rate in fed-batch MEC reactor.

(3) To design the *MEC* experimental system and validate the *MEC* mathematical model with on-line data and test its performance of *MEC* system.

(4) To design of *PI; PID* and neural network closed loop control for online system for biohydrogen production in fed-batch MEC reactor.

1.4 Scope of work

Literature review concentrates of the hydrogen gas as a renewable energy source and microbial electrolysis cells (*MEC*) process for producing hydrogen from organic waste. Mathematical model previously developed by (Pinto et al., 2010) will be modified to be appropriate with the suggested process design parameters in order to construct the experimental *MEC* fed-batch reactor setup for validation and control purposes. Statistical analysis was used to identify some important parameters that have significant effects on the hydrogen production rate using this reactor. Therefore, current is used to manipulate

the rate of hydrogen production. In order to determine the optimal production of hydrogen, several control strategies consist of conventional and advanced control are implemented. Their performance are tested and simulated to analyze their respective performance.

1.5 Structure of Thesis

This thesis is divided into six chapters. In overall outline, the thesis is organized as follows;

Chapter 1 describes an introduction to the study background, problem statement, and objectives of the research, scope and structure of research.

Chapter 2 studies the literature on the fundamental concepts and basic mechanism of biological hydrogen production processes, microbial electrolysis cell, irreversible energy losses in *MEC* and overview of current research on *MEC* systems. It starts with reviewing about biophotolysis processes, fermentation processes and electrochemical processes.

Chapter 3 discusses the detailed work about microbial electrolysis cell modelling & computer simulation. This is followed by the fundamental standards of microbial electrolysis cell consist of extracellular electron transfer, thermodynamic and kinetics. This chapter ends with overview of activation energy loss, concentration energy losses, electrode energy loss, ohmic energy losses and overview of current research on *MEC* systems. The dynamics simulation, system identification and open loop test to investigate the dynamics of the process are presented in this chapter. It consists of the *MEC* model development, behavior of microbial electrolysis cells, effect of varying changes of initial concentration on the *MEC*, influent of applied voltage on *MEC* current and hydrogen production rate and Analysis of the effect of internal and external parameter on *MEC* current and hydrogen production rate.

Chapter 4 highlights the *PID*, neural network model and controller design performance in the *MEC* reactor. *PID* and neural networks controller for process control design is

described in detail. This chapter starts with dynamic open loop behavior of *MEC* reactor, design of a conventional *PID* (Proportional-Integral-Derivative) controller of simulated *MEC* system and direct inverse neural network controller concepts. The results and discussion of conventional *PID* controller and neural network controller in *MEC* reactor is presented in this chapter for various set point and disturbance rejection studies. The neural network controller schemes i.e. internal model control (*IMC*) and hybrid control scheme are also designed and their performances investigated.

Chapter 5 presents the experimental reactor design and operation that are required for on-line measurement and computer studies on *MEC* reactor system. Description of palm oil mill effluent (*POME*) substrate, inoculum preparation and cultivation medium and pretreatment experiments and analytical method are discussed. In this chapter, the on-line implementation of advanced control strategies, start-up process value and noise filtering, open-loop validation models, Process and Instrumentation Diagram (*P&ID*), online signal flow diagram, closed-loop control for the online system, *PI* Closed loop control for online system and implementation of neural network control strategy will be discussed in detail.

Chapter 6 highlights the conclusions and summary of the thesis, importance of the proposed research and contributions to knowledge and some perspective and recommendations for future work are suggested.

CHAPTER 2: LITERATURE REVIEW

2.1 Introduction

This chapter discusses the detailed studies and literature reviews on mechanisms of possible biological hydrogen production processes. There are a variety of technologies for biological hydrogen production mechanisms including biophotolysis, photo fermentation, dark fermentation and hybrid biohydrogen production by electrochemical processes. In these studies, a review on the recent developments of biohydrogen production is presented. First, the theoretical principles of biophotolysis by cyanobacteria and green micro algae, as well as direct and indirect of biophotolysis process on hydrogen production are described. Secondly, practical aspects and fundamental of biological hydrogen production processes by photo and dark fermentation are reviewed. A new hybrid biological hydrogen production processes by using the electrochemical process is then proposed. Thirdly, the studies of microbial electrolysis cell (MEC), reactor design, electrode materials of MEC, substrates used in MEC and the unique and advantages of biohydrogen production processes will be discussed in the next chapter.

2.2 Fundamentals of biological hydrogen production processes

Increasing energy demands from a growing world population, and the depleting reserves of fossil fuels and their environmental impacts, are leading to a search for novel energy technologies. Most likely, a diverse portfolio of energy producing technologies will be needed to replace fossil fuels. These technologies may rely on renewable or non-renewable resources, the former being much more interesting because they do not depend on limited reserves. A portfolio of renewable energy technologies may include a variety of systems based on sunlight, wind, rain, tides, geothermal heat, and biomass. Hydrogen

gas is one element of an efficient energy source because it has 2.8 times the energy content when compared to the energy in gasoline. Besides being environmentally friendly, hydrogen gas can also be produced from organic industries wastewater and agriculture source so that production costs become cheaper (B. E. Logan et al., 2008).

The global interest in hydrogen based economy has been stimulated by possible harvest for cleaner energy production using hydrogen in fuel cells. A global reduction in CO_2 emissions will require sustainable hydrogen production based on renewable energy sources such as solar, wind, and biomasses. Hydrogen can be produced from certain forms of biomass by biological fermentation, but still the yields are significantly low. This bio-electrochemically assisted microbial system, when combined with the hydrogen fermentation process has the potential to produce as much as 8 to 9 mole H_2/ mol of glucose at energy cost equivalent of 1.2 mol H_2/mole of glucose. Production of hydrogen by electrochemical process is not limited only to carbohydrates, as in the fermentation process. Other biodegradable dissolved organic matter can theoretically be used to generate hydrogen from the complete oxidation of organic matter (Azwar et al., 2014).

According to (Hallenbeck & Benemann, 2002), hydrogen can be produced from different types of raw materials, including fossil fuels, water, and biomass. Hydrogen production from renewable sources can be obtained in different ways. There are several major renewable energy sources to produce from the water that flows, the heat from the earth, wind, solar, biomass and biological hydrogen production from microorganisms. Many microorganisms are known to produce hydrogen under certain conditions, including microalgae such as blue-green algae that use light energy to split water for hydrogen formation and cyanobacteria that usually use carbohydrates to store energy from photosynthesis to produce hydrogen from water (Hallenbeck and Benemann, 2002).

Production of biohydrogen has the potential to be a renewable alternative to current technologies. There are varieties of technologies for biological hydrogen production mechanisms including biophotolysis, photo fermentation, dark fermentation and hybrid biohydrogen production by electrochemical processes. Photo-fermentation produces hydrogen via algae and photosynthetic bacteria under the role of solar energy, so that the reaction is limited to light condition and intensity makes it slowly progress in application (Argun et al., 2008). Dark-fermentation produces hydrogen by microbial degradation of organic materials in an anaerobic environment with the maximum hydrogen yield of 12 mol/mol.glucose theoretically, but the "fermentation barrier" makes it only 2–3 mol in practice (Kotay & Das, 2008). The problems mainly reflect on: (1) low rate of carbon source utilization and incomplete substrate conversion which means the intermediate products cannot be spontaneously converted to H_2; and (2) accumulation of volatile fatty acids (*VFAs*) such as acetic acid, propionic acid, and butyric acid make the system instable.

2.2.1 Biophotolysis processes

Biophotolysis is associated with plant-type photosynthesis process, formerly known as blue-green algae that uses light to split water for hydrogen formation, and takes place under anaerobic conditions. Biophotolysis indirectly involve cyanobacteria usually use carbohydrates to store energy from photosynthesis to produce hydrogen from water.

2.2.1.1 Biophotolysis of water by Cyanobacteria and Green Micro Algae

Biophotolysis process can occur in various species of bacteria and algae, for example species of bacteria and algae that can produce hydrogen through biophotolysis like photosynthetic bacteria from soil or natural water, Anabaena species Cyan bacteria, or eukaryotic alga Chlamydomonas species Reinhardt. The hydrogen gas production in a sustainable and environmentally friendly to produce clean energy from renewable

resources can be obtained through biophotolysis of water by cyanobacteria and Green Micro Algae. Cyanobacteria and green algae can split water into hydrogen and oxygen molecules by using sunlight (Hallenbeck et al., 1978; Miyamoto et al., 1979) Mechanism of biohydrogen production through biophotolysis or photoautotrophic process is hydrogen gas formed from the water by using sunlight and CO_2 as the sole source for energy through the process of hydrogenase enzyme by bacteria and algae (Ghirardi et al., 2000). Figure 2.1 shows the ability to photosynthesis produce H_2 under anaerobic conditions using green alga Chlamydomonas reinhardtii.

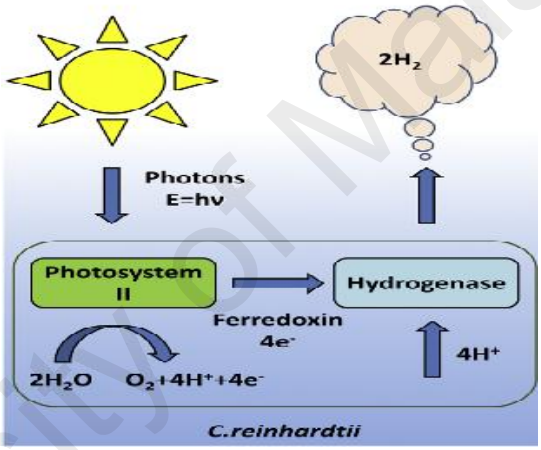

Figure 2.1: The green alga Chlamydomonas reinhardtii has the ability to photosynthetically produce H_2 under anaerobic conditions. Excerpted from (Tamburic et al., 2011)

The advantage of biophotolysis is that, there is no requirement of adding substrate as nutrients. Water is the primary electron donor required for the production of hydrogen gas. Sunlight and CO_2 are the basic inputs needed to grow the cyanobacteria or microalga on biophotolysis process through the hydrogenase enzyme.

Production of hydrogen gas by green algae and cyanobacteria is one of the methods that produce renewable energy which does not emit greenhouse gas effect with the availability of abundant resources, namely water as substrate and solar energy as a source

of energy. Thus, hydrogen gas produced could be used in a fuel cell to generate electricity as shown in Figure 2.2 (Maness et al., 2009).

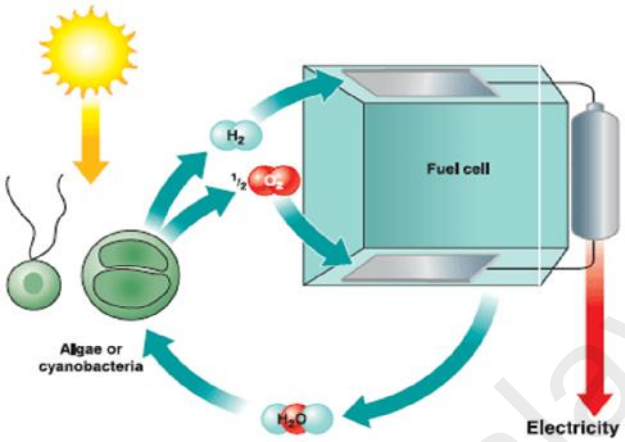

Figure 2.2: Schematic representation of the Vision for photobiological H_2 production and its utilization in a H_2 fuel cell. Adapted from (Maness et al., 2009)

In the biophotolysis process, light energy is absorbed by photosystem (*PSI* and *PSII*) of microalgae; this energy is then transferred through the electron transport chain, in turn reducing ferredoxin and provides electrons to the hydrogenase enzyme. In certain circumstances such as in anaerobic conditions, for example at a pressure of hydrogen is very low or low light, hydrogenases can provide a solution for excess electrons when carbon fixation component of the photosynthetic chain is disrupted (Akkerman et al., 2002).

A hydrogenase is an enzyme that catalyses the reversible oxidation of molecular hydrogen. The main purpose of studying about the hydrogenase is to understand the mechanism of hydrogen production, control of cell metabolism, and ultimately increase the production of hydrogen. Hydrogenases play a vital role in biophotolysis by Cyanobacteria and Green Micro Algae (Adams & Stiefel, 1998; Frey, 2002). Hydrogenases were classified according to the metals thought to be at their active sites; three classes were recognized: iron-only ([FeFe]-hydrogenases), nickel-iron ([*NiFe*]-

hydrogenases), and metal-free hydrogenses(P. M. Vignais et al., 2001). Among the three types of enzymes are most commonly found in various bacterial and algae are [*FeFe*]-hydrogenases and [*NiFe*]-hydrogenases except for metal-free hydrogenases found in some types of methanogens. Three types of this enzyme are monomeric [*FeFe*] -hydrogenases most involved in the evolution of hydrogen, features high sensitivity to oxygen (O_2) and carbon monoxide (*CO*) (Bleijlevens et al., 2004).

2.2.1.2 FeFe-Hydrogenases

[*FeFe*]-hydrogenase is an enzyme which plays a vital role in anaerobic metabolism, which is produced by green algae and become more efficient catalyst hydrogenases. [*FeFe*]-hydrogenase is able to catalyses the reversible oxidation of molecular hydrogen. Figure 2.3 highlights that the *FeFe*-hydrogenases only contains a dinuclear iron center that is attached to a protein with only one bond between cysteine residues and one of the two iron atoms. [*Fe-Fe*]-hydrogenases contain [*2Fe-2S*] and additional [*4Fe-4S*] cluster, an electron shuttle between sites the hydrogen activate, in proteins, and redox partners on the surface. Cysteine also functions as a ligand to a cluster of adjacent [*4Fe-4S*], so there is a sulfur bridge between two metal sites (Maness et al., 2009). Iron atoms from binding [*4Fe-4S*] center to the structure of proteins by three additional cysteine residues and linked through a protein cysteine residue to a 2Fe subcluster. Except for cysteine bridging cysteine, the iron atoms of the *2Fe* center coordinated to carbon monoxide (*CO*) and cyanide (*CN*) ligands. With the *CO* and *CN* is expected to allow for stabilization of low oxidation and spin state of iron is required for activity (Maness et al., 2009).

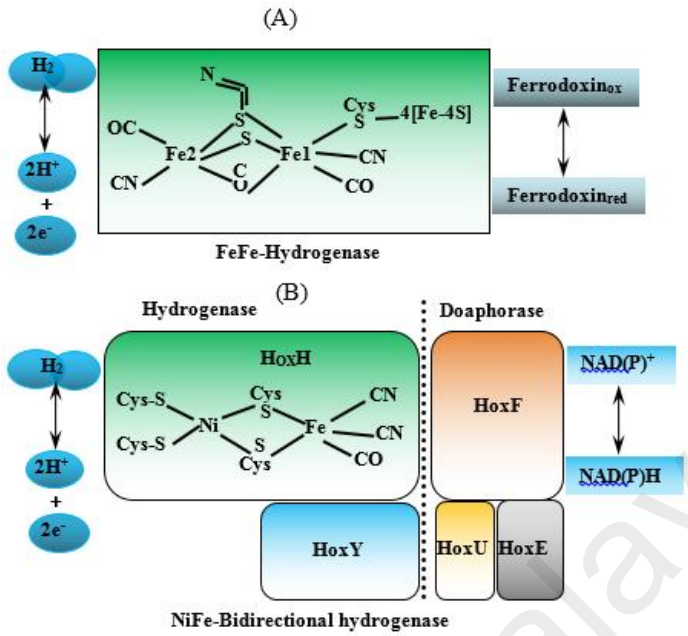

Figure 2.3: Schematic representation of the [F*eFe*]-hydrogenases and [*NiFe*]-hydrogenases. Adapted from (Maness et al., 2009)

2.2.1.3 Cyanobacterial NiFe-Bidirectional Hydrogenases

[*NiFe*]-hydrogenases produced by cyanobacteria consist of the center of several metals, including *Ni-Fe* bimetallic sites active, iron-sulfur and Mg^{2+} ions. *Ni-Fe* active site is located inside the protein molecules and functions as bidirectional hydrogenases that involve a number of lines in the catalytic reaction route like: route of electron transfer, proton transfer lines and gas-access channels (Rousset & Cournac, 2008; Seibert et al., 2008; Tamagnini et al., 2002).

[*NiFe*] hydrogenases function as the metabolism of hydrogen, which are grouped into two sub-units that are; hydrogenase large and small. Large subunit contains a core double [*NiFe*] active site and the small subunit binds at least one [*4Fe-4S*] cluster (P. Vignais & Colbeau, 2004). While the large subunit [*NiFe*]-hydrogenase and other nickel metalloenzymes synthesized as a precursor without metal active sites that experienced a post-translational maturation process of the complex (Blokesch et al., 2002; Casalot & Rousset, 2001). Synthesis and insertion of metallocentre of NiFe-hydrogenases is a

complex process, involving at least seven proteins and chemical components such as Adenosine triphosphate (*ATP*), Guanosine triphosphate (*GTP*), and karbamoilfosfat, which is the embryo of cyanide (Blokesch et al., 2002).

The *NiFe*-hydrogenases have higher levels of similarity and the complex among all the hydrogenase operons and *FeFe*-hydrogenases, so that the microbes have a very important role in hydrogen production process. Figure 2.3indicates that the bidirectional NiFe-hydrogenase of cyanobacteria consists of five subunits. Large as the center of the catalytic subunit of pentameric hydrogenase *HoxH* and containing atoms of *Fe* and *Ni* associated with the ligands *CN* and *CO* and sulfur atoms. While the small subunit hydrogenase, *HoxY*, contains a cluster [*4Fe-4S*] that are required to transfer electrons to the large catalytic subunit. For the remaining three subunits that form part of the complex is HoxF diaphorase, *HoxU*, and *HoxE* and function as an electron channel between the *NAD (P) H* and hydrogenase active site. The large number of genes involved in the maturation of the structural subunit of *NiFe*-hydrogenases, an indication of the complexity of the molecular structure of hydrogenase (Maness et al., 2009).

2.2.1.4 Direct biophotolysis

Direct biophotolysis is a biological process that can produce hydrogen directly from water using microalgae photosynthesis system to convert solar energy into chemical energy in the form of hydrogen, the reaction is generally as follows:

$$2H_2O + S \quad e \xrightarrow{(Pho \quad he)} 2H_2 + O_2 \qquad (2.1)$$

In indirect biophotolysis green algae or cyanobacterium (Figure 2.4), Hydrogen gas is produced through photosynthesis by using solar energy to split water molecules. In this process also decrease ferredoxin, hydrogenase or nitrogenase which these compounds are very sensitive to oxygen (Hallenbeck & Ghosh, 2009).

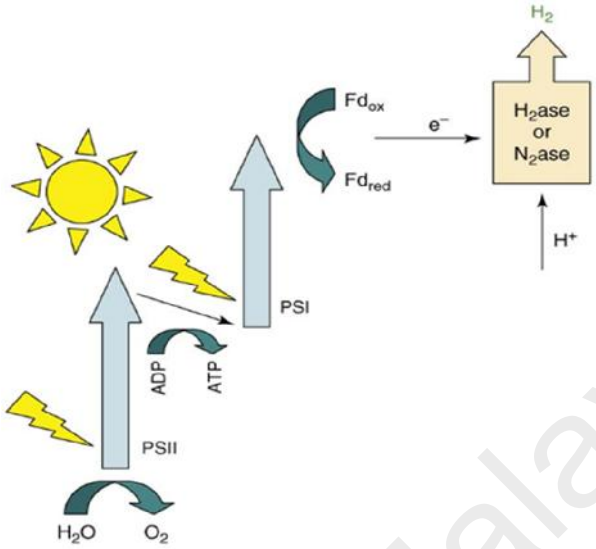

Figure 2.4: Direct biophotolysis of green algae or cyanobacteria. Adapted from Hallenbeck (Hallenbeck & Ghosh, 2009)

The advantage of this process is that, even in low light intentitas, green algae and anaerobic conditions are still able to convert almost 22% of light energy by using the hydrogen as an electron donor in the process of fixation of CO_2. From the results of further studies, even photosystem I-defective mutants of Chlamydomonas are able to produce efficiency twice as large as the wild type strain. Hydrogen production by green microalgae take place in anaerobic conditions in the dark to induce activation of enzymes involved in hydrogen metabolism. Hydrogenase sensitivity to oxygen is a big challenge for this method, so that further research is needed to develop engineered hydrogenase so that it is not sensitive to oxygen inactivation. Green microalgae have the genetic machinery, enzymatic, metabolic, and electron-transport to photoproduce hydrogen so that hydrogenase is able to combine a proton (H^+) in media with and release electrons to form hydrogen. Synthesis hydrogen permits the flow of electrons through the electron transport chain, which supports the synthesis of adenosine triphosphate (*ATP*) (Ghirardi et al., 2000).

In photosynthesis, photosystem process occurs in two-stage process, photosystem I (*PS I*) and photosystem II (*PS II*), both processes operate in series. In anaerobic conditions (lack of oxygen), electron (e-) from reduced ferredoxin (*Fd*) is used by the hydrogenase to reduce protons (H^+) and evolve hydrogen. Partial inhibition of *PS II* can produce anaerobic conditions for the cells in the photobioreactor, because there is less water oxidation activities to evolve O_2 and O_2 residues used by respiration (Wykoff et al., 1998).

$$2H_2O + li\ \ ht\ e^{\cdot} \rightarrow O_2 \uparrow + 4H^+ + F\ \ (r\ \ )(4e^-) \rightarrow F\ \ (r\ \ )(4e^-) + 4H^+ \rightarrow F\ \ (o\ \ ) + H_2 \quad (2.2)$$

In photosystem I (*PS I*) generate reductant for CO_2 reduction while in photosystem II (*PS II*), the separation of water and oxygen. In *PS II*, *P680*, the strongest absorption by the antenna pigments at wavelengths less than 680 nm (due to photon excitation energy of each) and then transferred to the *PS II* reaction center and produces a strong oxidant that is able to liberate electrons from water. Reductant that provides reducing equivalents through a series of electron carriers and cytochrome complex to the oxidized reaction center of *PS I*. While the *PS I* reaction center, the strongest absorption by antenna pigment at wavelength 700 nm, *P700*. The light energy absorbed by *PS I* is not only used to oxidize the reaction center, but also to produce a strong reductant capable of reducing oxidized nicotinamide adenine dinucleotide phosphate ($NADP^+$) to *NADPH* (Happe & Kaminski, 2002).

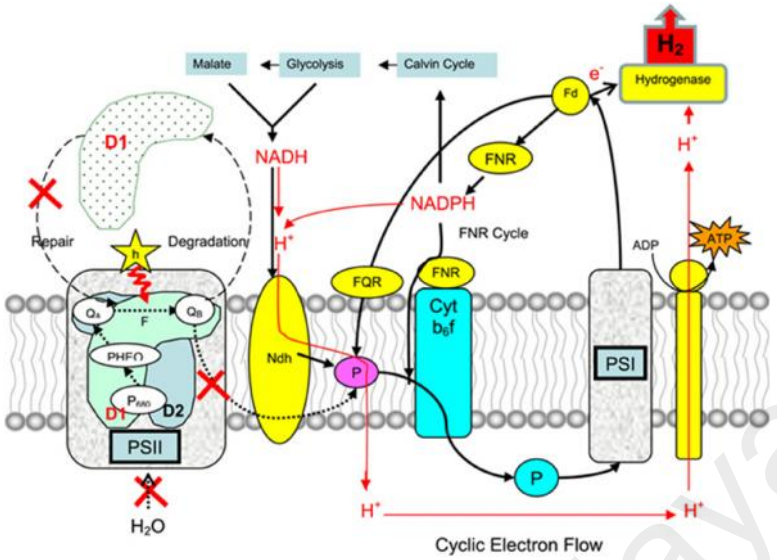

Figure 2.5: A schematic of the predicted photobiological pathway of hydrogen production in sulfur deprivation produces anoxic condition for induction of hydrogenase. Adapted from (Dasgupta et al., 2010)

Figure 2.5 illustrates the mechanism of sulfur deprivation anoxic conditions so that the induction of hydrogenase and *PS II* partially inhibited and electrons mostly come from sources of carbon reserves through plastoquinon. Anaerobic conditions induce expression of hydrogenases [*Fe*]-in algal cells (Forestier et al., 2003; Happe & Kaminski, 2002) so that continuous hydrogen production can be achieved (Ghirardi et al., 2000). Figure 2.5 also shows that overall sulfate permease mutants can grow without depleting hydrogen sulfate in the culture medium (H.-C. Chen et al., 2003). Some of the photosystem II inhibitors have also been used to inhibit the activity of water oxidation (Happe & Kaminski, 2002).

(Hallenbeck & Benemann, 2002) reported that the two photons from the water to form hydrogen gas and simultaneously produce CO_2 reduction by PS I. In the group of green plants, because of the lack of hydrogenase occurred only CO_2 reduction, contrary microalgaes and cyabobacteria have the ability to produce hydrogen, because it has a hydrogenase enzyme. In the process of *PS II*, the electron is transferred to ferredoxin (*Fd*) by using solar energy that is absorbed in *PS I*. Since hydrogenase is very sensitive to

oxygen, then the amount of oxygen levels should be controlled below 0.1% so that the production of hydrogen can be stored to maximum yield (Hallenbeck & Benemann, 2002).

2.2.1.5 Indirect biophotolysis

Indirect biophotolysis is a biological process that can produce hydrogen from water using a system of microalgae and Cyanobacteria photosynthesis to convert solar energy into chemical energy in the form of hydrogen through several steps: (i) biomass production by photosynthesis, (ii) biomass concentration, (iii) dark aerobic fermentation produces 4 glucose mol hydrogen / mol in the algal cells, together with 2 mol of acetate, and (iv) conversion of 2 mol of acetate into hydrogen. This process can be classified into two distinct groups, one of which is depending on the light and the other is light independent process. The reaction is generally as follows:

$$6H_2O + 6C_{\ 2} + li\ \ ht \rightarrow C_6H_1\ O_6 + 6O_2 \quad (2.3)$$

$$C_6H_1\ O_6 + 2H_2O \rightarrow 4H_2 + 2C_{\ 3}C \qquad + 2C_{\ 2} \quad (2.4)$$

$$2C_{\ 3}C \qquad + 4H_2O + li\ \ ht \rightarrow 8H_2 + 4C_{\ 2} \quad (2.5)$$

The overall reaction as follow:

$$12H_2O + li\ \ ht \rightarrow 12H_2 + 6O_2 \quad (2.6)$$

As above shown reactions, the mechanism of photosynthesis process to separate the O_2 and hydrogen undergo through several phases is highlighted. Oxidation of cyanobacteria stores carbohydrate and produces hydrogen. The energy required to produce hydrogen is also obtained from the starch reserves from previous photosynthetic activity. In stage two, the system sulfur limits C. reinhardtii to occur under aerobic conditions separate from the anaerobic conditions, although some of the electrons derived from the starch in the system. This phase was included in the photosynthesis biophotolysis

directly due to the operation of cells that are still functioning and provide electrons to hydrogenases during anaerobiosis (Hallenbeck & Ghosh, 2009).

Figure 2.6 shows the various mechanisms of oxygenic hydrogen production in green algae through hydrogenase and how the blue-green algae hydrogen produced through nitrogenase. Phenomenon of driving electrons is produced from photosynthetic anoxygenic reserve carbon source and hydrogen production in photosynthetic bacteria through nitrogenase, purple bacteria and green bacteria. In Figure 2.6, itis also seen the process of separation phase O_2 and hydrogen evolution in cyanobacteria, carbohydrate is oxidized to Produce hydrogen which took place in indirect phophotolysis (Dasgupta et al., 2010).

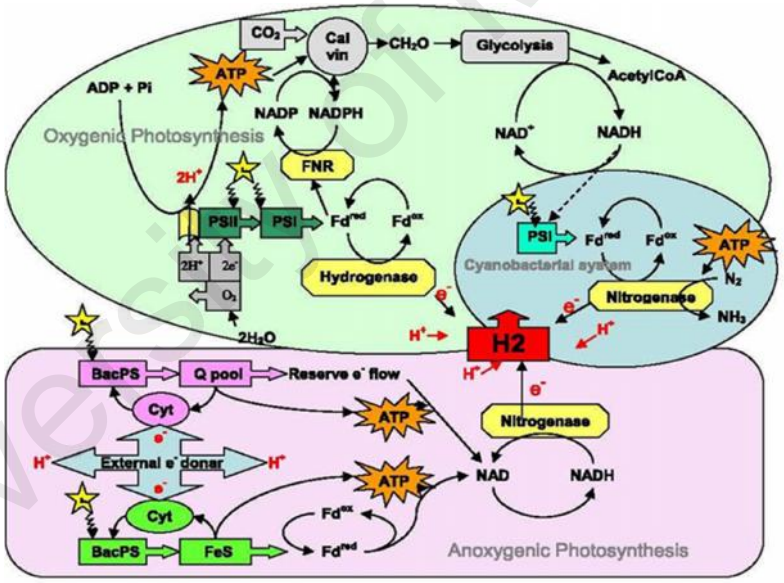

Figure 2.6: Schematic processes of electron flow on oxygenic and anoxygenic photosynthesis. Adapted from (Dasgupta et al., 2010)

In filamentous cyanobacteria, such as the genus Anabaena, spatially separating the two processes by forming heterocysts, nitrogenase is located in heterocycts with functional *PS I* then catalyzes the formation of hydrogen product. Where nitrogenase isoenzymes

vary on how many hydrogen ions paired with fixation. Equation (2.7) and (2.8) showed significant ATP requirement of nitrogenase (Stal & Krumbein, 1985).

$$N_2 + 8H^+ + F\ (r\ )(8H^-) + 16A \rightarrow 2N_{\ 3} + H_2 + F\ (o\ ) + 16A + P \quad (2.7)$$

$$8H^+ + 8e^- + 16A \leftrightarrow 4H_2 + 16A + 16P \quad (2.8)$$

Electrons donated to *PSI* in heterocyst derived from carbon transported from neighboring photosynthetic cells, so they do not have their own photosynthetic machinery, which will inhibit the function of the nitrogenase enzyme that catalyzes the O_2-sensitive nitrogen fixation (Brentner et al., 2010).

2.2.2 Fermentation processes

There are a variety of biological hydrogen production process, fermentation is one very effective method, because it can be operated and produce hydrogen continuously without the need for light. When compared with hydrogen production through biophotolysis, the hydrogen production by fermentation process has higher stability and efficiency. In industrial scale, the fermentation process is more appropriate to use because it uses a simple control system, so that the necessary operational costs are lower. One of the advantages of hydrogen production via fermentation process is using a variety of organic wastes as a substrate, so it can play a dual role of waste reduction and energy production. Thus, hydrogen production through fermentation process has received extensive attention from the researchers and scientists in recent years (Li & Fang, 2007; Wang & Wan, 2008).

Biohydrogen production by fermentation processes by using carbohydrates as a substrate has received significant attention from the researchers and scientists in recent years. Here are some reactions of hydrogen production by fermentation of glucose ((2.9), (2.10) and (2.11)) shows that the most desirable end-products is acetate, with production levels of four hydrogen mol^{-1} mol glucose (Claassen et al., 1999; F. Hawkes et al., 2002; Li & Fang, 2007; Mosey, 1983; Rodríguez et al., 2006). Theoretically, the maximum of

33% of chemical oxygen demand (*COD*) can be converted from glucose to hydrogen. The rest of the energy is released as acetate.

$$C_6H_1\ O_6 + 12H_2O \rightarrow 6H\ \ O_3^- + 12H_2 + 6H^+ \quad \Delta G^0 = 241\ k\ m\ \ ^{-1} \quad (2.9)$$

$$C_6H_1\ O_6 + 4H_2O \rightarrow 2CH_3C\ \ O^- + 2H\ \ O_3^- + 4H_2 + 4H^+ \Delta G^0 = -48\ k\ m\ \ ^{-1} \quad (2.10)$$

$$C_6H_1\ O_6 + 2H_2O \rightarrow CH_3CH_2CH_2C\ \ O^- + 2H\ \ O_3^- + 2H_2 + 3H^+\ \Delta G^0 = -137\ k\ m\ \ ^{-1} \quad (2.11)$$

$$C_6H_1\ O_6 + 3H_2O \rightarrow CH_3CH_2O\ \ + CH_3C\ \ O^- + 2H_2 + 3H^+ \quad \Delta G^0 = -97\ k\ m\ \ ^{-1} \quad (2.12)$$

Based on to the theory as shown in reaction (9) above, 12 moles of hydrogen can be produced from one mole of glucose (Hallenbeck & Benemann, 2002; F. Hawkes et al., 2002). In reaction (2.9), (2.10), (2.11) and (2.12) looks respective standard Gibbs free energy at a temperature of 25 °*C*, ΔG^0 value is calculated based on data from (Amend & Shock, 2001), where production of 12 moles of hydrogen (reaction (9)) is thermodynamically unfavorable. According to (Claassen et al., 1999), also due to this reaction at hyperthermophilic conditions while the transformation of acetate produced to hydrogen is feasible through photosynthesis in the partial pressure of hydrogen is very low and temperatures higher than 40 °*C*.

In contrast to the former reactions, production of propionate (Equation (2.13)) decreases the production of hydrogen (Li & Fang, 2007); (Mosey, 1983) as was proven experimentally by (F. R. Hawkes et al., 2007; Shin et al., 2004).

$$C_6H_1\ O_6 + 2H_2 \rightarrow 2CH_3CH_2C\ \ O^- + 2H_2O + 2H^+ \quad (2.13)$$

Undesirable consumption of hydrogen (reaction (2.14)) or glucose (reaction (2.15)) can be caused by the activity of homoacetogens such as *Clostridium aceticum*(F. R. Hawkes et al., 2007):

$$2H\ \ O_3^- + 4H_2 + H^+ \rightarrow CH_3C\ \ O^- + 4H_2O \quad (2.14)$$

$$C_6H_1\ O_6 \rightarrow 2CH_3CH_2C\ \ O^- + 2H^+ \quad (2.15)$$

In practice, the fermentation with butyrate as the main product is regarded as the most effective route to produce hydrogen (Lay, 2000; Lin & Chang, 1999). From the experimental results using the fermentation processes, the maximum hydrogen production with 2.9 mol of H_2 mol^{-1} glucose was achieved by Clostridium species (Lay, 2000; Taguchi et al., 1996).

2.2.2.1 Photo-Fermentation

Photo-fermentation is the fermentative conversion of organic substrates by a diverse group of photosynthetic bacteria that use sun light as energy to convert organic compounds into hydrogen and CO_2. For example photo-fermentation with Purple Non-Sulfur (*PNS*) bacteria can be used to convert fatty acids into hydrogen and small molecules between the products of other gases (namely CO_2). This process takes place in anoxic or anaerobic conditions and by using photosynthetic bacteria and sunlight as energy. Photo-hydrogen production was performed mainly through four species of Purple Non-Sulfur (PNS) bacteria. There are several types of bacteria that can be used in photo-fermentation process such as bacteria Rhodobacter sphaeroides (Sasikala et al., 1991), Rhodopseudomonas palustris (Barbosa et al., 2001), Rhodobacter capsulatus (Hillmer & Gest, 1977), and Rhodospirillum rubrum (Miyake et al., 1982) by using small molecule organic acids like acetate, lactate and butyrate as carbon and energy source of light that can change the carbon source to produce hydrogen (Shi & Yu, 2005; Uyar et al., 2009). While dark fermentation is the conversion of organic substrates by various groups of bacteria that take place in the dark (without the presence of light) with a series of biochemical reactions and takes place under anaerobic conditions (Redwood et al., 2009).

In the photo-fermentation process, Purple Non-Sulfur (*PNS*) bacteria is a group of photosynthetic bacteria has some advantage over compared to cyanobacteria and algae.

These bacteria use enzyme nitrogenase to catalyze nitrogen fixation for reduction of molecular nitrogen to ammonia. Nitrogenase has interesting property that it can evolve hydrogen simultaneously with nitrogen reduction. Stressful concentrations of nitrogen are therefore required for hydrogen evolution. Photo-heterotrophs make use of energy from sunlight to oxidize organic compounds and generate the electron potential needed to drive hydrogen production. By utilizing energy from the sun to drive thermodynamically unfavorable reactions, *PNS* bacteria can potentially divert 100% of electrons from an organic substrate to hydrogen production. In this processes, photo-heterotrophs typically utilize the smaller organic acids that are often produced but not metabolized, during dark fermentation. Thus, waste streams from photo-fermentation contain fewer by products as the organic compounds are fully reduced to form H_2 and CO_2 (Harwood et al., 2008).

In principle, photofermentations are able to fully convert organic compounds into hydrogen, even against a relatively high hydrogen partial pressure, because hydrogen evolution is driven by *ATP*-dependent nitrogenase and *ATP* formed is capture light energy through photosynthesis. Some researchers have conducted a study that non-sulfur purple photosynthetic bacteria capture light energy and use it to convert organic acids into hydrogen quantitatively (Basak & Das, 2007; Redwood et al., 2009).

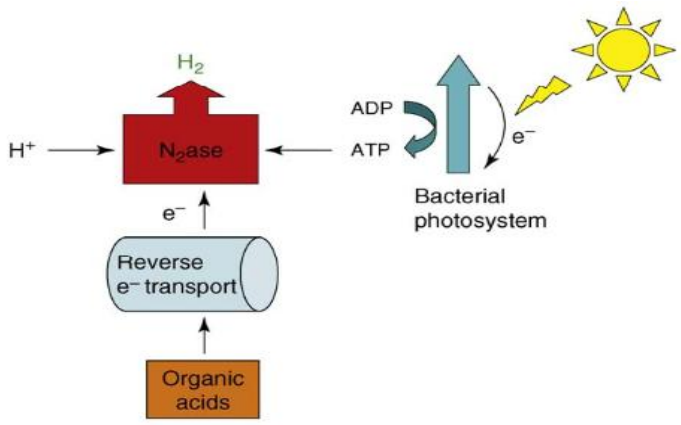

Figure 2.7: Photo-fermentation processes by Photosynthetic bacteria. Adapted from (Hallenbeck & Ghosh, 2009)

Figure 2.7 describes the non-sulfur photosynthetic bacteria to carry out a photosynthetic anaerobic purple, then captured using solar energy to generate *ATP* and high energy electrons through electron flow through, which then reduces ferredoxin. Reduction of *ATP* and reduced ferredoxin drives the hydrogen protons with nitrogenase. The organism is unable to obtain electrons from water and therefore the use of organic compounds, usually organic acids, as substrates (Hallenbeck & Ghosh, 2009).

Some researchers reported that although the stoichiometric conversion of several organic acids into hydrogen on photofermentation process can be obtained, but the light conversion efficiency and the level of production volume is still low. Results of recent studies have shown that to produce the maximum hydrogen is suggested to use two-stage system of photo-dark Fermentation (C.-Y. Chen et al., 2008; Nath et al., 2008; Tao et al., 2007). Moreover, photo-fermentation bacteria can utilize short chain organic acids which are produced in dark-fermentation, a combination of dark- and photo-fermentation can be achieved the highest theoretical hydrogen yield of 12 mol H_2/mol hexose, although results are still far below the stoichiometric (Miyake et al., 1984).

One group of Proteobacteria which have photosynthetic pigments and capable of photosynthetic are categorized as Purple Sulfur Bacteria (*PSB*). They are anaerobic or microaerophilic, and are often found in hot springs or stagnant water. Unlike plants, algae and cyanobacteria, they do not use water as their reducing agent, and consequently, do not produce oxygen. Instead, they use hydrogen sulphide or other reduced sulphur compounds as electron donor, which is oxidized to produce granules of elemental sulphur, which become visible in cells.

2.2.2.2 Dark-Fermentation

Dark Fermentation is the fermentative conversion of organic substrate and biomass materials to produce biohydrogen which takes place in anaerobic conditions and without

the presence of light. It is complex process manifested by various groups of bacteria by involving a series of biochemical reactions (Lay, 2000). Dark hydrogen fermentation has several advantages compared with other biological methods of hydrogen production such as photosynthetic and photo fermentation because of its ability to produce hydrogen continuously without the presence of light, higher hydrogen production rate, process simplicity, lower net energy input and utilization of low-value waste as raw materials (John Benemann, 1996; Chen et al., 2006; Levin et al., 2004; Nandi & Sengupta, 1998).

Dark fermentation produces hydrogen from organic compounds by anaerobic microorganisms (Fan et al., 2006; Noike et al., 2005; Oh et al., 2003; Shin et al., 2004; Taguchi et al., 1996). Dark fermentation can also produce hydrogen from organic waste as shown in the following equation (Hawkes et al., 2002; Kraemer & Bagley, 2008):

$$C_1\ H_2\ O_1\ + 9H_2O \rightarrow 4C\ _3C\ \ ^- + 8H^+ + 4H\ \ O_3^- + 8H_2 \qquad (2.16)$$

In order to increase the yield of more hydrogen in the dark fermentation process, it is necessary to control several parameters namely *pH*, organic food, nutrition, temperature, solids retention time (*SRT*), and P_{H2}. One of the most important parameters on hydrogen production is *pH*, because *pH* is one factor that influence on the activities of the enzyme hydrogenase. There have been several studies reported that the hydrogenase activity are directly correlated with dark Fermentation of hydrogen, this indicates that the *pH* plays a very important role on hydrogen production (Bhaskar, et al., 2007). Many studies have reported that the effect of *pH* in fermentative hydrogen production from glucose and sucrose using mixed microflora (Cai et al., 2004; Ginkel et al., 2001; Kawagoshi et al., 2005; Lee et al., 2002; Liu & Fang, 2003).

Many studied have been reported that the *pH* value is maintained in conditions of low and shortening the shorter solids retention time (*SRT*), thus limiting the growth of

methanogens. In general, studies based on several studies dark fermentation, *pH* value was maintained at a *pH* range of 5.5 to 8.0 either by adjusting the initial *pH*, buffer usage, or using an automatic *pH* controller. By applying these techniques, the maximum conversion efficiency has been increased by 60-70% (Ginkel et al., 2005). (Fang & Liu, 2002) also have obtained the optimum pH value in the range of 5.5 to the production of hydrogen in chemostat culture using a mixture of holding time for 6 h so that the growth of methanogens can be slowed.

Several studies have been conducted for the hydrogen production on a batch, anaerobic sequencing batch reactor (*AnSBR*), fed-batch, fluidized bed bioreactor (*FBR*), continuously stirred reactor (*CSTR*) and continuous of dark Fermentation using different raw materials as shown in Table 3. Sagnak and his team successfully fermented acid hydrolyzed waste ground wheat using anaerobic sludge as bacterial strains for hydrogen gas production by anaerobic dark fermentation (Sagnak et al., 2011). Microbial tri-saccharides species and anaerobic digester sludge were used for dark fermentation of hexose in batch systems has been done by (Quéméneur et al., 2011). (Ozmihci et al., 2011) used Clostridium butyricum-NRRL 1024 from waste wheat starch for dark fermentative bio-hydrogen production using continuously.

2.2.2.3 Photo-Dark Fermentation

The main problem faced by using a dark Fermentation biohydrogen production is low yield and energy efficiency, for example in dark fermentation for 1 mol hexose can only produce 2 to 4 moles of hydrogen with acetate and butyrate as byproduct (Su et al., 2009). In addition to producing hydrogen also byproducts contain many organic acids, which lead to energy waste and environmental pollution. While in photofermentation, organic acids can be used side by photosynthetic bacteria for further processing and then be converted into hydrogen production (Liu et al., 2010). Various efforts have been done so

that new approaches such as byproduct of organic acid produced by fermentation dark for further methane and hydrogen production in other processes (Cooney et al., 2007; Zong et al., 2009).

The best solution to solve this problem is by using sequentially between dark-Fermentation process and photofermentation. This concept is very promising for the production of biohydrogen because hydrogen production is greater than the dark phase of the fermentation process or a single photofermentation. So, the two-stage process combining dark and photofermentation can improve the hydrogen production, theoretical from 4 to 12 mol H_2/mol hexoses and from 2 to 10 mol of H_2/mol pentose (Chen et al., 2008). During the dark fermentation of carbohydrate containing substrate is converted into organic acids, CO_2 and hydrogen by mesophilic and thermophilic bacteria. In the second stage, dark fermentation waste containing organic acids such as acetic and lactic bacteria used in photofermentation by photosynthetic or Purple Non-Sulfur (*PNS*) for hydrogen production further. (Su et al., 2009) also reported that sequential technological dark and photo-fermentative been used to increase the yield of hydrogen from glucose and starch cassava.

2.2.3 Electrochemical processes

Bio-electrochemical system is an alternative technology using microorganisms as electrochemical catalyst. Microorganisms are capable of catalyzing the oxidation-reduction reaction at the anode and cathode electrode. Bio-electrochemical systems (*BESs*) are divided into two major groups which are microbial fuel cells (*MFCs*) and microbial electrolysis cells (*MECs*). Production of hydrogen from protons and electrons are produced directly by bacteria with increasing electrochemical potential in the cathode chamber of *MEC* reactor. The most interesting part of the process of electrochemical is

the occurrence of two simultaneous processes that produce hydrogen gas and electro-coagulation process.

Hydrogen can be produced from certain forms of biomass by biological fermentation (Nath & Das, 2004), but yields are low. The maximum hydrogen production from fermentation, assuming only acetate or butyrate is produced from glucose, is

$$C_6H_1\ O_6 + 2H_2O \rightarrow 4H_2 + 2C\ _2 + 2C_2H_4O_2 \quad (2.17)$$

$$C_6H_1\ O_6 \rightarrow 2H_2 + 2C\ _2 + 2C_4H_8O_2 \quad (2.18)$$

4 mol of H_2/mol glucose could be obtained if only acetate was produced, but only 2 mol H_2/mol if butyrate is the sole end product. Current fermentation techniques produce a maximum of 2-3 mol H_2/mol glucose. Thus, most of the remaining organic matter is essentially wasted as a mixture of primarily acetic and butyric acids, despite a stoichiometric potential of 12 mol H_2/mol glucose (BE Logan, 2004). The largest hydrogen yield theoretically possible using microorganisms (without an external source of energy) is therefore at 4 mol H_2/mol glucose based on production of acetic acid. Higher yields can be achieved using photobiological process and supplemental light, or using pure enzymes, but neither of these methods so far show promise for economical production of hydrogen (J Benemann et al., 2004; Miyake et al., 1999; Woodward et al., 2000). Moreover, of all the different types of biomass available for making hydrogen, only materials rich in carbohydrates such as glucose are suitable fermentation substrates.

2.2.3.1 Microbial Fuel Cells

Microbial Fuel Cells (*MFC*) and Microbial Electrolysis Cells (*MEC)* are among such bioelectrochemical systems. Together, *MFC* and *MEC* could be represented by the acronym *MxC*. Performance of *MxC* largely depends on anaerobic biofilm occupied by anodophilic (electrogenic) microorganisms, which transfer electrons to the anode during

their metabolism (Bond et al., 2002). Though anodic compartments in all *MxC* are similar, the cathode reactions differ. *MFC* operate with cathodes exposed to air resulting in oxygen reduction reaction at the cathode and electricity production (B. E. Logan et al., 2006). In contrast, *MEC* require a small additional input of electrical energy provided by an external power supply to facilitate the reaction of hydrogen formation on the cathode (René A Rozendal et al., 2006). A *MFC* consists of two electrodes (anode and cathode), where bacteria grows on organic materials dissolved in the anode chamber in anaerobic conditions. Due to the activities of bacteria, chemical energy from organic matter in the wastewater is converted into electrical energy. Microorganisms oxidize substrates to produce electrons and transfer to the anode electrode. Then electrons through an external circuit to the cathode electrode and produce an electric current (Hong Liu & Logan, 2004).

By electrochemically augmenting the cathode potential in a *MFC* circuit it is possible to directly produce hydrogen from protons and electrons produced by the bacteria. This approach greatly reduces the energy needed to make hydrogen directly from organic matter compared to that required for hydrogen production from water via electrolysis. In a typical *MFC*, the open circuit potential of the anode is ~ -300 mV (Hong Liu & Logan, 2004; Hong Liu et al., 2004). If hydrogen is produced at the cathode, the half reactions occurring at the anode and cathode, with acetate oxidized at the anode, are as follows:

Anode : $C_2H_4O_2 + 2H_2O \rightarrow 2C_{\ 2} + 8e^- + 8H^+$ (2.19)

Cathode: $8H^+ + 8e^- \rightarrow 4H_2$ (2.20)

Producing hydrogen at the cathode requires a potential of at least E^0= - 410 *mV* at *pH* 7.0 (Plambeck, 1995), so hydrogen can theoretically be produced at the cathode by applying a circuit voltage greater than 110 *mV* (i.e., 410-300 *mV*). This voltage is substantially lower than that needed for hydrogen derived from the electrolysis of water,

which is theoretically 1210 *mV* at neutral *pH*. In practice, 1800-2000 *mV* is needed for water hydrolysis (under alkaline solution conditions) due to over potential at the electrodes (X. Chen et al., 2002).

It is shown here that this biochemical barrier can be circumvented by generating hydrogen gas from acetate using a completely anaerobic microbial fuel cell (*MFC*). More than 90% of the protons and electrons produced by the bacteria from the oxidation of acetate were recovered as hydrogen gas, with an overall Coulombic efficiency (total recovery of electrons from acetate) of 60-78%. This is equivalent to an overall yield of 2.9 mol H_2/mol acetate (assuming 78% Coulombic efficiency and 92% recovery of electrons as hydrogen). This bio-electrochemically assisted microbial system, if combined with hydrogen fermentation that produces 2 to 3 mol of H_2/mol glucose, has the potential to produce 8 to 9 mol H_2/mol glucose at an energy cost equivalent to 1.2 mol H_2/mol glucose (Hong Liu et al., 2005).

2.2.3.2 Microbial Electrolysis Cell

Research on the production of hydrogen gas using the *MEC* has been conducted since 2005, some of the articles relating *MEC* began publication in 2007 (Bruce Logan et al., 2007). A *MEC* is a slightly modified *MFC* where a small amount of electricity is applied to the anode chamber to suppress the production of methane and oxygen is kept out of the cathode chamber to assist bacterial oxidation of organic matter present in wastewater to produce hydrogen, a gas to become the most attractive energy source in the 21st century. While Microbial Electrolysis Cell (*MEC*) has tremendous potential, the development of this technique is still in its infancy. Information about the anode materials and microorganisms used in *MFCs* are also applicable to *MEC* systems due to their similar anodic process. Yet, efficient and scalable designs are required and investigated by

biologists for the successful applications of the microbial electrolysis process (Hu et al., 2008).

The dark and photo fermentation process has many disadvantages compared to the *MEC*. At this process the formation of other compounds such as volatile fatty acids (*VFAs*), so that hydrogen gas cannot be produced optimally. In bioelectrocatalysis technologies such as *MEC*, the organic material used as an electron donor to be degraded by bacteria is exoelectrogenic. Because of the drive voltage supplied from the outside, the compounds *VFAs* will break down into protons. When protons are released from the anode and met with electrons in the cathode and then the hydrogen gas formed (Hong Liu et al., 2005). If compared with other processes, the *MEC* is one technology that has a very bright prospect in the future and when viewed in economic terms, *MEC* has a market and commercial potential is very large. To achieve these conditions, some studies need to be given special attention, such as: how to reduce the required electrical input reactor, the material for the cathode to be cheaper and how to increase the current density in the reactor (Hallenbeck & Ghosh, 2009).

2.3 Fundamental of Microbial Electrolysis Cell

One of the newest and promising approaches for the production of hydrogen from organic materials and wastewater is to use bio-electrochemical system or microbial electrolysis cell (*MEC*). This technology has outperformed other processes such as photo-dark biophotolysis and fementation. In *MEC* reactor, exoelectrogenic bacteria oxidize the organic matter then generate electrons, protons and CO_2. The electrons released by bacteria into the anode then combine with the protons at the cathode and react to form hydrogen gas. This reaction does not occur spontaneously but needed supply some energy from outside. Minimum required electrode potential is suggested at 0.414 *V*. Such *MEC* reactor is a schematic diagram as shown in Figure 2.8.

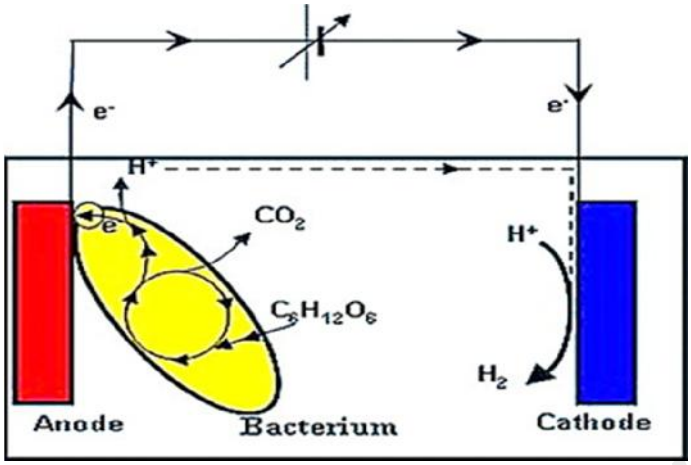

Figure 2.8: Schematic construction and operation for *MEC* reactor with typical single chamber

Here's one example ofthe reaction between electrons and protons in the *MEC* reactor using acetate as a substrate:

$$C_2H_4O_2 \rightarrow C_{\ 4} + C_{\ 2} \quad (2.21)$$

$$C_{\ 2} + 4H_2 \rightarrow C_{\ 4} + 2H_2O \quad (2.22)$$

$$H_2O + e^- \rightarrow O^{\ -} + H_2 \quad (2.23)$$

The following is the reaction in the MEC when acetate is used as the substrate:

Anode:

$$CH_3COO^- + 4H_2O \rightarrow 2HCO^{3-} + 9H^+ + 8e^- \quad (2.24)$$

Cathod:

$$8H^+ + 8e^- \rightarrow 4H_2 \quad (2.25)$$

2.3.1 Reactor design

The structure of the *MEC* reactor is directly related to the internal resistance and current density, and these factors can affect the rate of hydrogen production. Currently, there are 3 types of *MEC* reactor types encountered, i.e. *H*-type, cube-type and rectangular-type. The third type of the reactor structure has characteristic and advantages

of them. As a comparison for each reactor structure, the advantages and disadvantages can be seen in Table 2.1.

Table 2.1: Comparative different structures, advantages and disadvantages of MEC reactor

Structure:	Characteristics	Advantages and disadvantages
H-type	Two bottles separated by a membrane	Structure is simple and the separated chambers could prevent the mixing of oxygen and hydrogen; but the electrodes space cause the large system resistance
Cube-type	Single chamber without membrane	Significantly increase the current density and hydrogen recovery rate, enhance the reaction performance; but the hydrogen could be used by the methanogens
Rectangular-type	Reaction be separated by a membrane into two chambers	Membrane could prevent the mixing of oxygen and hydrogen gas; but increase the pH gradient

When observed from the ion exchange membrane, *MEC* reactor is divided into two parts, namely the membranous reactor and reactor membranless. Meanwhile, when observed from the structure of space, then the *MEC* reactor chamber can be divided into single and double chamber. By using the ion exchange membrane, the H_2 and O_2 can be separated so that the oxidation of H_2 at the anode can be avoided. By using anion exchange membrane, this will reduce the internal resistance of the reactor, reducing the *pH* gradient, reduce energy loss, increase the level of energy recovery, the imbalances in the oxidation process at the anode will be better and the production of hydrogen will be higher. Hence, *MEC* performance will be optimized so as to boost the production of hydrogen gas up to 1.1 m3 m-3 d-1 (Call & Logan, 2008; C.-Y. Chen et al., 2008).

MEC reactor with a single chamber without membrane has its own advantages, when the applied voltage is less than 0.6 *V* and the distance between the two electrodes is

controlled at 0.2 cm, the hydrogen yield will reach its maximum value. Optimum electrode spacing should be a serious concern for researchers in order to prevent the use of hydrogen ions by hydrogen-consuming microorganism's inhabitation and transform into methane.

2.3.2 Electrode materials of *MEC*

2.3.2.1 Anode

There are several types of material used in the anode *MEC* reactor such as carbon-based materials, stainless steel, iron, platinum and others. Carbon-based materials is one of the most widely used material as electrode materials in *MEC* reactor because it has several advantages such as; low cost, low over-potentials, non-corrosive, abundance in nature, low toxicity to living organisms, biocompatibility and versatility in morphologies, and are also excellent conductivity (Logan et al., 2008).

2.3.2.2 Cathode

In the *MEC* process, hydrogen gas is formed at the cathode. To encourage the production of hydrogen gas is formed faster in *MEC* reactor, the right amount of supply overpotential is required to be supplied into the reactor. In order to keep overpotentials lower, the selection of appropriate cathode material has to be done properly. Platinum (*Pt*) is one type of material that has overpotentials very low and usually used as the catalyst in *MEC* reactor. But the cost is very expensive, so that the selection of platinum as the electrode material becomes less attractive to the *MEC* reactor. Stainless steel is one alternative to replace platinum as well as low overpotentials and also low cost. Another advantage of the stainless steel material is stability in highly alkaline solution (Selembo et al., 2009).

2.3.3 Substrates used in *MEC*

MEC has been known as one of the renewable technologies that are environmentally friendly. This technology is one of the alternative methods of producing hydrogen gas by utilizing different types of organic waste water. Abudukeremu Kadier et al. (2014) reported that there have been many studies done on the production of hydrogen gas from a wide variety of organic wastes such as domestic wastewater, swine wastewater, fermentation effluent, refinery wastewater samples, industrial, food processing, wastewater, potato processing wastewater & dairy manure wastewater.

Hydrogen gas can also be produced from glucose, cellulose, glycerol, fermentable organics and various types of substrates nonfermentable such as acetic acid, butyric acid, lactic acid, valeric acid, propionic acid (Cheng and Logan, 2007). Hydrogen recovery from the substrate sodium acetate (CH_3COONa) approaches the theoretical value that is 4 mol H_2 / mol acetate. This substrate is the end product of the fermentation general such as photo and dark fermentation. From the literature it was reported that the final product of this process is the most widely used in the *MEC* reactor (Call & Logan, 2008). By using this substrate highest hydrogen production rate reaches 50 $m^3\ H_2\ /\ m^3\ d$ with an applied voltage of 1 V (Jeremiasse et al., 2010).

2.4 The uniqueand advantages of biohydrogen production processes

Table 2.2 shows the characteristics, uniqueness and common to each of biohydrogen production processes. Every of biohydrogen production processes have advantages and lack of each system. One of the best alternatives to maximize the production of hydrogen gas is by combining these three processes. The three of processes used in sequence, namely photo-fermentation, dark-fermentation and bio-electrochemical processes. This concept is very promising for the maximum biohydrogen production when compared to the dark-fermentation or photo-fermentation phase only. By using each process separately

the maximum hydrogen gas obtained only is 60-70%. So, by combining these three processes in sequence, namely dark-fermentation, photo-fermentation and bio-electrochemical process can increase the hydrogen gas production to 91% (Call & Logan, 2008).

Table 2.2: Comparison of the unique or common processes of biohydrogen production by cyanobacteria and green micro algae, photo-fermentation, dark-fermentation and bio-electrochemical process

No	Processes	Common	Unique	Ref.
1	Cyanobacteria and green micro algae	1. Uses carbohydrates to store energy 2. Take place in anaerobic condition	1. Using biophotolysis process. 2. No requirement of adding substrate as nutrients 3. Only using water, CO_2 and sunlight energy as a source of energy 4. H_2 can be produced directly from water and sunlight 5. It has the ability to fix N_2 from atmosphere	(Miyamoto et al., 1979; Ghirardi et al., 2000; Akkerman et al., 2003 & Maness et al., 2009)
2	Photo-fermentation	1. Uses organic wastes as a substrate 2. This process takes place in anoxic and anaerobic conditions	1. Can use a variety of organic wastes as a substrate 2. Using photosynthesis bacteria. 3. Using sunlight as energy to convert organic compounds into hydrogen 4. A wide spectral energy can be used by photosynthetic bacteria	(Wykoff et al., 1998; Tao et al., 2007; Zhua et al., 2007 & Harwood et al., 2008)
3	Dark-fermentation	1. Takes place in anaerobic conditions 2. Using organic substrate and biomass to produce biohydrogen	1. It is ability to produce hydrogen continuously without the presence of light 2. This process take place in dark condition 3. Higher hydrogen production rate. 4. Process very simplicity 5. Lower energy input 6. Can use low-value organic waste as raw material	(Benemann, 1996; Taguchi et al., 1998; Mulin et al., 2004 & Liu et al., 2010)

			7. No oxygen limitation 8. Can produce several metabolites as by-products	
4	Bio-electrochemical process	1. Takes place in anaerobic conditions. 2. Using organic substrate to produce biohydrogen	1. This process is also used to remove organic contaminants in wastewater 2. It is possible to directly produce hydrogen from protons and electrons produced by the bacteria 3. More than 90% of protons and electrons produced by the bacteria	(Liu et al., 2004; Call et al., 2008)

In summary, biological hydrogen production is the most challenging undertaking issue in the last decade, while world energy demand increases, fossil fuel resources is reduced and the need to minimize greenhouse gas is becoming increasingly concerned. Hydrogen gas will be one of realistic energy future as the growing science of biotechnology so that it can overcome environmental problems and social changes. It is a fact that hydrogen is clean and efficient energy carrier, produce zero emissions and can be generated by renewable sources such as biomass and waste.

Since steam reforming or partial oxidation hydrocarbon fossil fuels operate at high temperatures the chemical methods require very high operating costs. It is necessary to develop a new process to obtain hydrogen fuel with a low production cost. Biological method has potential as an alternative to the current renewable technologies because it offers promising advantages such as operating under mild conditions and a specific conversion. The sources of raw materials can be obtained from a variety of organic-based starch, cellulose containing solid wastes, food industrial wastewater, industrial waste biodiesel, palm oil mill effluent etc.

There are various technologies used for biological hydrogen production is to include the biophotolysis of water by cyanobacteria and green micro algae, photo fermentation, dark fermentation, photo-dark fermentation and bio-electrochemical processes. Hydrogen production using biophotolysis systems by cyanobacteria and green micro-algae to become an alternative method of gaseous energy recovery and has the potential to be applied in the production of renewable energy. Research on photobiological hydrogen metabolism has increased significantly; further studies need to be more innovative to increase the effectiveness of photobioreactors. Direct biophotolysis is a biological process that can produce hydrogen directly from water, even though productivity of hydrogen production is relatively limited, but has provided new knowledge about the phenomenon hydrogenases enzymes, biomaterial and the nature of electron carriers in the photosynthesis system. Indirect biophotolysis has its advantages and potential to enable hydrogen energy co-generation involves the steps of photosynthesis and biomass production of dark anaerobic fermentation of biomass to produce hydrogen.

In the dark fermentation, the conversion of organic compounds into hydrogen gas through a complex process involving a diverse group of bacteria with a complex series of biochemical reactions. While the photo-fermentation, the conversion of organic compounds into hydrogen gas can only take place in the presence of light. By combining the two processes is dark and photo-fermentation, this being the most interesting approach that can be used to increase the production of hydrogen gas. In this process besides having excess levels of hydrogen production, fast and simple operation, also can be used a variety of organic wastes as substrates. Thus, compared with the production of hydrogen through the process of photosynthesis, the production of hydrogen fermentation is more suitable to be used as well as produce a very clean energy and also can treat organic waste.

One of the advantages of the *MEC* is able to produce high hydrogen production, H_2-capture efficiency up to 91%. Because the performance of the *MEC* is determined by the physiology of microorganisms and on the other hand is also determined by the physical chemical transport processes involved. Results of high H_2 and can provide multiple benefits in terms of maximum H_2 yield and minimize the *BOD* of the waste. It's one of the advantages when compared with the fermentation process.

CHAPTER 3: MATHEMATICAL MODELING AND SIMULATION OF THE BIOHYDROGEN PRODUCTION PROCESSES IN MICROBIAL ELECTROLYSIS CELL REACTOR

3.1 Introduction

This chapter presents a dynamic modeling and simulation model of microbial electrolysis cell (*MEC*) in fed-batch reactor. The *MEC* model used here has been simplified from the model presented by Pinto et al. (R. Pinto et al., 2011), ignoring the conversion of organic matter to acetate hydrolysis process involving fermentation. In particular the emphasis in this chapter was to study the fundamental of bioelectrochemical systems as thermodynamic and kinetics for *MEC* process, irreversible energy potential losses and the dynamic performance of *MEC* involving the mathematical model and electrochemical process for *MEC* system. In addition, the mathematical model used here applies to operating *MEC* on wastewater involving anodophilic (x_a), acetoclastic (x_m) and hydrogenotrophic (x_h) microorganisms and substrate concentration(S). Furthermore, the behaviour of *MEC*, effect of the influent of applied voltage, analysis of the effect of internal and external parameter involving the effect ofvaryingchanges of the anodic compartment volume (V_r), initial concentration of anodophilic microorganisms (X_a) and the maximum growth rate of the hydrogenotrophic ($\mu_{m\ \ ,h}$) on *MEC* current and hydrogen production rate will be discussed in this chapter.

This chapter begins with a literature review focusing on introducing about hydrogen gas, thermodynamics in bioelectrochemical systems, irreversible energy potential losses and some of *MEC* models that were developed in this field and gather the sources of information and data required to develop a *MEC* simulation model.

As a result of the use of fossil fuels in excess and without considering the negative impact on the global climate and human health, causing safety ecosystems around the world is threatened. Dilemmas and concerns over the impact of these resources will not be resolved without the proper completion. To save future generations, need to be an exhaustive review of other sources of alternative energy has properties characteristic of sustainable and renewable, clean, free of greenhouse gas emissions, acid rain and air pollution. One of the great challenges in the coming decade is how to get new renewable energy sources that are environmentally friendly and to replace high dependency on fossil fuels. Until recently, almost all of the energy needed is derived from the conversion of fossil energy sources, such as for power generation, industrial and transportation equipment that uses fossil fuels as a source of energy. Fossil fuels are source of non-renewable energy and also have seriously negative impacts on the environment, e.g. soil, water, air, and climate. The use of fossil fuels cause excessive global climate change because emissions of greenhouse pollutants and the formation of compounds *COx , NOx, SOx, CxHy*, ash, and other organic compounds that are released into the atmosphere as a result of combustion (Das & Veziroğlu, 2001; Yokoi et al., 2002). One of the other energy sources that qualify above is hydrogen gas. At the end of this decade, the talk about hydrogen fuel is not only discussed among scientists alone but has become a major issue and a hot topic in several car manufacturers, the mass media and even political leaders. In some developed countries, public enthusiasm was so great, and they had been ready to welcome the hydrogen gas as a vehicle fuel of the future. This is one solution for modern society and as a way out to overcome the threat of global warming accelerating, so that almost all the country's dependence on fossil fuels can be resolved. One of the interesting things is that when hydrogen gas used in vehicles or fuel cell, the result is much more efficient than the internal combustion engine. When these compounds react with air, the by-product is in the form of water. Because of these advantages that hydrogen gas is

known as a low-carbon energy source. Most likely, a diverse portfolio of energy-producing technologies will be needed to replace fossil fuels in the future. These technologies may rely on renewable or non-renewable resources. A portfolio of renewable energy technologies may include a variety of systems based on sunlight, wind, tides, geothermal heat, and biomass. Those are much more interesting because they do not depend on limited reserves (B. E. Logan et al., 2008). Based on the above considerations, in recent years various studies has been conducted to obtain a sustainable source of energy that can replace fossil fuels and which do not have a negative impact on the environment. Hydrogen is one alternative fuel substitute for fossil fuels and is considered as an "energy carrier" with a promising future. It has a high energy content of 122 kJ/g, that is 2.75 times greater than those of hydrocarbon fuels (Argun et al., 2008).

Hydrogen plays a very important role and contribution in the global era that is based on clean renewable energy supplies and sustainably which will provide major contributions to the world economic growth. Hydrogen fuel is environmentally friendly, clean and is the most abundant element in the universe in its ionic form. Hydrogen gas is also colorless, tasteless, odorless, light and non-toxic. When its gas is used as fuel, it will not produce pollution to the air but it produces only water as its end-product when it burns (Kotay & Das, 2008). Hydrogen gas which is produced by biological processes becomes very interesting and promising because they can be operated at ambient temperature and pressure with minimal energy consumption, and become more environmentally friendly.

Microbial electrolysis cells (*MEC*) used for wastewater treatment are a novel and promising renewable energy technology that can produce H_2 while the treatment is being performed. Currently, several studies of the *MEC* system have been reported in the literature. One important and interesting phenomenon of the *MEC* model is a competition between anodophilic and methanogenic microorganisms to consume the substrate in the

anode compartment (Pinto et al., 2010). Competition among these microbial populations has severe effects on the performance of the *MEC* bioreactor.

An initial study of this system used a model involving competition among anodophilic, methanogenic acetoclastic and hydrogenotrophic methanogenic microorganisms in the biofilm as reported by (R. P. Pinto et al., 2011). Others have reported improvements in the modeling and simulation of a two-chamber microbial fuel cell (Kato Marcus et al., 2007), conduction-based modeling of the biofilm anode of a microbial fuel cell (Marcus et al., 2011), analysis of a microbial electrochemical cell using the proton condition in biofilm model and a multi-population model of a microbial electrolysis cell (R. Pinto et al., 2011). (Picioreanu et al., 2008; Picioreanu et al., 2010) provided detailed descriptions of the mathematical model for microbial fuel cells with anodic biofilms and anaerobic digestion. The model was based on evaluation of the effect of pH and electrode geometry on microbial fuel cell performance.

However, the *MEC* presents many technological challenges that are beyond modeling studies that need to be overcome before it can be used for commercial applications. For instance, the nonlinear and highly complex processes in this hydrogen production process are due to microbial interaction, which depends on the microbial activity. Its complexity makes the MEC system difficult to operate and control under the best of conditions. However, these problems can be alleviated using an integrated process system engineering approach involving process modeling, optimization, and control simultaneously.

3.2 Bioelectrochemical systems (*BESs*)

Bio-electrochemical systems (*BESs*) are an alternative technology that uses microbial as catalysis in the electrochemical reactions. Microorganisms are known to have capability of oxidizing a substrate to catalyze oxidation-reduction reactions at the

electrode surface. In this process, the chemical energy of organic materials from the waste water can be converted into electrical energy and is known as the microbial fuel cell (*MFC*). And from the waste water can also produce hydrogen gas by adding a number of potential energy into the system, and now more popularly known as microbial electrolysis cell (*MEC*) process.

The basic principle of bio-electrochemical is the process of oxidation-reduction between the substrate and enzyme activities that involve certain bacteria or microbes in the system. In the process, the bacteria transfer electrons to the anode electrode and the cathodic electrode can be used as a source of energy which later became known as *MFC* and *MEC* process. Reduction oxidation process that occurs at the anode will produce hydrogen ions and protons diffuse into the cathode to balance the pH of the organic compound (Bond et al., 2002). In contrast to the reactor *MFC*, the oxidation-reduction process that occurs on the cathode has hindered the formation of hydrogen proton gradient due to diffusion of air from outside. Both anode-cathode can be connected through an electrical circuit, so that the energy of the proton gradient that passes from the anode to the cathode can be utilized as much as possible (Bond et al., 2002; Bond & Lovley, 2003).

Besides knowledge of the basic principles in a biochemical system, it is necessary also a broader study on the field of design and process as well as appropriate managerial preferences so that the loss of energy in the system can be minimized. For example, the loss of biological and electrochemical cell ohmic resistance and *pH* gradient should be minimized as small as possible. Current and voltage are two important variables that need to be controlled so that the hydrogen gas can be continuously produced optimally.

3.2.1 Thermodynamics in *BESs*

Figure 3.1 shows a diagram illustrating the mechanism of the difference between the *MFC* with *MEC*. In the *MFC* and *MEC*, exoelectrogenic bacteria oxidize organic

compounds and form a biofilm layer around the solid anode. For the *MEC* process, all the oxidation-reduction reaction takes place under anaerobic conditions and allows the formation of hydrogen gas at the cathode. Especially in the cathodic reaction, both the *MFC* and *MEC*, through dissociation constant water so that protons and hydroxyl, the reaction among each other is always in balance.

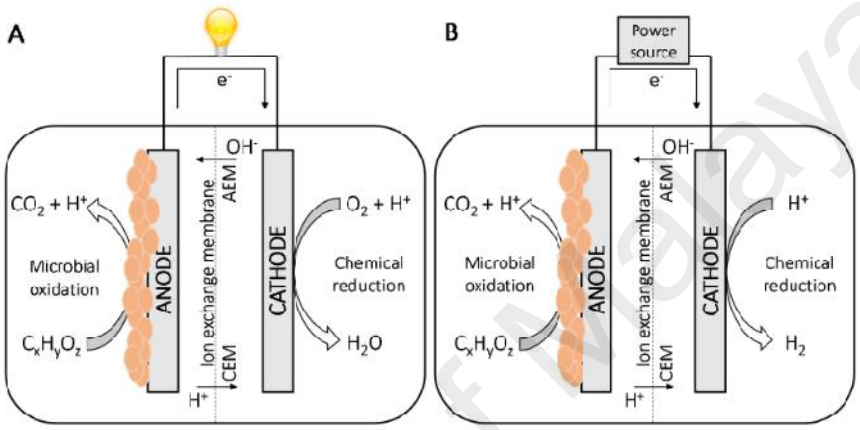

Figure 3.1: The mechanism of oxidation-reduction reaction in (A) microbial fuel cell (MFC) and (B) the microbial electrolysis cell (*MEC*)

The following is a standard half-reactions and Potential (E^0) at the anode and cathode of an *MFC* using acetate, ferricyanide and Manganese dioxide as an electron donor. The anode and cathode half-reactions (B. E. Logan et al., 2008)as given as follows :

$$2HCO_3^- + 9H^+ + 8e^- \rightarrow CH_3COO^- + 4H_2O \qquad E^0(V) = 0.187 \qquad (3.1)$$

$$O_2 + 4H^+ + 4e^- \rightarrow 2H_2O \qquad E^0(V) = 1.229 \qquad (3.2)$$

$$O_2 + 2H_2O + 4e^- \rightarrow 4OH^- \qquad E^0(V) = 0.401 \qquad (3.3)$$

$$MnO_2(s) + 4H^+ + 2e^- \rightarrow Mn^{2+} + 2H_2O \qquad E^0(V) = 1.230 \qquad (3.4)$$

$$O_2 + 2H^+ + 2e^- \rightarrow H_2O_2 \qquad E^0(V) = 0.695 \qquad (3.5)$$

$$Fe(CN)_6^{3-} + e^- \rightarrow Fe(CN)_6^{4-} \qquad E^0(V) = 0.361 \qquad (3.6)$$

And here are the half-reaction of the cathode and anode to *MEC* process by using acetate as the electron donor, the reaction as given as follow:

$$CH_3COO^- + 4H_2O \rightarrow 2HCO_3^- + 9H^+ + 8e^- \qquad E^0(V) = 0.187 \qquad (3.7)$$

$$2H^+ + 2e^- \rightarrow H_2 \qquad E^0(V) = 0 \qquad (3.8)$$

$$2H_2O + 2e^- \rightarrow H_2 + 2O^- \qquad E^0(V) = -0.828 \qquad (3.9)$$

3.2.2 Thermodynamics Principles

In MFC and MEC, thermodynamic analysis is needed, especially to assess changes in the energy and entropy, such as heat absorption and energy released by the system, the energy consumed or useful for system and others. For example, if the results of thermodynamic calculations showed that the Gibbs free energy is positive, the required energy input from the outside is required to drive the reaction. Conversely, if the Gibbs free energy is negative, then the reaction will occur spontaneously without requiring the input of energy from outside the system.

Here is the equation to measure the Gibbs free energy in the system or electromotive force so that electrical energy can flow in a circuit. Standard reaction Gibbs free energy can be calculated as:

$$\Delta G_r = \Delta G_r^0 + R \ln(\prod) \qquad (3.10)$$

where ΔG_r is the Gibbs free energy for the specific conditions, while ΔG_r^0= Gibbs free energy for standard conditions and it is defined as 298.15 K, whereas *R* (8.31447 J mol)is the universal gas constant and *T* (K) is the absolute temperature and $\prod$ is reaction quotient of the products divided by the reactants (B. E. Logan et al., 2008).

In the electrochemical system, the overall potential electromotive force (E_e) is obtained from the potential difference between the cathode and the anode. Theoretically the reaction of potential electromotive force (E_e) can be achieved spontaneously if the value E_e > 0. If the value E_e < 0, the necessary energy from the outside to push the reaction of non-spontaneous process is required. The relationship between ΔG_r and E_e is obtained from the following equation:

$$W_m = E_e . (Q) = E_e . (n.F) = -\Delta G_r \quad (3.11)$$

where Q is the charge transferred in the reaction determined by the number of electrons in the exchange reactions and are expressed in Coulomb (C). Whereas n is the number of electrons per mole of reaction, and F is Faraday's constant (9.64853x 104 C / mol). From the above equation is obtained:

$$E_e = -\frac{\Delta G_r}{n} \quad (3.12)$$

If all of the reaction is assumed to standard conditions, $\prod$ = 1, then

$$E_e^0 = -\frac{\Delta G_r^0}{n} \quad (3.13)$$

According to (B. E. Logan et al., 2006), the maximum conditions of the system on the standard state will be achieved when Gibbs free energy is negative. Theoretically, the value of potentials (E_e) can be calculated from the difference between the cathodic and anodic of MFC or MEC system. The equation can be described as follows:

$$E_e = E_{c\ ho} - E_a \quad (3.14)$$

Where $E_{c\ ho}$ is the potential electromotive force of a specific reaction that occurs in cathode and E_a is the potential value of electromotive force of a specific reaction that takes place at the anode chamber section.

3.2.2.1 Thermodynamics of *MFC*

Despite the development of research for the *MFC* very rapidly, but it still has many shortcomings such as the lack of terminology and methods for analysis and proper system performance. It required more in-depth scientific studies, such as on microbiology, electrochemistry, performance systems, environmental engineering and all things associated with the *MFC* process.

In Figure 3.2 shows that the number of microorganisms at the anode compartment to transfer electrons from an electron donor (substrate) to the anode electrode either directly or through intermediaries. The electrons then flow to the cathode via an external resistance and then react with oxygen. The anode compartment also produced a number of protons which then migrate to the cathode chamber via the cation exchange membrane (*CEM*).

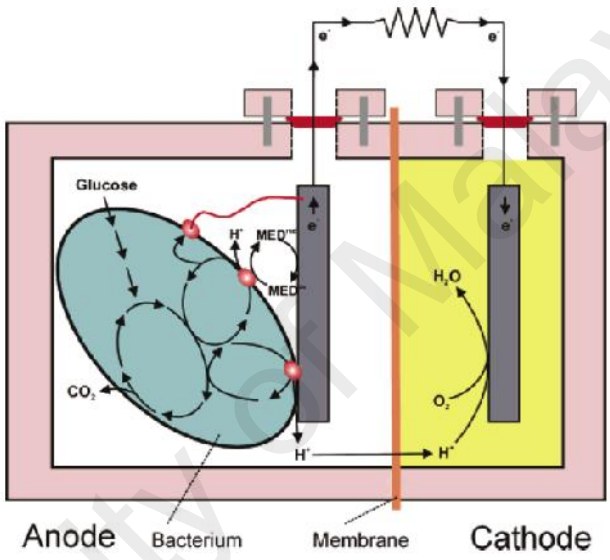

Figure 3.2: General description of the operating principle of the *MFC* (Bard et al., 1985)

In *MFC*, electrode potentials occurred between interfaces the electrodes and the electrolyte, which is a measure of energy per unit charge available from oxidation-reduction reactions. Potential energy occurs because of the transfer of electrons and ions specific adsorption on the entire interface anode and cathode. Here are a half-cell reaction in the standard state (at 298 K, 1 bar, 1 M) for acetic acid oxidation by bacteria that occurs in the anode and the cathode (Bard et al., 1985).

In *MFC*, electrode potentials occurred between interfaces the electrodes and the electrolyte, which is a measure of energy per unit charge available from oxidation-reduction reactions. Potential energy occurs because of the transfer of electrons and ions

specific adsorption on the entire interface anode and cathode. Half-cell reaction in the standard state (at 298 K, 1 bar, 1 M) for acetic acid oxidation by bacteria that occurs in the anode and the cathode (Bard et al., 1985).

$$2H\ _3^- + 9H^+ + 8e^- \rightarrow C\ _3C\ \ ^- + 4H_2O \tag{3.15}$$

The normal hydrogen electrode (*NHE*) at standard conditions has the potential to zero, so as to obtain the theoretical potential of the anode (E_A^+) then use the general equation of the standard cell electromotive force, namely:

$$E_A\ = E_A^0\ - \frac{R}{8F} ln\left(\frac{[C\ _3C\ \ ^-]}{[H\ \ _3^-]^2[H^+]^9}\right) \tag{3.16}$$

The theoretical reduction potential for the anode where acetate is oxidized in certain conditions can also be written as follows (B. E. Logan et al., 2006):

$$E_a^e\ \ = E_{an}^0\ \ - \frac{R}{b_A\ F} ln\left(\frac{C_C\ _3C\ \ ^-}{[H\ \ _3^-]^2[H^+]^9}\right) \tag{3.17}$$

At the cathode, oxygen is used as an electron acceptor in which oxygen is reduced to water and can be calculated as in the following equation (B. E. Logan et al., 2006; Rene A Rozendal et al., 2007).

$$O_2 + 4H^+ + 4e^- \rightarrow 2H_2O \tag{3.18}$$

$$E_c\ = E_{C}^0\ - \frac{R}{4F} ln\left(\frac{1}{p\ _2[H^+]^4}\right) \tag{3.19}$$

The theoretical reduction potential at cathode part for H^+ and $O\ \ ^-$ concentration can be calculated as in equation 3.20 and 3.21:

$$E_{c\ \ ho}^e\ = E_{c\ \ ho\ \ \_H^+}^0 - \frac{R}{b_{O_2}F} ln\left(\frac{1}{p\ _2[C_{H^+}]^4}\right) \tag{3.20}$$

$$E_{c\ \ ho}^e\ = E_{c\ \ ho\ \ \_O\ \ }^0 - - \frac{R}{b_{O_2}F} ln\left(\frac{[C_O\ \ -]^4}{p\ \ _2}\right) \tag{3.21}$$

where $E_{c\ ho\ \_H^+}^0$ and $E_{c\ ho\ \_O}^0$ – are indicates as the standard reduction potentials for reactions 3.2 and 3.3, respectively. b_{O_2}stand for moles of electrons transferred per mole of oxygen, pO_2 (atm) is the partial pressure of oxygen and C_O – (mol L^{-1})described the concentration of hydroxyls.

Theoretically, the maximum voltage on the *MFC* can reach 1.1 V. However, when the measured value is much smaller at around 0.62 *V* (Rabaey & Verstraete, 2005) and 0.80 *V* in open circuit without current flow (Hong Liu et al., 2005). This is due to a number of energy losses in the system and in general, overpotentials of ohmic electrodes and the loss of the system can be written as follows;

$$E_{c\quad} = E_{e\quad} - (\sum \eta_{la} + |\sum \eta_{lc}| + I_{\iota\ \Omega}) \tag{3.22}$$

Where $E_{e\quad}$ is standard cell electromotive force; $\sum \eta_{la}$ and $\sum \eta_{lc}$overpotentials that occur in the anode and cathode, and $I_{\iota\ \Omega}$ is the sum of all ohmic losses.

The potential value of electromotive force ($E_{e\quad}$) for an *MFC* with acetate as an electron donor can be calculated by use of equation 3.13. From theoretical calculations at *pH* 7, the maximum voltage value obtained for the difference between the cathodic and anodic potentials is 1.1 *V*. In the *MFC* process, because the anodic potential is lower than the cathodic potential so that the reaction can occur spontaneously. The Figure 3.3 shows a schematic diagram of the electron flow spontaneously from a low potential to a higher potential for *MFC* and *MEC*.

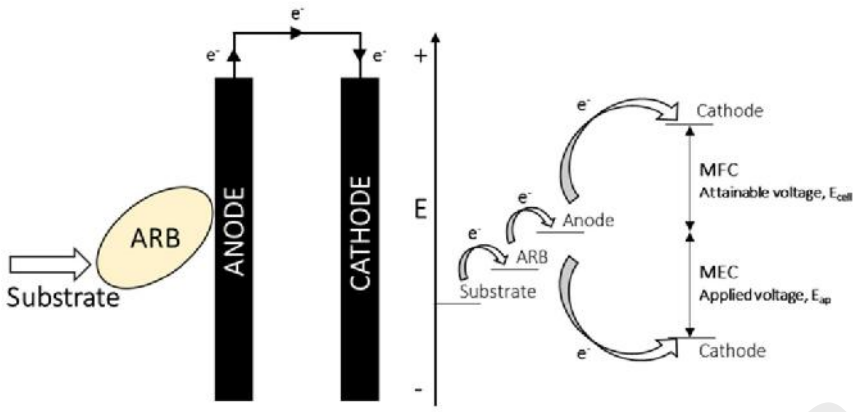

Figure 3.3: Illustrates the direction of electron flow in the electrode potential of the *MFC* and *MEC* reactor (B. E. Logan et al., 2006)

3.2.2.2 Thermodynamics of H_2 production in *MEC*

One of the advantages of *MEC* is the microorganism capable of oxidizing organic substrate to catalyze the oxidation-reduction reaction to produce hydrogen. Many organic compounds that cannot be extracted by microorganisms through photo or dark fermentation process such as acid butyric acid, propionate, butane and ethanol, but however able to be extracted through the *MEC* process. The compound is a dead end product of the fermentation process because the bacteria in the process are not able to extract energy from the reaction.

Conversion of organic compounds generally have a Gibbs free energy (ΔG_r) of reaction were positive, whereas the main requirement for generating hydrogen gas is the Gibbs free energy of reaction must be negative. Following is reaction at standard conditions (T = 25 ° C, P = 1 bar, pH=7) for the oxidation of acetate (Thauer et al., 1977):

$$C_3C^- + 4H_2O \rightarrow 2H_3^- + H^+ + 4H_2O \qquad (\Delta G_r = +104.6\, k\ /m\ ) \qquad (3.23)$$

The above reaction is fermentation reaction of acetate to the hydrogen. The main problem is the Gibbs free energy is positive so that hydrogen should not be formed spontaneously. It is required to supply a number of energy into the system to encourage the bio-electrochemical reactions, so that the above acetate oxidation reaction can evolve

releasing hydrogen ions. To overcome the thermodynamic limit the applied voltage must be greater than ($\frac{\Delta G_r}{n}$).The reaction to acetate in standard biological conditions:

$$E_e = -\frac{\Delta G_r}{n} = -\frac{1 \quad .6x1^{\ 3}}{8x9} = -0.14\ V \tag{3.24}$$

where, n is the number of electrons in the reaction, and F= 96 485 C / mol $e^{-1}$is Faraday constant.

The negative sign indicates that the Gibbs free energy of reaction (ΔG_r) is positive so that the reaction cannot take place spontaneously so that the required supply the number of voltage into the system for to continue the reaction.Equilibrium potential (E_e) value can be obtained for the theoretical to the anode (E_a) and cathode potentials (E_c) as

$$E_e = E_c - E_a \tag{3.25}$$

By using the Nernst equation so that the energy potential anode for acetate in standard conditions can be calculated as;

$$C\ {}_3C^{\ -} + 4H_2O \rightarrow 2H\ {}_3^{-} + 9H^+ + 8e^- \tag{3.26}$$

$$E_a = E_a^0 - \frac{R}{8F} ln \left(\frac{[C\ {}_3C^{\ -}]}{[H\ {}_3^{-}]^2[H^+]^9}\right) \tag{3.27}$$

Where, at the standard conditions, the value of E_a^0 = 0,187 V, R = 8,314 J / K mol , T (K) isthe absolute temperature and the anode potential = 0.279 V(B. E. Logan et al., 2006). In standard biological conditions, the anode potential equals to - 0.279 V. Thus, the cathode potential is theoretically defined as;

$$2H^+ + 2e^- \rightarrow H_2 \tag{3.28}$$

$$E_c = -\frac{R}{2F} ln \left(\frac{p_{H_2}}{[H^+]^2}\right) \tag{3.29}$$

with p_{H_2} = hydrogen partial pressure and the cathode potential is equal to -0.414 V. Thus, the equilibrium voltage obtained;

$$E_e = (-0.414\ V) - (-0.279\ V) = -0.14\ V \quad (3.30)$$

This is the same value calculated with the above equation 3.15, and theoretical energy requirement of 0.29 kWh/m^{3}H$_2$. The *pH* value is related to the value of the hydrogen evolution reaction. At *MEC* reactor, the higher the pH value of a system, then the reaction katodic increasingly negative potential. So that the required energy from the outside to push for the reaction to take place spontaneously.

Theoretically, the value of reduction potential of acetate both at *MFC* and *MEC* for anodic reaction is 0.27 vs hydrogen evolution reaction at *pH* 7. For the hydrogen evolution reaction (*HER*), equations 3.29 can also be written:

$$E_{c\ ho}^{e} = E_{c\ ho\ \_H^+}^{0} - \frac{R}{b_{H_2}F} ln\left(\frac{p_{\ 2}}{[C_{H^+}]^2}\right) \quad (3.31)$$

$$E_{c\ ho}^{e} = E_{c\ ho\ \_O}^{0} - - \frac{R}{b_{H_2}F} ln\,(p_{\ 2}[C_{O\ -}]^2) \quad (3.32)$$

where $E_{c\ ho\ \_H^+}^{0}$ and $E_{c\ ho\ \_O}^{0}$ – represents the theoretical cathode potential at standard conditions for reaction 3.8 and 3.9, b_{H_2} indicates the moles of electrons transferred per mole of hydrogen and pH_2 is the partial pressure of hydrogen.

In the MEC reactor, applied voltage (E_a) must be greater than the voltage (E_e), because of the loss of internal energy system. There are some losses that occur in the MEC, as losses caused anodic overpotential (φ_a), cathodic overpotential (φ_c) and ohmic losses ($I_{\ \Omega}$), while the potential loss caused by bacterial metabolic included in the category biocathoda and anode overpotential. The equation is given as follows:

$$E_a = E_e - (\sum \varphi_a + |\sum \varphi_c| + I_{,\Omega}) \quad (3.33)$$

In the *MEC*, the production of hydrogen gas is directly related to the amount of current in the system. When the amount of voltage added to the system then automatically the amount of current will also be increased. Hence that the possible loss of energy will also increased. The voltage applied to the system is not entirely lost because most of the energy is also stored as chemical energy in the molecules of hydrogen. In other words, the higher the applied voltage, the input electrical energy per amount of hydrogen (kWh/m^3H_2) generated will also be higher. From various experiments, it is show that the amount of voltage supplied to the reactor must be greater than 0.2 V or equal to 0.43 kWh/m^3H_2. Hence allowing all to be fully recovered hydrogen ions at the cathode.

The purpose of inserting a number of energy into the system is to encourage the formation of hydrogen ions reaction can take place in the reactor. But because of the energy loss in the system, the voltage applied to the *MEC* reactor must be greater than the required system. The equation that is the relationship between the voltage applied from the outside (E_a) with voltage from a power source (E_p) is given by:

$$E_a = E_p - I_{,e} \quad (3.34)$$

where, E_a is a source of applied voltage, $I = V/R_e$ is current-voltage resistors, and E_p is the voltage of the power source.

3.2.3 Irreversible energy potential losses in the bioelectrochemical system

In bioelectrochemical system, the loss of energy through the overpotential is associated with a voltage efficiency of the system. The potential loss of the system is the reduction of potential losses determined by the half-reaction thermodynamics. To encourage that reaction can take place in the system is required recovery more energy than is required of the system. One cause of increasing overpotential on *MFC* and *MEC* are due to the

increased rate and current density in the system. There are several other possible causes of the polarity of the overpotential system is when it uses more energy than is required of the system. Thermodynamically anode cell electrolyte should be more positive, and the cathode is more negative. When energy is supplied to the system is less than required, the cell anode will have less negative nature. And if the supply of energy to the system at the cathode is less than that required of thermodynamic calculations, then a cell cathode will have a less positive nature. In this section, further discussion about the possibility of overpotential caused by the ohmic voltage loss, overpotentials activation, overpotentials concentration, and bacterial metabolic losses will be presented.

3.2.3.1 Ohmic voltage losses

Energy potential losses due to ohmic voltage is caused by the configuration of the cell and resistivity difference of various types of conductors such as electrodes, collectors, cable, membrane, and electrolyte. Overpotential ohmic resistance occurs because of the transfer and the flow of electrons through the electrode or electrolyte ions. One way to determine the ohmic voltage losses on the membrane is to measure the voltage difference on both sides of the membrane between two electrodes (Ter Heijne et al., 2006). There are two methods that can be used to measure the resistance ohmic namely the current interrupt method (Aelterman et al., 2006) or electrochemical impedance spectroscopy (He & Angenent, 2006; Rene A Rozendal et al., 2007). The mathematic equation for calculating the ohmic voltage losses are referring to Ohm's law:

$$\eta_{ohm} = I.R_{in} \tag{3.35}$$

Where R_{in} (Ω) is the internal resistance of the cell.

3.2.3.2 Activation Energy Loss

Activation energy losses are the activation energy required for the system to transfer electrons from the electrodes anolyte. Potential differences in the value of the balance required to produce current is directly related to the activation energy system. The slow redox reaction is due to the activation overpotential, the higher the activation overpotential in the system, the exchange current density becomes lower. Conversely, if the exchange current density in the higher system, the activation overpotential becomes lower.

The linear correlation of the exchange current density in the system between the activation overpotential and logarithmic values can be shown on the Butler-Volmer equation and Tafel (Freguia et al., 2007; Popat et al., 2012). Activation Energy Loss is also associated with the type of catalyst used. The better the catalyst activity types used in the system, the activation losses will decrease. The relationship can be described by the Butler-Volmer equation for the oxygen reduction reaction (ORR) at MFC are as follows (Popat et al., 2012):

$$I = I_{0,C}\left[\left(\frac{C^*_{O_2}}{C^B_{O_2}}\right)\left(\frac{C^*_{H^+}}{C^B_{H^+}}\right)^4 e^{\left(\frac{-\alpha\ n_{O_2}F\ a\ ,c}{R}\right)} - e^{\left(\frac{(1-\alpha)b_{O_2}F\ a\ ,c}{R}\right)}\right] \quad (3.36)$$

$$I = I_{0,C}\left[\left(\frac{C^*_{O_2}}{C^B_{O_2}}\right) e^{\left(\frac{-\alpha\ n_{O_2}F\ a\ ,c}{R}\right)} - \left(\frac{C^*_{H^+}}{C^B_{H^+}}\right)^4 e^{\left(\frac{(1-\alpha)b_{O_2}F\ a\ ,c}{R}\right)}\right] \quad (3.37)$$

Where *I (A)* is indicated as the current intensity, $I_{0,C}$ stands for the exchange of current intensity, C^*(mol L^{-1}) is the concentration at the catalyst surface, C^B(mol L^{-1}) is a concentration at the bulk solution and α is described as the transfer coefficient. Both $I_{0,C}$ and α are two parameters associated with the catalyst activity.

By using the Butler-Volmer equation, the relationship of the activation energy loss with evaluation hydrogen reaction (*HER*) at the cathode to the *MEC* system can be described in equation 3.38 and 3.39 as follows:

$$I = I_{0,c}\left[\left(\frac{C_{H^+}^{*}}{C_{H^+}^{B}}\right)^{2} e^{\left(\frac{-\alpha\ H_2 F\ a\ ,c}{R}\right)} - \left(\frac{C_{H_2}^{*}}{C_{H_2}^{B}}\right) e^{\left(\frac{(1-\alpha) b_{H_2} F\ a\ ,c}{R}\right)}\right] \tag{3.38}$$

$$I = I_{0,c}\left[e^{\left(\frac{-\alpha\ H_2 F\ a\ ,c}{R}\right)} - \left(\frac{C_{OH^-}^{*}}{C_{OH^-}^{B}}\right)^{2}\left(\frac{C_{H_2}^{*}}{C_{H_2}^{B}}\right) e^{\left(\frac{(1-\alpha) b_{H_2} F\ a\ ,c}{R}\right)}\right] \tag{3.39}$$

In the Butler-Volmer equation above is to describe the electron transfer kinetics on the cathode. While at the anode, in addition to the electron transfer kinetics is also the process of enzyme kinetics. Respiration anode bacteria (*ARB*) serve as a catalyst and can reduce losses activation of the oxidation reaction. At the anode involves two electron transfer process as well as the enzyme kinetics and electron transfer kinetics which describe the process of electron transfer from microorganisms to the anode. On enzyme kinetics is the conversion of organic compounds into carbon dioxide, protons and electrons. Nernst-Monod model below is illustrates the current intensity of kinetics bioanode as a function of the concentration of the substrate and the potential of the anode. In the Nernst-Monod model of this, the anode is assumed as a final electron acceptor (Torres et al., 2008).

$$I = I_m \left(\frac{1}{1+e^{-\frac{F}{R}(E_a \quad -E_K\ )}}\right)\left(\frac{C_s}{K_s+C_s}\right) \tag{3.40}$$

where I_m (A) is described as the maximum current intensity determined by the enzymatic reaction, E_K (V) is demonstrated anode potential, K_s (mol L^{-1}) is an abbreviation of the substrate concentration at the which the current intensity is half the I_m and C_s is the substrate concentration (mol L^{-1}).

3.2.3.3 Concentration Energy losses

Concentration losses (η_{c}) is a phenomenon that involves the decomposition of the charge-carrier and occurs due to limited diffusion of the reactants or products between the bulk solution and the electrode surface. Because the rate of the chemical reaction is so fast that affects the reaction thermodynamics and physical formation of bubbles on the surface of the electrode. Concentration loss at the cathode and anode can be calculated using the following equation:

$$\eta_{c} = E_{c}^{e} - E_{c}^{*} \quad (3.41)$$

$$\eta_{c} = E_{a}^{e} - E_{a}^{*} \quad (3.42)$$

where, E_{c}^{e} and E_{a}^{e} is the bulk solution concentration at cathode and anode, while E_{c}^{*} and E_{a}^{*} each is the local electrode concentrations.

At the *MFC*, in the cathode overpotential concentration related to oxygen, protons and hydroxyl. Overpotentials associated with oxygen can be ignored so that equation 3.41 may be combined with equations 3.20 and 3.21, so the following equation are obtained:

$$\eta_{c} = \frac{R}{b_{O_2}F} ln \left(\frac{C_{H^+}^{B}}{C_{H^+}^{*}}\right)^{4} \quad (3.43)$$

$$\eta_{c} = \frac{R}{b_{O_2}F} ln \left(\frac{C_{O^-}^{B}}{C_{O^-}^{*}}\right)^{4} \quad (3.44)$$

Similarly in the MEC, overpotential associated with the concentration of hydrogen can be ignored, so that by combining the equation 3.41 with equations 3.31 and 3.32, respectively, so the equations below can be written as such:

$$\eta_{c} = \frac{R}{b_{H_2}F} ln \left(\frac{C_{H^+}^{B}}{C_{H^+}^{*}}\right)^{2} \quad (3.45)$$

$$\eta_{c,c} = \frac{R}{b_{H_2}F} ln \left(\frac{C_O^B}{C_O^*}\right)^2 \quad (3.46)$$

In the case of proton transport limitations, the overpotentials concentration related to anodic reaction reactants (acetate), bicarbonate and products (protons). Due to transportation limitations proton, then the *pH* value in the biofilm decreased. This will have an impact on reaction thermodynamics and kinetics bioanodes (biofilm anode).

3.2.3.4 Bacterial metabolic losses

Bacterial metabolic losses are biological activity and biocatalyzing microorganisms which are directly related to the surface area and the intrinsic electron transfer rate and the rate of enzyme or redox system. The biological activity of the biocatalyzing microorganisms is also influenced by environmental conditions such as temperature, the composition in the reactor, the electrode potential, and biological competition of microbes (Cheng & Logan, 2007a; Clauwaert et al., 2007; Hong Liu et al., 2005; Rabaey & Verstraete, 2005). In bioelectrochemical system, especially on the part of the anode, the energy metabolism of the bacteria resulting from the difference of the redox potential and transfer electron substrat to the final electron acceptor (B. E. Logan, 2009). To improve the performance of MFC and MEC reactor, it would require the selection of the anodic and cathodic microbial community's to optimize the functionality of microbial community (Boon et al., 2008).

3.3 Microbial electrolysis cell (*MEC*) model development

The biohydrogen production process in an *MEC* is a nonlinear and complex process. One of the ways to overcome the problems posed by the *MEC* is to build a mathematical model used for process design, optimization and developing control strategies. This model makes several assumptions, such as uniform distribution of the carbon sources from wastewater in the anode compartment and neglecting of the acetate gradient in the

biofilm (R. Pinto et al., 2011). Because the porosity and circulation rate of the fluid is very high, it is also assumed that the microorganisms in the anodic compartment are distributed homogeneously within each layer. Biofilm formation and retention of the *MEC* fed-batch reactor in each biofilm layer is based on a two-phase biofilm growth model with the assumption that *pH* and temperature are fully controlled and maintained at a constant value. It is also assumed that there is an absence of biomass growth in the anodic liquid and perfect mixing in the anode compartment occurs.

The main objective of the model is to simulate hydrogen production using organic waste from wastewater in a simple and easily identifiable dynamic model. The model equations presented here are based on multi-population *MEC* models, and the following modifications were made to modify the model proposed by (R. Pinto et al., 2011) for our case study.

The model here is modified for a fed-batch reactor; where the Pinto model assumed a continuous system but in this proposed model, the biofilm formation and retention consists of a two-phase model with biofilm growth incorporating, anodic biofilms (Layer 1) and a cathode biofilm population (Layer 2). The Pinto model uses three phases, an outer biofilm layer (Layer 1), an inner biofilm (Layer 2) and cathode biofilms (Layer 3), but using the two-phase model will be more practical and easier to apply in modeling and controlling the real plant.

This proposed model involves metabolic activities of acetoclastic methanogenic, anodophilic and hydrogenotrophic microorganisms without involving the fermentation used in the Pinto model. We also assume in our modeling steps that it is very difficult to observe two different processes in the same reactor, for instance fermentation and bio-electrochemical process simultaneously (Picioreanu et al., 2010). The model is applied to a real pilot plant-scale reactor with a volume of 10 liters. In comparison, Pinto applied

the model to a lab-scale reactor with a volume of only 50 ml. This modification aims to make the model closer to a real plant for such a system and more practical in nature.

3.3.1 Reactions at electrodes

The mathematical models presents here simulate the competition of three microbial populations in the *MEC*. The model considers competition between anodophilic and methanogenic microorganisms for the carbon source. The reactions at the anode and cathode are described as follows:

At anode:

$$C_2H_4O_2 + H_2O + 4M_o \rightarrow 4M_r + C_2 \quad (3.47)$$

$$4M_r \rightarrow 4M_o + 8e^- + 8H^+ \quad (3.48)$$

$$C_2 + HC_3^- + 8e^- + 8H^+ \rightarrow C_3C^- + 3H_2O \quad (3.49)$$

Cathode:

$$C_2H_4O_2 \rightarrow C_4 + C_2 \quad (3.50)$$

$$C_2 + 4H_2 \rightarrow C_4 + 2H_2O \quad (3.51)$$

$$H_2O + e^- \rightarrow O^- + H_2 \quad (3.52)$$

The overall reaction of acetate acid at the anode and cathode is described as

$$C_3C^- + 3H_2O \rightarrow HC_3^- + 4H_2 \quad (3.53)$$

Acetate is represented in the substrate concentration, and M_{ox} and M_{red} are the reduced and oxidized forms of the intracellular mediator (R. Pinto et al., 2011). The proposed simplified diagram for the *MEC* reactor system is shown in Figure 3.4. The *DAQ* system is also introduced in the setup for possible implementation of the control system in real time.

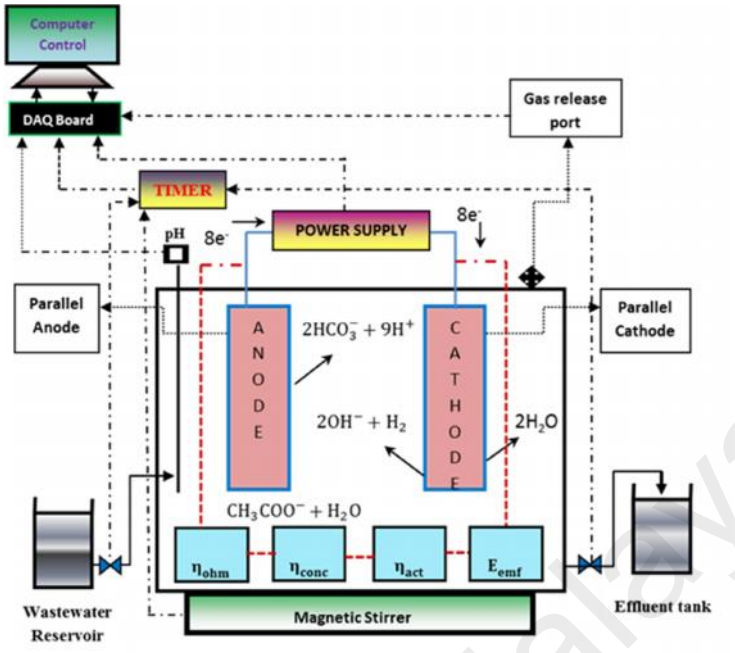

Figure 3.4: The simplified diagram for microbial electrolysis cells fed-batch reactor

3.3.2 Mass balances and stoichiometric equations for the *MEC* system

The dynamic mass balance equations for the components *S*, X_a, X_m, X_h and M_{ox} in the reactor system are given below as follows:

$$\frac{d}{d} = -q_m \quad ,a \frac{S}{K_S + S} \frac{M_o}{K_M + M_o} x_a - q_m \quad ,m \frac{S}{K_{S,m} + S} \tag{3.54}$$

$$\frac{dx_a}{d} = \mu_m \quad ,a \frac{S}{K_{S,a} + S} \frac{M_o}{K_M + M_o} x_a - K_{d,a} x_a - \alpha_1 x_a \tag{3.55}$$

$$\frac{d \ m}{d} = \mu_m \quad ,m \frac{S}{K_{S,m} + S} - K_{d,m} x_m - \alpha_1 x_m \tag{3.56}$$

$$\frac{d \ h}{d} = \mu_m \quad ,h \frac{H_2}{K_h + H_2} - K_{d,h} x_h - \alpha_2 x_h \tag{3.57}$$

$$\frac{d \ o}{d} = \frac{\gamma}{V_r x_a} \frac{I_M}{m} - Y_M q_m \quad ,a \frac{S}{K_{A,a} + S} \frac{M_o}{K_M + M_o} \tag{3.58}$$

$$Q_{H_2} = Y_{H_2} \left(\frac{I_M}{m} \frac{R}{P} \right) - Y_h \mu_h x_h V_r \tag{3.59}$$

Where S is the substrate concentration; x_a, x_m, and x_h are the concentration of the anodophilic, acetoclastic, and hydrogenotrophic microorganisms, respectively; M_o is the oxidized mediator fraction per electricigenic microorganism; and Q_{H_2} is the hydrogen production rate (mL/day).

3.3.3 Intracellular material balancesfor the *MFC* and *MEC*

The rate oxidized of formation of intracellular mediators in the *MFC* and *MEC* reactor can be described by using Faraday's law. The reduced form and a constant pool of the mediator per anodophilic or electricigenic microorganism in the system are assumed. The following balance equation involves every electricigenic or anodophilic microorganism and the value of M_T are assumed to be constant:

$$M_T = M_r + M_o \tag{3.60}$$

$$d_o/d = -Y_M q_e + \frac{\gamma}{V_e}\frac{I_M}{m} \tag{3.61}$$

Where M_o is the oxidized mediator fraction per anodophilic microorganism and M_r is the reduced mediator fraction per each anodophilic microorganism. M_T is to describe the total mediator fraction per microorganism in the reactor. *Y* is the mediator yield; *γ* is the mediator molar mass and *m* is the number of electrons transferred per mol of mediator.

3.3.4 Kinetic equationsfor the MEC

Especially for anodophilic, acetoclastic metanogen and fermentative microorganisms, the growth rate was assumed only limited by the concentration of organic substrates, while for electricigenic bacteria, the growth rate is limited by the oxidised form of the mediator concentrations of substrate. By using the multiplication kinetics Monod equation, the Kinetic equations can be described as follows:

$$\mu_f = \mu_{m,f}\frac{S}{K_{S,f}+S} \tag{3.62}$$

$$\mu_e = \mu_{m,e}\frac{A}{K_{A,e}+A}\frac{M_o}{K_M+M_o} \tag{3.63}$$

$$\mu_m = \mu_{m,m}\frac{A}{K_{A,m}+A} \tag{3.64}$$

$$\mu_h = \mu_{m,h}\frac{H_2}{K_h+H_2} \tag{3.65}$$

$$q_f = q_{m\ ,f}\frac{S}{K_{S,f}+S} \tag{3.66}$$

$$q_e = q_{m\ ,e}\frac{A}{K_{A,e}+A}\frac{M_O}{K_M+M_O} \tag{3.67}$$

$$q_m = q_{m\ ,m}\frac{A}{K_{A,m}+A} \tag{3.68}$$

3.3.5 Hydrogenotrophic methanogens

The hydrogenotrophic methanogens grow around the biofilm layer. The hydrogenotrophic consume hydrogen produced in the cathode part, so that the growth is very dependent on the H_2 concentration in water. At *MEC* reactors, gas transfer to liquid is ignored, so it is assumed the concentration of hydrogen dissolved is saturated. While the *MFC*, because no hydrogen was produced and the growth rate is equal to zero so that the concentration of dissolved hydrogen is assumed to be equal to zero. This dependence can be described by the following equation:

$$\mu_h = \mu_{m\ ,h}\frac{H_2}{K_h+H_2}, where \begin{cases} H_2 = H_2^* & if\ Q_{H_2} > 0 \\ H_2 = 0 & if\ Q_{H_2} = 0 \end{cases} \tag{3.69}$$

$$\mu_h \begin{cases} \mu_{m\ ,h} & if\ I_M > 0 \\ 0 & if\ I_M = 0 \end{cases} \tag{3.70}$$

Where H_2 is the hydrogen saturation concentration in water, K is the half-saturation (Monod) constant and $\mu_{m\ ,h}$ is the maximum growth rate of the hydrogenotrophic microorganisms.

3.3.6 Electrochemical Balances

The potential losses of internal resistance can give additional information about the performance of an *MEC*, especially when comparing different systems (Y. Fan et al., 2008). Since the voltage needed for hydrogen production is constant, the current density depends on the total internal resistance of the system, which in itself is a function of the

current density. The total internal resistance is a sum of the partial resistances of the system (Bard & Faulkner, 2001).

Figure 3.5 gives an overview of partial internal resistances in an *MEC*, which can be represented by a series of resistances in an equivalent circuit. These partial resistances consist of: (i) counter-electromotive force (E_C), (ii) activation loss (η_a), concentration loss (η_c), ohmic loss (η_{ohm}). Each of these polarizations has a different magnitude for different current density degrees. At low current densities, activation losses are dominant due to reaction energy barriers at the electrode-electrolyte interface, which need to be overcome to start the reaction. At high current densities, reactant and product diffusion limitations lead to high concentration losses (Noren & Hoffman, 2005).

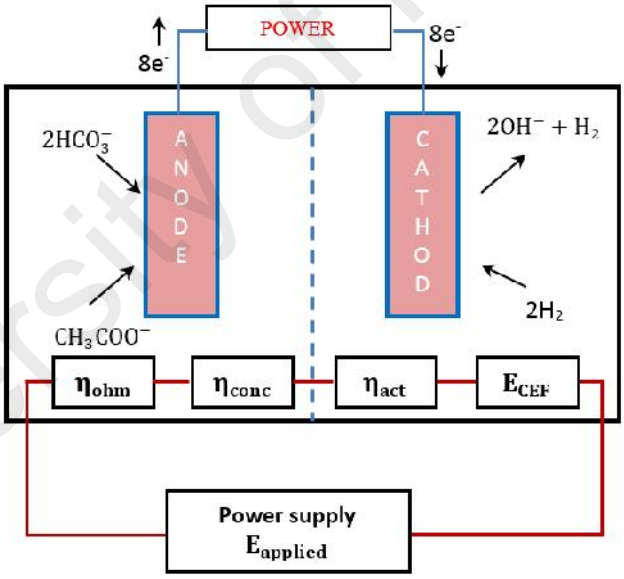

Figure 3.5: Overview of the potential losses of Microbial Electrolysis Cells in batch reactor

Finally, ohmic losses increase linearly with current due to electron and ion conduction at the electrodes, electrolytes, and contact resistance across each material's interface, and interconnections to electrodes. Note that the output voltage of a fuel cell is directly proportional to the cell current, following Ohm's law:

$$E_o \quad = R_e \; I_c \tag{3.71}$$

MEC voltage can be calculated using theoretical values of the electrode potentials by subtracting the ohmic, activation, and concentration losses. Therefore the following electrochemical balance can be written as (Fuel Cell Handbook, 2005):

$$-E_a \quad = E_C \quad - \eta_{ohm} - \eta_{c} \quad - \eta_a \tag{3.72}$$

Here, concentration losses at the cathode will be neglected due to the small size of H_2 molecules resulting in a large diffusion coefficient of H_2 in a gas diffusion electrode used as a cathode. The concentration losses at the anode can be calculated using the Nernst equation (Pinto et al., 2010).

$$\eta_{c} \quad _{,A} = \frac{R}{m} ln \left(\frac{M_T}{M_r}\right) \tag{3.73}$$

The cathodic activation losses can be calculated by the Butler-Volmer equation. Assuming that the reduction and oxidation transfer coefficients that express the activation barrier symmetry are identical, the Butler-Volmer equation can be approximated as suggested by (Noren & Hoffman, 2005):

$$\eta_{a} \quad _{,C} = \frac{R}{\beta} S \quad h^{-1}\left(\frac{I_M}{A_S \quad _{,A} i_0}\right) \tag{3.74}$$

Therefore, the *MEC* current can be calculated by combining eqs. 21-23:

$$I_M \quad = \frac{E_C \quad + E_a \quad - \frac{R}{m} ln \left(\frac{M_T}{M_r}\right) - \eta_{a} \quad _{,C}(I_M \quad)}{R_{in}} \frac{M_r}{\varepsilon + M_r} \tag{3.75}$$

where ε is constant [mg-M mg-x^{-1}]; ε ~0, eq.(24) can be written as:

$$I_M \quad = \frac{E_C \quad + E_a \quad - \frac{R}{m} ln \left(\frac{M_T}{M_r}\right) - \eta_{a} \quad _{,C}(I_M \quad)}{R_{in}} \tag{3.76}$$

To improve model accuracy during the start-up period the R_{ii} values were linked to the concentration of electricigenic microorganisms (Pinto et al., 2010):

$$R_{ii} = R_M + (R_M - R_M)e^{-K_R x_a} \quad (3.77)$$

Which is determines the curve steepness [L mg-x^{-1}].

3.4 Parameter estimation and model revision

A microbial electrolysis cell (*MEC*) is a modified microbial fuel cell that can produce hydrogen gas at the cathode from the current generated by bacteria during the breakdown of organic matter (B. E. Logan et al., 2008). Biohydrogen production process through microbial electrolysis cell is a complex and nonlinear processes. One of the solutions to overcome the problems posed by the *MEC*s is to build a mathematical model that can be used for process design, optimization and to develop process control strategies.

This study presents a model for *MEC* in the batch reactor based on the two-population *MFC* model developed by (Pinto et al., 2010), that will be used for analysis and tested with open-loop identification. *MEC* model presented here describes the competition between the three populations of microbes that is anodophilic, hydrogenotrophic and acetoclastic microorganism. An *MEC* batch reactor operated on wastewater contains a complex microbial community consisting of fermentative, hydrogenotrophic methanogenic, acetoclastic methanogenic and anodophilic microorganisms, it is similar to anaerobic digestion (Arcand et al., 1994; B. E. Logan & Regan, 2006; Moletta et al., 1986; Quarmby & Forster, 1995). Many studies have been reported that anodophilic consume more organic matter at low substrate concentrations due to low substrate half-saturation constant (Torres et al., 2008), whereas methanogens perform well at high substrate concentrations.

Equation model presented here is called unified models describing microbial activity in the anodic compartment of a microbial fuel cell and a microbial electrolysis cell in the cathodic reactions leading to hydrogen production. The parameters for system characteristics, kinetic and stoichiometric parameters of the model used for the simulation is presented in Table 3.1.

Table 3.1: System characteristics, kinetic and stoichiometric parameters of the model used for the simulation in *MEC*

Parameter	Value	Nomenclature
$\mu_{m\ ,m}$	0.3	The maximum growth rate of the acetoclastic methanogenic microorganism [d^{-1}]
$\mu_{m\ ,a}$	1.97	The maximum growth rate of the anodophilic microorganism [d^{-1}]
$\mu_{m\ ,h}$	0.5	The maximum growth rate of the hydrogenotrophic microorganism [d^{-1}]
$q_{m\ ,a}$	13.14	The maximum reaction rate of the anodophilic microorganism [mg-A mg-x^{-1} d^{-1}]
$q_{m\ ,m}$	14.12	The maximum reaction rate of the acetoclastic methanogenic microorganism [mg-A mg-x^{-1} d^{-1}]
$K_{S,a}$	20	The half-rate (Monod) constant of the anodophilic microorganism [mg-AL^{-1}]
$K_{S,m}$	80	The half-rate (Monod) constant of the acetoclastic methanogenic microorganism [mg-AL^{-1}]
K_M	0.01	Mediator half-rate constant [mg-M L^{-1}]
H_2	1	H_2 saturation in water [mg-A L^{-1}]
K_h	0.001	Half-rate constant [mg L^{-1}]
Y_{H_2}	0.9	The dimensionless cathode efficiency [dimensionless]
Y_h	0.05	The yield rate for hydrogen consuming methanogenic microorganisms [mL-H_2 mg-x^{-1} d^{-1}]
R	8.314	The ideal gas constant [mL-H_2atm K^{-1} mol-H_2^{-1}]
T	298.15	The MEC temperature [K]
m	2	The number of electrons transferred per mol of H_2 [mol-e^- mol-H_2^{-1}]
F	96.485	The Faraday constant [A d mol-e^{-1}]
P	1	The anode compartment pressure [atm]
M_T	800	Mediator fraction [mg-M mg-x^{-1}]
β	0.5	The reduction or oxidation transfer coefficient [dimensionless]
$A_{s\ ,A}$	0.01	The anode surface area[m^2]
i_0	0.005	The exchange current density in reference conditions[A m^{2-1}]
R_M	20	The lowest observed internal resistance[Ω]
R_M	2000	The highest observed internal resistance[Ω]
K_R	0.024	The constant, which determines the curve steepness[L mg-x^{-1}]
E_C	-0.35	The counter-electromotive force for the MEC [V]
E_a	10	The electrode potentials [V]
$X_{m\ ,a}$	512.5	Anodophilic biofilm space limitation [mg-x L^{-1}]
$X_{m\ ,m}$	$1680/Y_h$	Methanogenic biofilm space limitation [mg-x L^{-1}]
$K_{d,a}$	0.04	The microbial decay rates of the anodophilic microorganism [d^{-1}]

$K_{d,m}$	0.01	The microbial decay rates of the acetoclastic methanogenic microorganism [d^{-1}]
$K_{d,h}$	0.01	The microbial decay rates of the hydrogenotrophic microorganism [d^{-1}]
Y_M	34.85	The oxidized mediator yield [mg-M mg-A^{-1}]
γ	663400	The mediator molar mass [mg-M mol_{med}^{-1}]
V	10	The anodic compartment volume [L]
F_{in}	2.5	The incoming flow rate [L d^{-1}]
S_0	2000	The initial conditions of organic substrate concentration in the influent and in the anodic compartment.
X_{h0}	10	The initial conditions of hydrogenotrophic methanogenic microorganisms
X_{a0}	1	The initial conditions of anodophilic microorganisms
X_{m0}	50	The initial conditions of acetoclastic methanogenic microorganisms

3.5 The behaviour of Microbial Electrolysis cells

In developing this model made several assumptions earlier that carbon sources or wastewater is distributed both in the anode compartment and acetate gradient in biofilm is neglected. Due to the porosity of the fluid and the circulation rate is very high that it is assumed that the microorganisms in the anodic compartment distributed homogeneously within each layer (Rauch et al., 1999). Biofilm formation and retention of *MEC* batch reactor in each biofilm layer is based on a two-phase biofilm growth model. Layer1 represents the anode biofilm, containing anodophilic and acetoclastic methanogens microorganisms, while layer 2 is occupied by the cathode biofilm hydrogenotrophic methanogenic microorganisms.The transformation of organic substrates by glucose to acetate takes place in anode biofilm layer 1. There after the acetate is consumed by acetoclastic methanogenic microorganism's anodophilic and produce methane and carbon dioxide formation. M_r and M_o are the reduced due to oxidation by intracellular mediator anodophilic microorganisms. Layer 2 assumed the cathode biofilm populated by hydrogenotrophic methanogenic microorganisms. Hydrogen consumed by microbes in this layer which convert hydrogen produced at the cathode into methane and resulted in the formation of biofilm layer adjacent to the cathode. Finally, *pH* and temperature assumptions are considered fully controlled and maintained at a constant value. The absence biomass growth in anodic liquid and mixing in the anode compartment is ideal.

In this works, the model which was previously developed by (R. Pinto et al., 2011) was used to study the sensitivity of stoichiometric and kinetic parameters on biohydrogen production via the microbial electrolysis cells (*MEC*) in batch operation. Detailed experimental data, characterization, operation and design used in this study can be found in (R. P. Pinto et al., 2011).In all simulations studies, the total of time was set at 9 days. Simulation results for each of the cases are given below.

Figure 3.6 shows the behaviour of substrate concentration (S) and hydrogenotrophic microorganism (X_h) with time. It is clear from the figure that the concentration of substrate (S), decreased sharply at the early of period until to 2 days but increased slowly during 2 to 3.5 days and then decreased slowly till the end of the period.

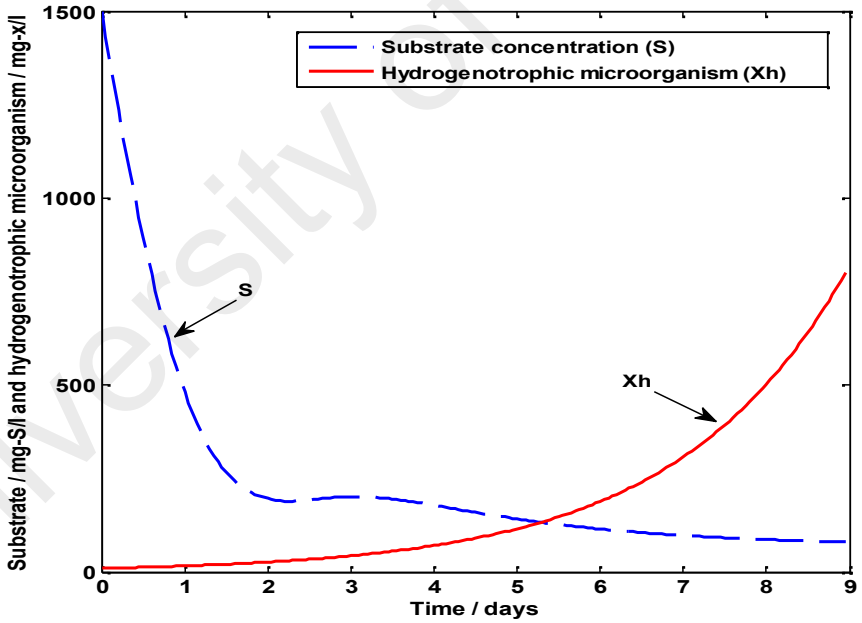

Figure 3.6: The behaviour of substrate concentration (S)and hydrogenotrophic microorganism (x_h)

Initial substrate concentration was 1500 mg/l and then decreased to 80 mg/l. This is due to the carbon source was consumed by the hydrogenotrophic microorganism. Figure 3.6 shows that the occurrence of metabolic activity and increased growth hydrogenophilic

microorganism is of 0 mg/l to 1600 mg/l for 10 days. The increasing consumption of organic materials by microorganism hydrogenophilic is as correlation with the increase in the production of hydrogen gas in the MEC batch reactor.

Figure 3.7 shows the behaviour of anodophilic (x_a) and acetoclastic (x_m) microorganism. It is clear from the figure that the concentration anodophilic (x_a), increased sharply at the beginning of the period up to 2 days and then declined sharply until the 4th day and then continued to decrease slowly until the end of the period.

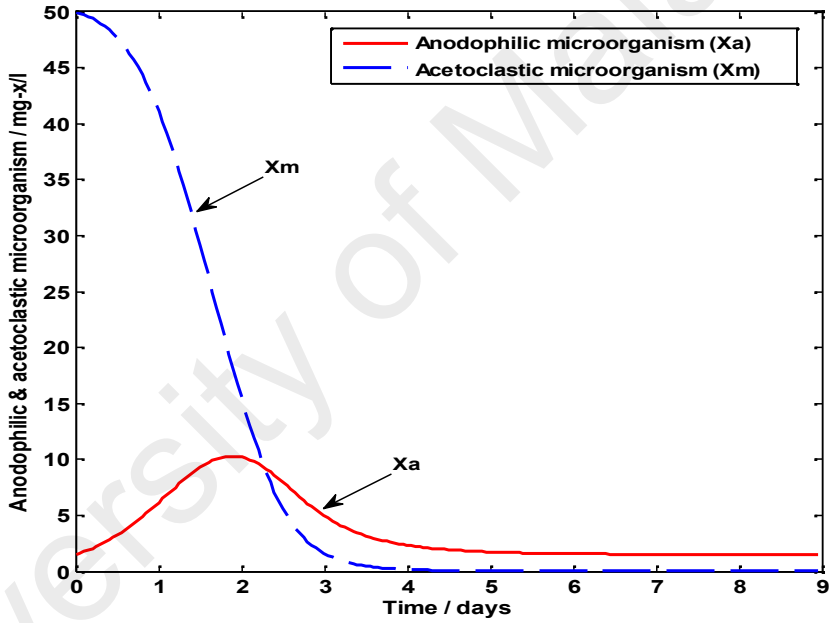

Figure 3.7: The behaviour of anodophilic $(x_a)$and acetoclastic (x_m) microorganism

Initial condition of anodophilic concentration is 1 mg-x/l and then increased to 10 mg-x/l. From Figure 3.6 and Figure 3.7, strong competition can be observed between hydrogenotrophic methanogens and anodophilic microorganisms in using the available carbon source. From both figures it can be seen that hydrogenotrophic methanogens can consume microorganisms substrate concentration better and faster compared with the concentration of substrate consumed by anodophilic microorganisms.

From figure 3.7, it can be seen that the initial condition of acetoclastic methanogenic concentration is 50 mg-x/l and fell sharply to 0 mg-x/l. In this process, acetoclastic methanogenic microorganisms (x_m) consume most of the carbon source and then produce methane and carbon dioxide, the reaction occurs at the anode biofilms Layer 1. From figure 3.7, it is also are clear that the growth of acetoclastic methanogenic microorganisms (Xm) is 0, this means that the rate of methane formation can be reduced in layer 1 so that the rate of formation of H_2 at cathode layer 2 can be increased.

From Figure 3.8, it can be seen that there is close relationship between I_{MEC} current (I_M) and hydrogen production rate (Q_{H2}). The hydrogen production rate (Q_{H2}) increased sharply with time due to the reduction of substrate and then decreases linearly with time as shown in Figure 3.8. The effect of methane production in this simulation was not observed because acetoclastic methanogenic microorganisms were unable to compete with the anodophilic microorganisms as shown in Figure 3.7. To maintain the level of hydrogen production in the cathode compartment requiressufficiencarbon source and supply current to the reactor. Figure 3.8 shows the effect of influent substrate concentration and applied voltage to the *MEC* on the hydrogen production. The hydrogen production rate increased sharply and reached a peak value of 1.52 mL/sec on the 2nd day, then decreased linearly until was steady at a value of 0.84 mL/sec on the 10th day. The I_{MEC} current increased sharply reaching a peak value of 0.13A on the 2nd day, and then gradually decreased slowly to remain steady at a value of 0.10A. It is clear from the figure that the hydrogen production rate (Q_{H2})in the MEC operated mainly depends on influent substrate concentration and supply current with continuously applied voltage to *MEC* reactor. Volumetric of hydrogen production rate also can be improved significantly by reducing the electrode spacing and increase the ratio of electrode surface area or cell volume.

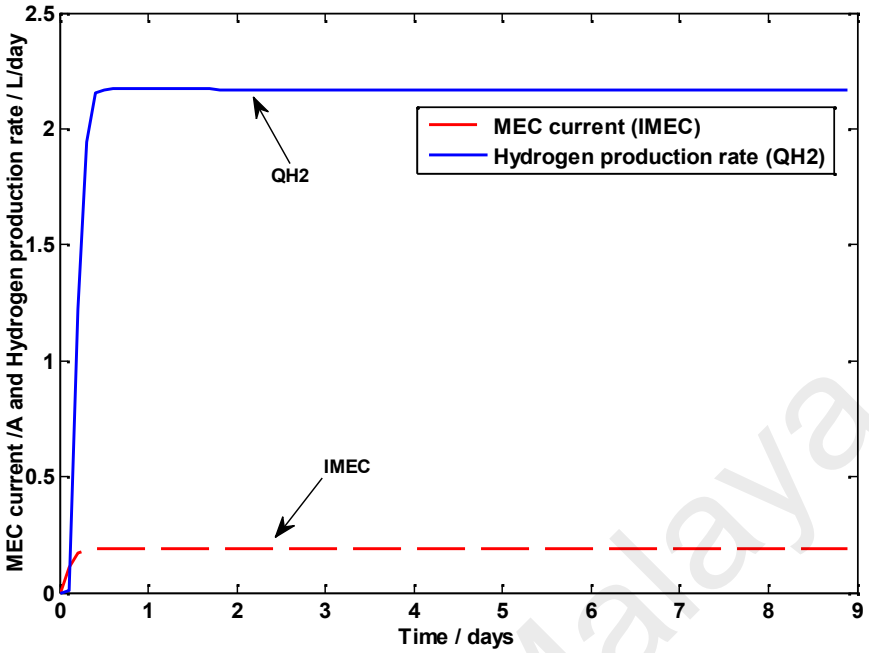

Figure 3.8: The behaviour of MEC current (I_M) and hydrogen production rate(Q_H)

In this investigation, the model which was previously developed by (Pinto et al., 2010) on MEC is used to study the sensitivity of the model predictions to changes in the values of the various kinetic parameters included in the model. The effect of varying the anodic compartment volume *(L)*, varying the electrode potentials (E_a), effect of varying changes of initial concentration on the *MEC* and the kinetic will be investigated. Changes of the various parameters to study the sensitivity of the system performance are described in the following subsections.

3.6 Effect of varying changes of initial concentration on the *MEC*

3.6.1 Effect of initial concentration (X_a)

Figure 3.9 and Figure 3.10 illustrate the simulation results for the effect of anodophilic microorganisms initial concentration (X_a) varied at 0.1 mg/l, 0.5 mg/l, 1.0 mg/l and 1.5 mg/l on the I_{MEC} current and the hydrogen production rate profiles. The investigation was carried out for an anodophilic microorganisms initial concentration (X_a) range of $0.1 \leq$

$X_a \leq 2$, the balance (ie the difference from the base value X_a which is 1.0) was either added to X_a .

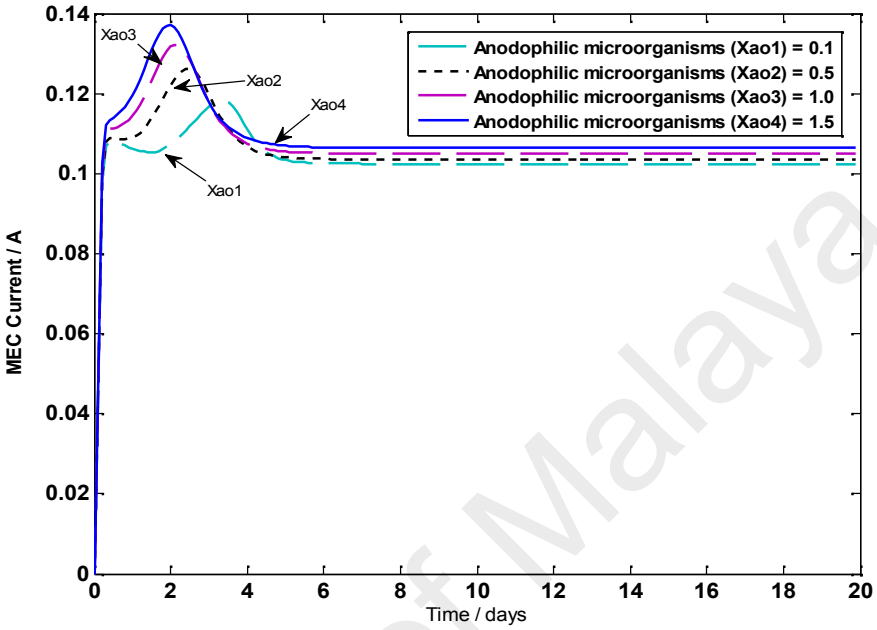

Figure 3.9: Effect of anodophilic microorganisms initial concentration (X_a) on the I_{MEC} current

In this narrow range of investigation, the system performance of I_{MEC} current and the hydrogen production rate were affected significantly by variations in the anodophilic microorganisms initial concentration (X_a). As the initial concentration of X_a is increased, the I_{MEC} and hydrogen production rate also increased which was manifested as higher of substrate concentrations during at the early of period until to 2 days.

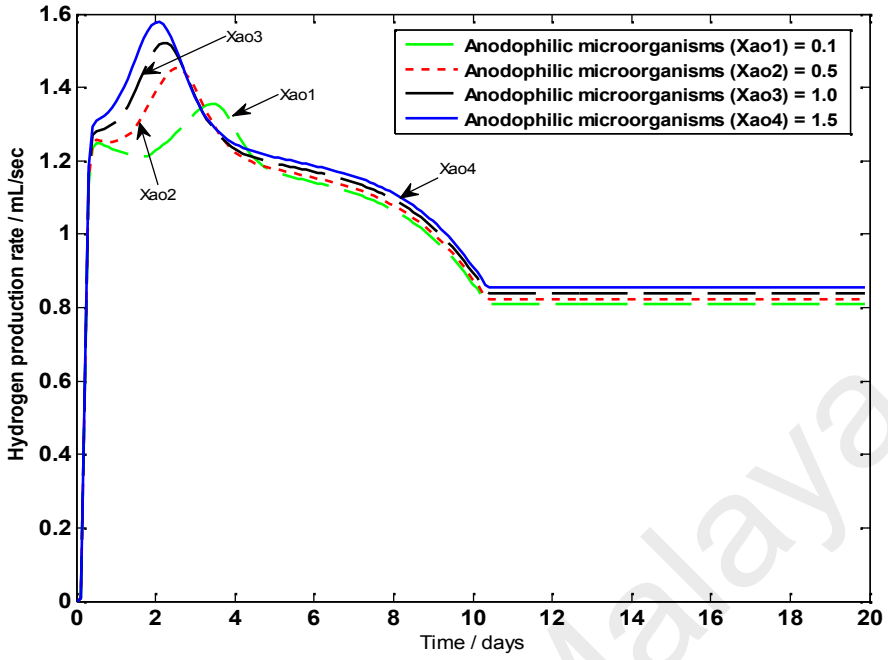

Figure 3.10: Effect of anodophilic microorganisms initial concentration (X_a) on the hydrogen production rate

However it is evident from figure 3.9 and 3.10 that performance of the I_{MEC} current and the hydrogen production rate were greatly affected by effect of varying changes of initial concentration of anodophilic microorganisms.

3.6.2 Effect of initial concentration (X_h)

The result for the effect of varying the hydrogenotrophic microorganism's initial concentration (X_{ho}) on the performance of MEC batch reactor is given in Figure 3.11 and Figure 3.12 The investigation was carried out for hydrogenotrophic microorganism's initial concentration (X_{ho}) range of $1 \leq X_a \leq 15$mg/l. Hydrogenotrophic methanogens are very sensitive to pH, oxygen, heat, and chemicals(Li & Fang, 2007). Increasing pH in a *MEC* batch reactor will impact to bioactivityhydrogenotrophic methanogens significantly. So that the hydrogen formed in the cathode will be consumed by hydrogenotrophic methanogens and then converted into methane gas and carbondioxide. This will have a negative impact on the rate of hydrogen production. From the figures

shown, the higher value of initial concentration of hydrogenotrophic microorganism led to a higher hydrogen production rate.

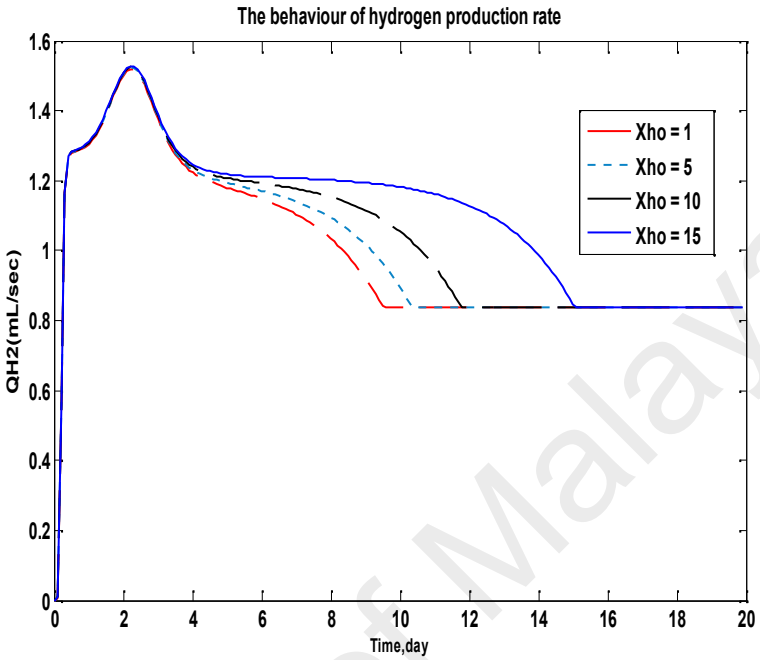

Figure 3.11: Effect of hydrogenotrophicmicroorganisms initial concentration (X_h) on the hydrogen production rate

Figure 3.12 illustrates the simulation results for the effect of hydrogenotrophic microorganisms initial concentration (X_{ho}) varied at 1 mg/l, 5 mg/l, 10 mg/l and 15 mg/l on the I_{MEC} current profiles. However it can see from figure 3.12 that the changes in the initial concentration of hydrogenotrophic microorganisms (X_{ho}) did not provide significant effect on the performance of I_{MEC}.

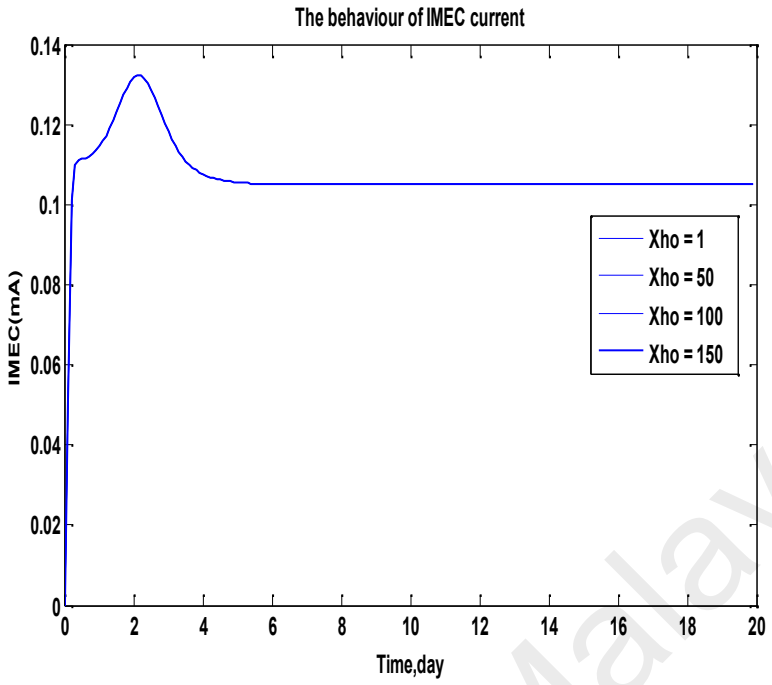

Figure 3.12: Effect of hydrogenotrophicmicroorganisms initial concentration (X_{ho}) on the I_{MEC} current

3.7 Effect of varying changes of *MEC* volume (*L*) and the electrode potentials (E_a) on MEC performances

3.7.1 Effect of anodic compartment volume (*L*)

Anodic compartment volume (*L*) is an important parameter in *MEC* bioreactors. Since hydrogen production rate correlates with the rate of anodic compartment volume (*L*). Figure 3.13 shows that the hydrogen production rate increased with increasing volume of bioreactor and reached a maximum at an anodic compartment volume of 24 *L*. As mentioned previously, by increasing the volume of the reactor the hydrogen production rate also increased, this is due to the increase of organic compounds in the system available so that microbes can convert the organic compounds into hydrogen gas.

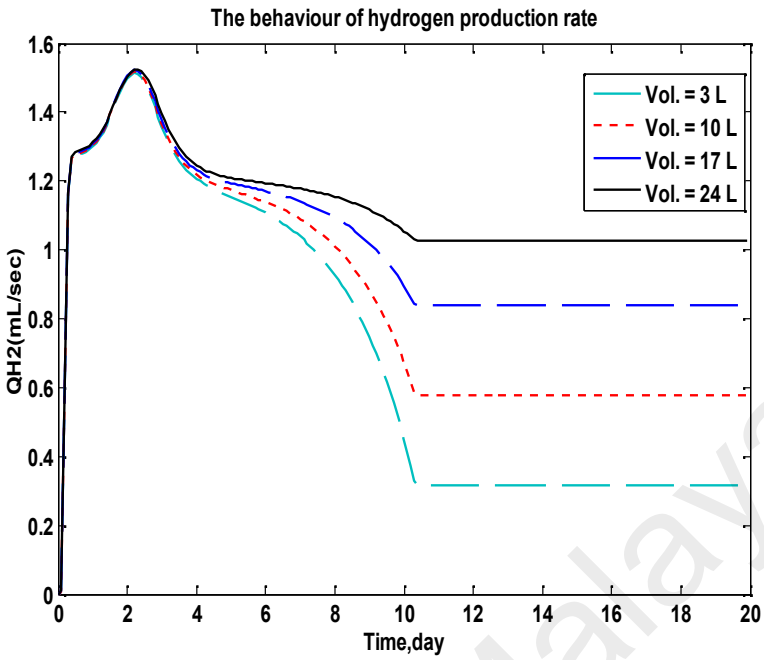

Figure 3.13: Effect of varying the anodic compartment volume *(L)* on the hydrogen production rate

The Figure 3.14 shows the effect of various anode compartment volume (*L*) on the current MEC profiles varied at 3 *L*, 10 L, 17 *L* and 24 *L*. As shown in the figure, changes in the anodic compartment volume (*L*) in the reactor do not provide significant effect on the performance of *MEC* current.

From the literature review done in this study, it does not explain in depth the existence of a direct relationship between the volume of the reactor to the hydrogen production rate and the concentration of organic in the *MEC* reactor is an important parameter in the study of hydrogen bioreactor. To optimize the process in order to obtain the maximum hydrogen production so that the volume or the organic loading rate to a certain level is very important to note.

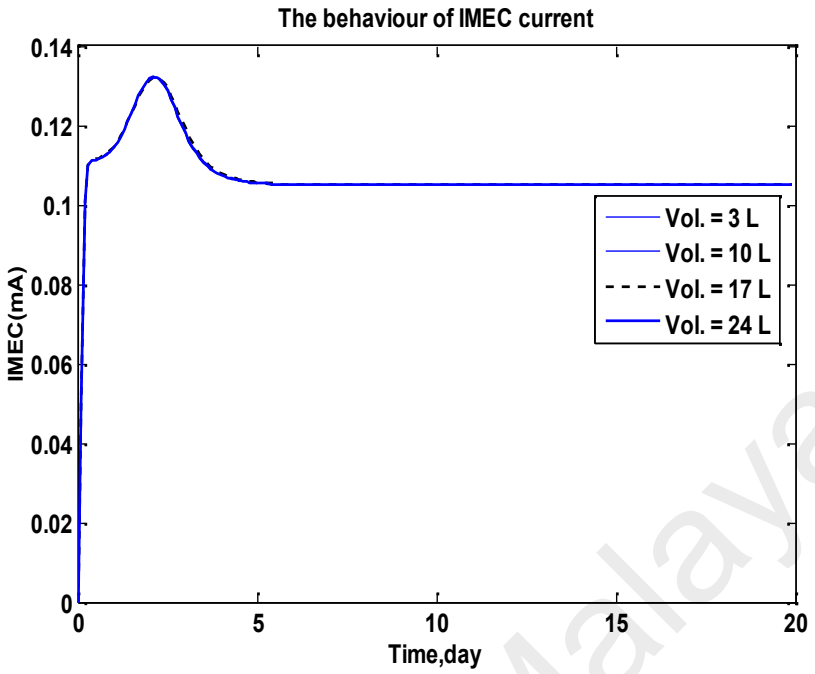

Figure 3.14: Effect of varying the anodic compartment volume (*L*) on the I_{MEC} current

The *MEC* system can be dealt with effectively and hydrogen production rate obtained maximum. Several studies have reported that in some cases the high organic loading rate is even lower hydrogen gas production (Van Ginkel et al., 2005) while other studies explain that the higher organic loading rate will increase the hydrogen production rate (H. Zhang et al., 2006).

3.7.2 Effect of varying the electrode potentials (E_a)

Figure 3.15 and 3.16 show the effect of voltage applied on the performance of *MEC* Fed-batch reactor. As shown in the figure, the dependence of hydrogen production and I_{MEC} current are very significant to the voltage applied to the process. In this process the *MEC* Fed-batch reactor operates at a voltage variation in the range of $2 \leq E_a \leq$ 14 Volt. The behaviour of the system differs significantly as the value of applied voltage (E_a) is changed. Applied voltage is given a significant influence on the performance of *MEC*. The Figure 3.16 shows the performance at 10*V* higher than 6*V* in

terms of the production of hydrogen, while the minimum voltage of $2V$ is applied to achieve a measurable level of hydrogen production in the *MEC* system. It is clear that the hydrogen production rate and I_{MEC} current increased with a higher value of electrode potentials (E_a) to the process.

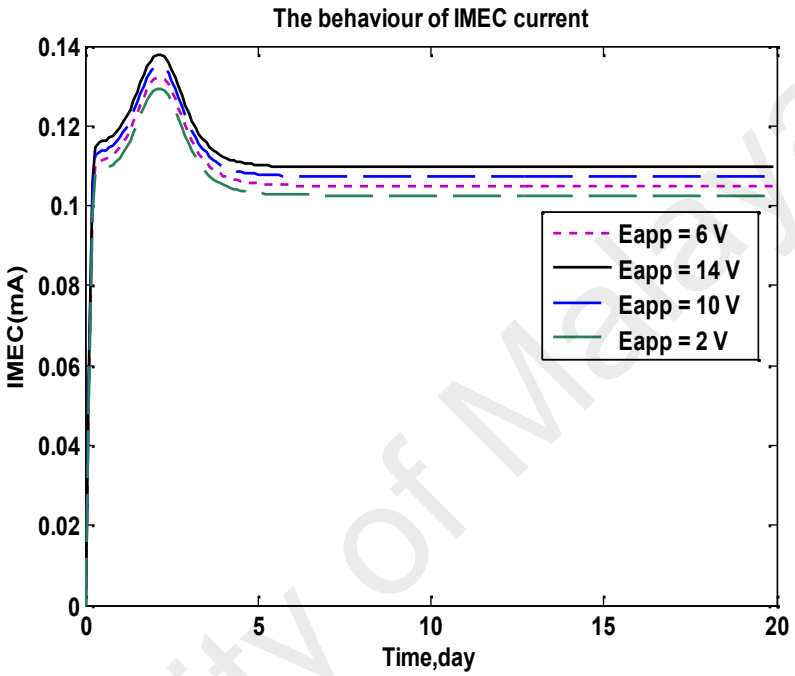

Figure 3.15: Effect of varying the electrode potentials (E_a) on the I_{MEC} current

I_{MEC} current depends on their action dynamics of anodophilic intracellular mediator in the process. M_{ox} is a fraction of oxidized mediator mediator while M_{red} fraction reduced by microbes anodophilic in the anodic compartment. Since I_{MEC} depends on M_{ox} and M_{red} thus increasing the voltage applied to the process will increase the concentration of M_{ox} to achieve maximum value. After concentrations maximum of M_{ox} reached, the current value will be constant despite I_{MEC} applied voltage increasing. So that the *MEC* of operating at high voltages will result in loss of energy and water electrolysis process takes place in the process.

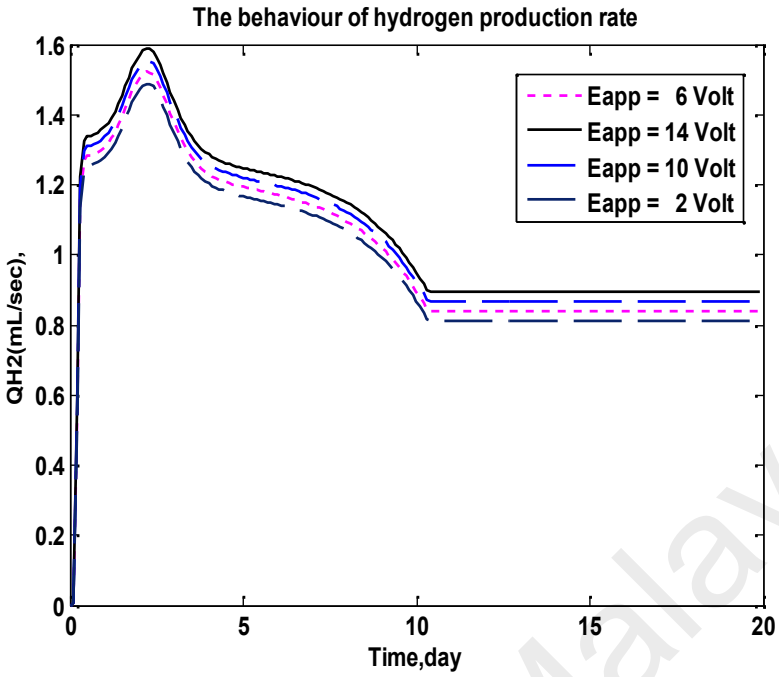

Figure 3.16: Effect of varying the electrode potentials (E_a) on hydrogen production rate

3.8 Analysis of the effect of changes of Kinetic Parameters on the hydrogen production rate

3.8.1 Effect of varying the maximum growth rate ($\mu_{m\ ,a}$)

The sensitivity analysis of the system performance to the maximum growth rate ($\mu_{m\ ,a}$) by anodophilic microorganism were presented in Figure 3.17 and Figure 3.18 performed in the range $1.5 \leq \mu_{m\ ,a} \leq 3.0\ h^{-1}$. In the range of investigation, this parameter was determined to have insignificant effect on the system performance. It is clear that changes in the value of the maximum growth rate only provides a change at the beginning of the process and not a significant effect on then I_{MEC} current and the rate of hydrogen production.

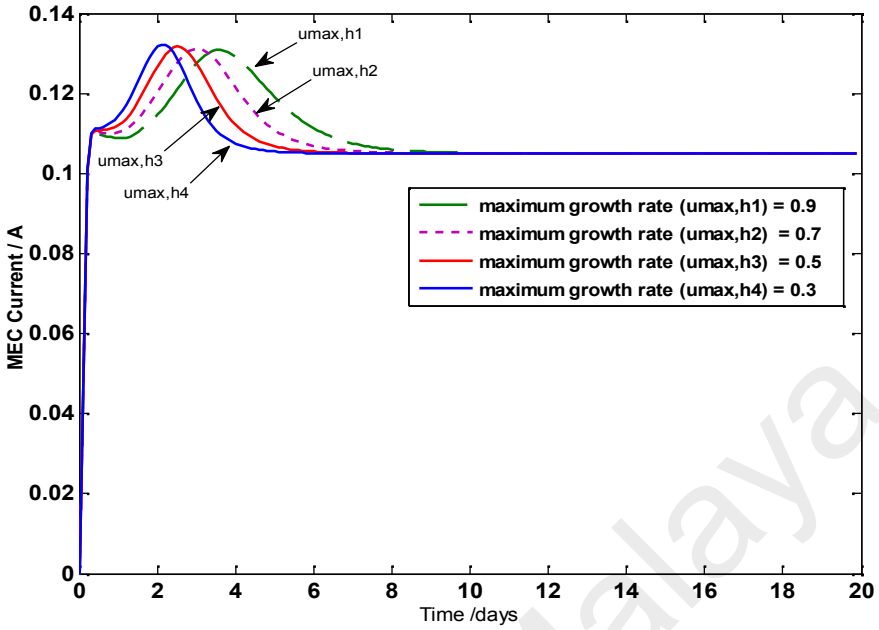

Figure 3.17: Effect of varying the maximum growth rate ($\mu_{m\ \ ,a}$) by anodophilic microorganism on the I_{MEC} current

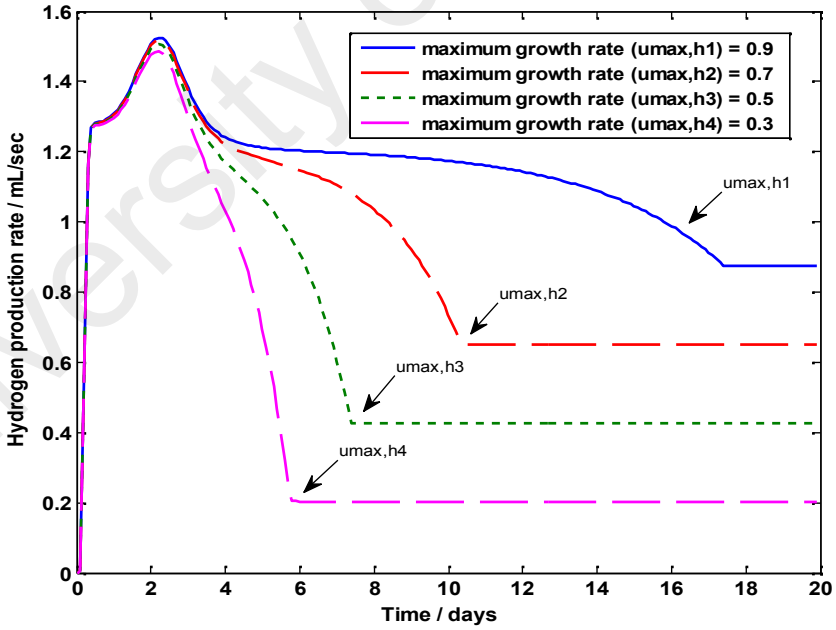

Figure 3.18: Effect of varying the maximum growth rate ($\mu_{m\ \ ,a}$) by anodophilic microorganism on the hydrogen production rate

3.9 Optimum parameters for H_2 production and applied current

From the dynamic studies of the previous model, it is clearly evident that the *MEC* system is a highly complex, nonlinear and multivariable system. It also shows that the internal parameters have a significant effect on the rate of hydrogen production, which is closely related to the electrode potential and the I_M current applied to the system.

In this study, the statistical analysis of *MEC* was performed where the response surface method (RSM) was applied to identify the optimum process condition. After collecting the data according to the design procedures, the optimization process is developed with a variety of process variables along with the *RSM* procedures. The regression analysis model was performed to get the optimum process response by using the quadratic models as follows (Khan et al., 2014):

$$Y = \beta_o + \sum_{i-1}^{k} \beta_i x_i + \sum_{i-1}^{k} \beta_{ii} x_i^2 + \sum_{i-1}^{k-1} \sum_{j-i+1}^{k} \beta_{ij} x_i x_j + \varepsilon \quad (3.78)$$

where, Y is the response, β_o is the constant coefficient, β_i, β_{ii}, and β_{ij} are the coefficients estimated by the model, pure-quadratic, cross-product effects of the x_i and ε is the error vector. In this process, the independent variables considered are concentration of anodophilic microorganisms (x_1), electrode potentials (x_2) and MEC current (x_3). The independent variables in this process werex_1, x_2 and x_3 where the low and high levels were coded as -1 and +1, respectively. The total number of experiments to be conducted is 15 runs and proposed combination parameters for the specific hydrogen production rate are listed in Table 3.2. The method used here is the Box Benhken method by using Design Expert software. Fifteen (15) runs were suggested for conducting experiments. Six runs were suggested to be repeated. This suggested repetition is advantageous to obtain the center point of the developed experimental design and to get the standard error of the sum of squares.

The statistical model was developed by applying the least squares method and multiple regression analysis study using the experimental data for the hydrogen production rate, which can be described as:

$$Y=1.17+0.22x_1+0.18x_2+0.77x_3-0.093x_1^2+0.18x_2^2-0.044x_3^2+0.038x_1x_2-0.09x_1x_3+0.18x_2x_3 \quad (3.79)$$

Where Y is hydrogen production rate (L/day); x_1 is anodophilic microorganisms (mg/l); x_2 is electrode potential (*V*); x_3 is MEC current (*A*).

Table 3.2: Specific hydrogen production rate at several of initial concentration of anodophilic microorganisms, electrode potentials and *MEC* current

Run	Anodophilic microorganisms (*mg/l*)	Electrode potentials (*V*)	MEC current (*A*)	Maximum hydrogen production rate (*L/d*)
1	425.00	0.80	0.16	1.17
2	750.00	0.10	0.01	0.74
3	750.00	0.10	0.30	1.74
4	425.00	0.80	0.16	1.17
5	100.00	1.50	0.30	2.22
6	100.00	0.10	0.30	1.54
7	425.00	0.80	0.16	1.17
8	972.00	0.80	0.16	1.18
9	425.00	1.98	0.16	1.89
10	425.00	0.80	0.16	1.17
11	425.00	0.80	0.16	1.17
12	750.00	1.50	0.01	0.84
13	100.00	0.10	0.01	0.14
14	425.00	0.80	0.16	1.17
15	100.00	1.50	0.01	0.12

The main problem in this case is to determine the value of voltage and current required without excessive external energy to produce maximum hydrogen gas. In order to address this challenge, the optimum value of the electrode potentials (*V*) and *MEC* current need to be determined corresponding to this situation, and these values need to be controlled to continuously produce the maximum and optimal hydrogen gas production. In this study, the *RSM* is applied to determine the optimum electrode potentials and counter-electromotive force conditions to achieve the optimum hydrogen production rate and current (I_M) in the reactor. In this process, the hydrogen production rate is affected by

various levels of process variables such as the concentration of microorganisms anodophilic, electrode potentials and current *MEC*. Three-dimensional response surface plot using equation (3.79) can be used to find the optimal response of the process variable at the highest point of the surface.

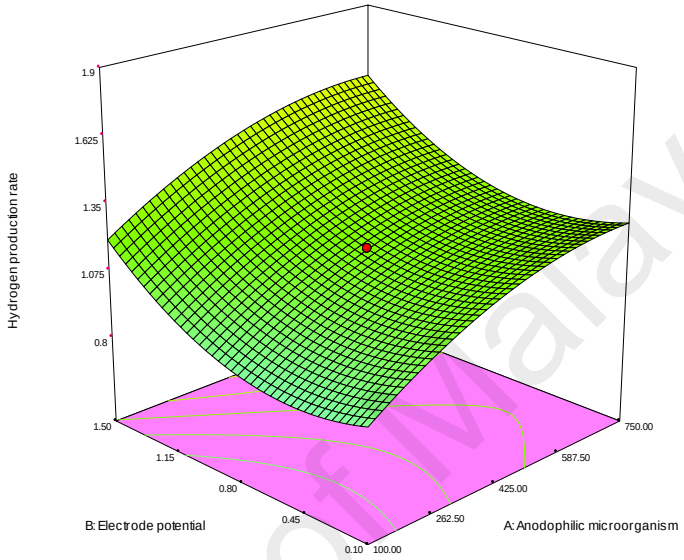

Figure 3.19: 3D Response surface of electrode potential vs anodophilic microorganism on hydrogen production rate

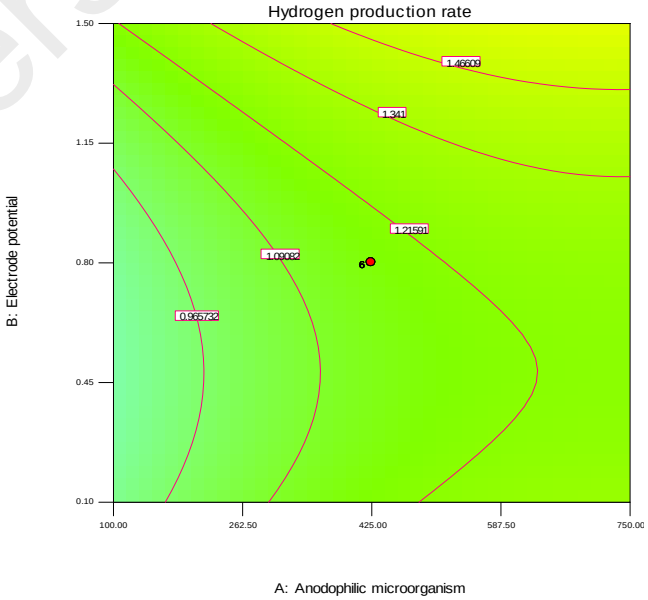

Figure 3.20: Contour plot of electrode potential vs anodophilic microorganism on hydrogen production rate

As the rate of hydrogen gas production will increase with increasing current *MEC*, it can be observed from the Figure 3.19 and Figure 3.20 that the value of current in the *MEC* process showed a positive linear effect on the hydrogen production rate. The optimum conditions for biohydrogen production rate of this study is at 1.17 l/day, where the concentration of microorganisms anodophilic obtained at 425 mg/l, the electrode potential at 0.8 *V* and the *MEC* current is at 0.16 *A*. From the contour plot, it is clearly shows that the current decline will lower the rate of hydrogen gas production in the *MEC* system while increased concentration acidophilic microorganisms and the electrode potential does not have significant impact on the rate of production of hydrogen gas. The red dot area in the figure shows the optimal results of hydrogen gas production while other colors indicate a lower value of the response.

3.10 Control variable selection

MEC is a technology using electrochemically active microorganisms to oxidize organic materials. The conversion of biomass which is more efficient and effectiveat the anode is one factor that is important to generate maximum production of hydrogen gas. This rate can be maximized without excessive energy consumption by minimizing the resistance within the *MEC* reactor. Knowledge of *MEC* performance changes caused by variations in the organic load, the nature ofthe carbon source, and hydraulic retention time, needs to be studied further in order to avoid excessive power consumption. To optimize the performance of the reactor, it is necessary to supply the optimum amount of electrical energy from outside which aims to reduce the potential of the cathode within the *MEC* reactor (B. E. Logan et al., 2008).

The addition of energy potential can be carried out by supplying of electric current (*DC*) into the reactor. Changes energy potential in the anode depends on the type and

concentration of the substrate, the amount of voltage applied to the system and the type of microbes used. The production of hydrogen gas can be achieved maximally by maintaining the stability and performance of the current density production in the reactor. One way to evaluate the performance of the electrode potential at *MEC* Reactor is to supply a voltage gradually. Experimentally observation shows that the potential difference between two electrodes increases with the applied voltage (Y. Zhang et al., 2010).

Knowledge of the internal resistance of the reactor system is indispensable. The production of hydrogen gas in *MEC* reactor will increase with the increasing amount of current in the reactor. One important factor that affects the performance of *MEC* reactor is the amount of voltage supplied to the reactor. Loss of energy will be greater if the amount of voltage supplied to the reactor excessive. To determine the exact voltage value without excessive external energy supply, it is necessary to control the amount of current in a reactor. To optimize the *MEC* current in the reactor, it is necessary to design appropriate control systems so that the amount of voltage supplied to the reactor can be controlled and regulated continuously. To address this challenge, the optimum value of the electrode potential (*V*) and *MEC* current in therector need to be determined.

In this study, the *MEC* current is controlled by adjusting the electrode potential charge (*V*). The performance of the controller is evaluated by observing the response of the process through tracking the set-point changes when the *MEC* current is maintained approximately at the optimal operational value of 0.16 *A*. To evaluate the performance of the controller, various simulation tests will be studied involving multiple set-point changes, disturbances rejection and noise measurement.

CHAPTER 4: CONTROL OF MICROBIAL ELECTROLYSIS CELLS BATCH REACTOR: SIMULATION STUDY

4.1 Introduction

This chapter will discussed a wide range of controllers used for *MEC* reactor system such as the *PID* and neural networks for process control design. In the first part of this chapter will be assessed on various closed loop control system for the *MEC* reactor involving proportional integral derivative (*PID*) algorithm and adaptive-*PID* controllers. As for the second part of this chapter will be discussed about the neural network controller such as direct inverse neural network (*DINN*) controller, the design of neural networks for process control systems, internal model control (*IMC*) and hybrid neural network (*HNN*) controller scheme. Results and discussion of the conventional *PID* controller and neural network controller includes closed loop control studies for constant set-point study, multiple set-point tracking study, disturbance rejection and measurement noise, respectively.

In this chapter, the design and development of the conventional *PID* and neural network based controllers performance for *MEC* process in batch reactor are presented. The simulation study and controller performance utilizes the MATLAB R2013b software (Appendix 2). Prior to considering an advanced control method to the process, it is important to assess the controllability of the system using conventional control methods. In this case, a well-known fixed-gain scheme is employed. The design of basic neural network controller which covers features essential in the development of the neural network model is studied. Inverse neural network model with feed-forward structure is used as the controller in this case. The control method proposed utilizes feed forward neural networks in the direct inverse neural network control method. The proper control

strategy is developed after preceded by simulation study with using the neural network based inverse model for set point tracking and disturbance rejection tests. The models were chosen in an effort to identify the one that best represent the system. The development includes the selection of input-output variable for the model, the data used for training and validation, and neural network model formulation. The design and performance of neural network controller for the basic, internal model-based control and hybrid schemes are also in this chapter.

4.2 Closed loop control system for the *MEC* reactor

Before describing in detail about the reasons for the use of neural network based controllers for *MEC* process, it will be presented in advance of the performance of closed loop control system for proportional integral derivative (*PID*) algorithm.

4.2.1 Proportional Integral Derivative (*PID*) Controllers algorithm

The *PID* controller is one of the most widely used feedback controllers and has been successfully used in various engineering applications such as industrial process control, flight control, motor drives, automotive, instrumentation, and so on (Isaksson & Hagglund, 2002; O'Dwyer, 2009). Among the advantages of proportional-integral-derivative (*PID*) are its simplicity and robustness for process control application (Shamsuzzoha & Skogestad, 2010). For this purpose, the well-known conventional controller, i.e., *PID* controller (with both fixed and adaptive gain schemes), was employed. The control law for the *PID* controller can be expressed mathematically as:

$$u(t) = k_c e(t) + k_c \tau_d \frac{d}{d} e(t) + \frac{k_c}{\tau_i} \int_0^t e(t) d \ + u_s \qquad (4.1)$$

Where k_c is proportional gain, τ_i is the integral action time, τ_d is the derivative time, $e(t)$ is the error and u_s is the control action control values when the error.

In the past few decades, many systems using various *PID* tuning formulae have been studied and currently it is easier for the operator to select the appropriate controller gain. However, conventional *PID* controller tuning requires repeated trials because of possible instability during the tuning or modeling experimental processes (Åström & Hägglund, 2006). The above equation (4.1) is served in analog form, while for the automatic control system by using software such as computer control, generally using a digital approach. For the implementation of digital control, as for the formula given in the form of discrete and can be written as follows:

$$u(t_k) = u(t_{k-1}) + K_p\left[\left(1 + \frac{\Delta t}{T_i} + \frac{T_d}{\Delta t}\right)\right] e(t_k) + \left(-1 - \frac{2T_d}{\Delta t}\right) e(t_{k-1}) + \frac{T_d}{\Delta t} e(t_{k-2}) \quad (4.2)$$

where $e(t_k) = y_s - y_t$ and subscripts t_k and t_{k-1} denote the sampling time; $t_k$stands for the current time sampling, t_{k-1} stands for the sampling at the previous time t_{k-1} and t_{k-2} stands for the sampling at the previous time t_{k-2}.

In digital control implementation, the formula is given in discrete form expressed as follows:

$$u(t) = k_c\left(e_t + \frac{\Delta t}{k_I}\sum_{i=1}^{t} e_i - \frac{k_d}{\Delta t}(e_t - e_{t-1})\right) \quad (4.3)$$

Where

$$u_{t+1} = u_t + \Delta u_t \quad (4.4)$$

$$e_t = y_s - y_t \quad (4.5)$$

and subscripts t and $t-1$ denote the sampling time; $t$stands for the current time sampling, and $t-1$ stands for the sampling at the previous time $t-1$.

By considering electrode potentials ($E_{applied}$) as the manipulated variable (control output) and *MEC* current (I_M) as the controlled variable, the control law can be written as follows:

$$\Delta E_{a\ (t+1)} = k_c\left(e_t - e_{t-1} + \frac{\Delta t}{k_I} e_t\right) \quad (4.6)$$

$$E_{a\ (t+1)} = E_{a\ (t)} + \Delta E_{a\ (t+1)} \quad (4.7)$$

$$e_t = \left(I_{M\ s} - I_{M\ t}\right) \quad (4.8)$$

Where $I_{M\ s}$ is the current set point, and $I_{M\ t}$ is the current response.

The performance of the various controllers was assessed in this section based on the response characteristics, which were investigated by observing the responses of the process under nominal and varying operating conditions. Because the system is highly non-linear in nature with constantly changing operating conditions over time, it gives rise to a difficult problemin terms of identification and control. The block diagram the PID controller can be seen in Figure 4.1.

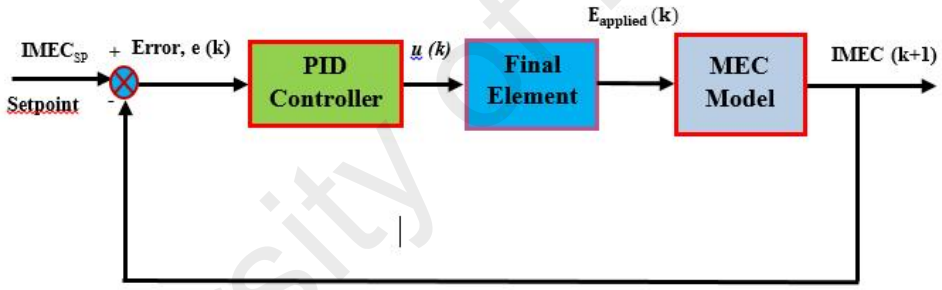

Figure 4.1: Block diagram of PID closed loop design

4.2.1.1 Closed Loop Control studies for constant set-point study

Figure 4.2 shows the performance of *PID-ZN* tuning method for constant set-point study. The Ziegler-Nichols method (ZN) for the PID controller obtained on the proportional gain (k_c) value is 9, the integral action time (τ_i) is 700 and the derivative time (τ_d) is 1.8. The controller performs well and is successful in managing the process to follow the given set point changes to keep up around at 0.18A. From this figure, It can be seen that the controller performs reasonably well when responding to deviation, but it

becomes sluggish when responding to large deviations in the process response. However, the controller is also capable of following the time-varying characteristic of the process in most conditions.

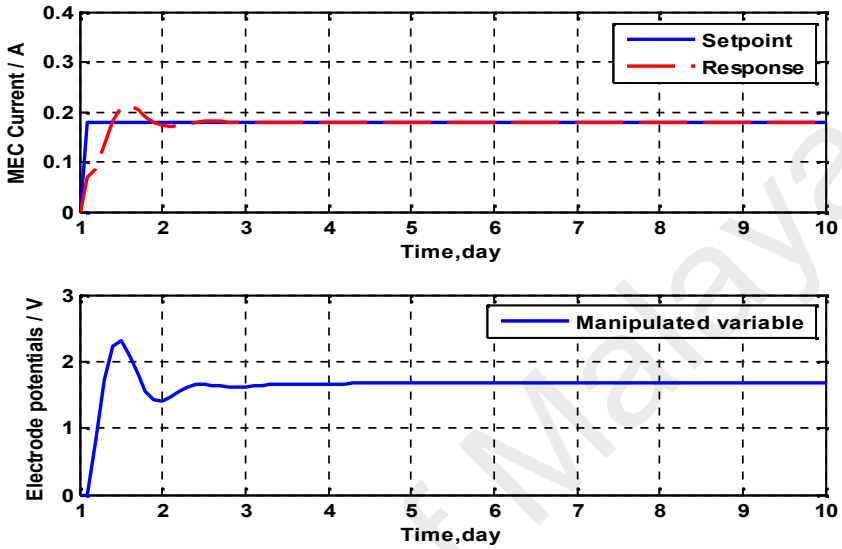

Figure 4.2: PID controller using Ziegler-Nichols tuning method

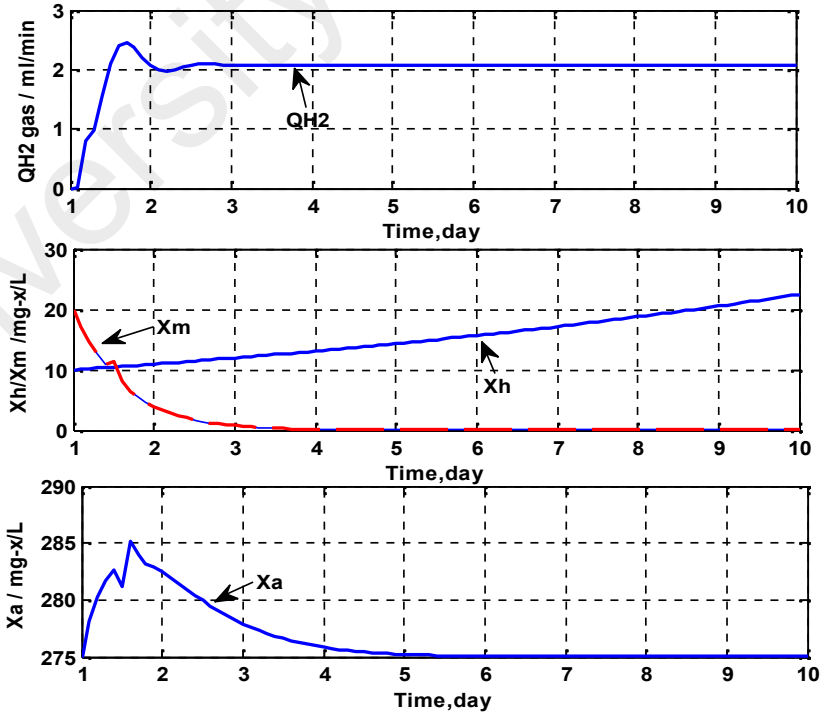

Figure 4.3: The dynamic behavior of H_2 production rate, *Xh*, *Xm* and *Xa* for *PID* controller

Figure 4.3 illustrates the dynamic behavior of the hydrogen production rate (Q_{H2}), concentration of hydrogenotrophic microorganism (x_h), concentration of acetoclastic microorganism (x_m) and concentration of anodophilic microorganisms(x_a) for the *PID-ZN* method. It can be seen that, when the set point is kept at around the nominal value of 0.18 A, operation at the optimal hydrogen production rate can be maintained.

4.2.1.2 Closed Loop Control studies for constant set-point study with noise and disturbance rejection

Figure 4.4 shows the performance of the controller when the measurement of the controlled variable is corrupted by noise under nominal operating conditions. The noises are assumed to come from the measurement of the *MEC* current in the reactor. From these studies, it can be seen that the *PID* responses are still stable with fewer oscillations.

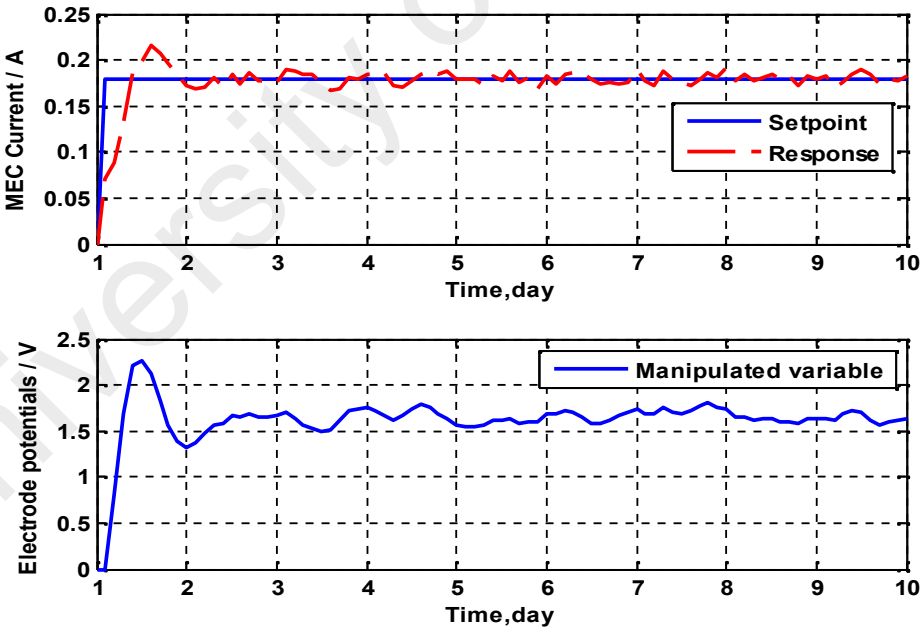

Figure 4.4: PID controller for constant set-point study with measurement noise

Figure 4.5 shows the *PID* controller for constant set-point study with disturbance rejection in the *MEC* system. The performance of *PID* controller has tested by using

counter-electromotive force (*V*) as the internal disturbance rejection The variation in disturbance was generated by changing the counter-electromotive force at nominal value of -0.3 *V*, -0.2 *V*, -0.1 *V* and 0.1 *V*, respectively. Based on these results, the performance of this controller is generally acceptable and the *PID* controller gave smoother responses in the *MEC* system.

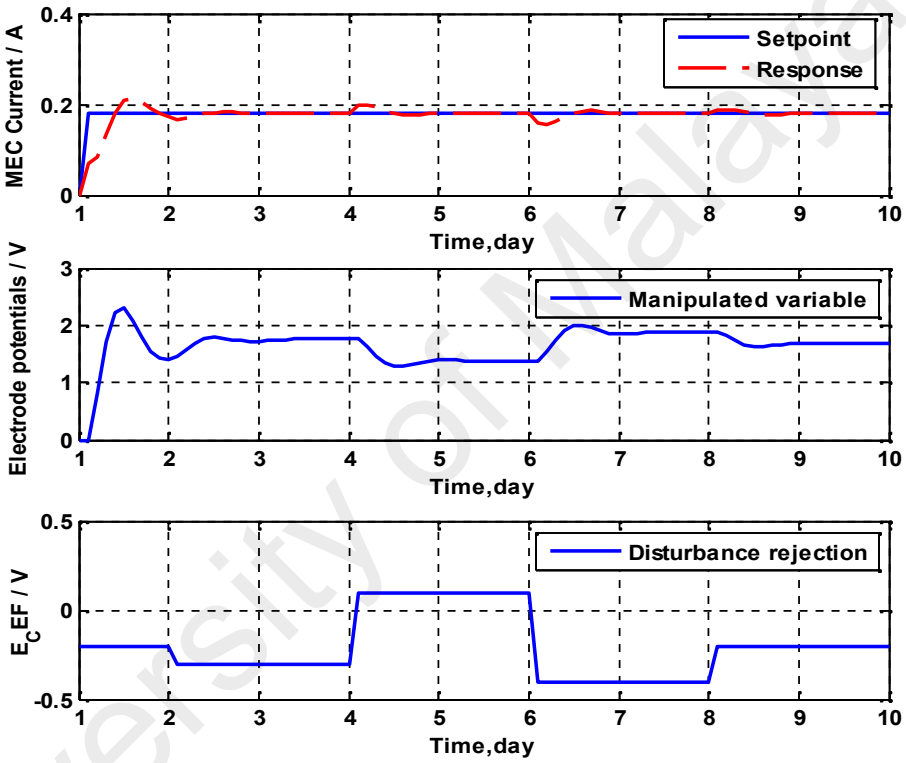

Figure 4.5: *PID* controller for constant set-point studywith disturbance rejection

Figure 4.6 shows the performance of the controller when the measurement of the controlled variable is corrupted by noise and disturbance rejection under nominal operating conditions in the set-point tracking study. In this process, the noises and disturbance are assumed to come from the measurement of the *MEC* current in the reactor. From these studies, when the systems reach a steady state and suddenly disturbances and noise occur together, the *PID* controller is able to bring the process variable to a set-point.

In generally, the performance of *PID* controller is good and can be applied to control the *MEC* reactor.

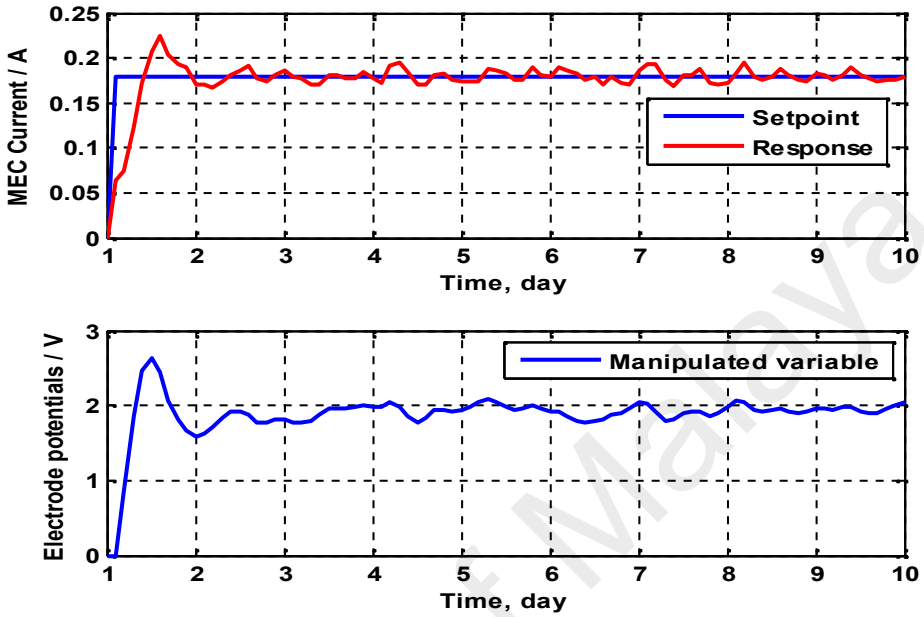

Figure 4.6: *PID* controller for constant set-point studywith disturbance rejection and measurement noise

In summary, from all the results and figures, it can be seen that, despite the fluctuations, the process can roughly be directed by the controllers to follow the set-point changes, and disturbance rejection can be performed satisfactorily. However, the controller is susceptible to noise, leading to severe fluctuations in the controller action as observed in the profiles shown in Figure 4.4 and 4.6. This is further evident in the comparison of the error in terms of the Integral Square Error (*ISE*), Integral Absolute Error (*IAE*) and Integral Time Absolute Error (*ITAE*) for PID controller as shown in Table 4.1.

Table 4.1: The *ISE*, *IAE* and *ITAE* for *PID* controller performance

Comparison Control Performance for constant study	ISE	IAE	ITAE
Set-point change	0.016945	0.32103	1.6719
Disturbances rejection	0.016966	0.33515	2.3268
Noise measurement	0.020738	0.72437	24.9153
Disturbances and noise	0.019895	0.68216	20.0381

4.2.2 Adaptive-*PID* controllers

Although *PID* control has several advantages, such as robustness in operating, flexibility and has a simple structure, but it is also has many short comings, such as poor tuning and slow to adapt when the change of parameters or external disturbances on the system (Mueller et al., 2007). In this study, the adaptive *PID* controller has been chosen because it has many advantages when compared with conventional *PID* controller. The adaptive *PID* controller is able to control the process dynamics change rapidly or unexpectedly and can continuously update the internal model of the process. Furthermore, adaptive control is a good solution that can serve as a feedback law to achieve the control objectives so the system can cope with external disturbances (Dey & Mudi, 2009; Golbert & Lewin, 2004; Yang et al., 2007). However, comparisons were also made with the controller tuned by the conventional *PID* Ziegler-Nichols method (*ZN*) because this is the most popular tuning method used (Dey & Mudi, 2009; Gyöngy & Clarke, 2006).

The controller gains are adjusted adaptively depending on the model error with respect to the changing conditions of the process, represented by the *MEC* model. The model-based identifier is the model constructed based on the bounded dynamic characteristic, which are developed based on the overall and simplified dynamic behavior of the complex nonlinear fed-batch *MEC* system.

In order to operate the *MEC* effectively at the optimal conditions obtained in the previous section, the controllers were applied to the *MEC* system under various conditions in association with the change in the electrode potentials (*V*), which affects the *MEC* current and the hydrogen production rate. The performance of the various controllers was assessed based on their response characteristics for set-point tracking under nominal and varying operating conditions, such as with disturbance and noise effects.

Adaptive-*PID* controller is able to control the system dynamics in the event of a non-nominal process condition. Consider the *MEC* process model given by:

$$y(k) = A_1x(k-1) + A_2x(k-2) + [B_1u(k-1) + B_2u(k-2)]u(k) \qquad (4.9)$$

For the case at nominal condition, A_i and B_i for i = 1, 2, and 3 are known through least-square regression technique. The control action is derived as:

$$u(k) = \frac{K_P\left[e(k)+\frac{1}{\tau_I}\int_0^t e(k)d + \tau_D\frac{d}{d}e(k)\right] - A_1x(k-1)+A_2x(k-2)}{B_1u(k-1)+B_2u(k-2)} \qquad (4.10)$$

The block diagrams show the method of adaptive PID as in Figure 4.7.

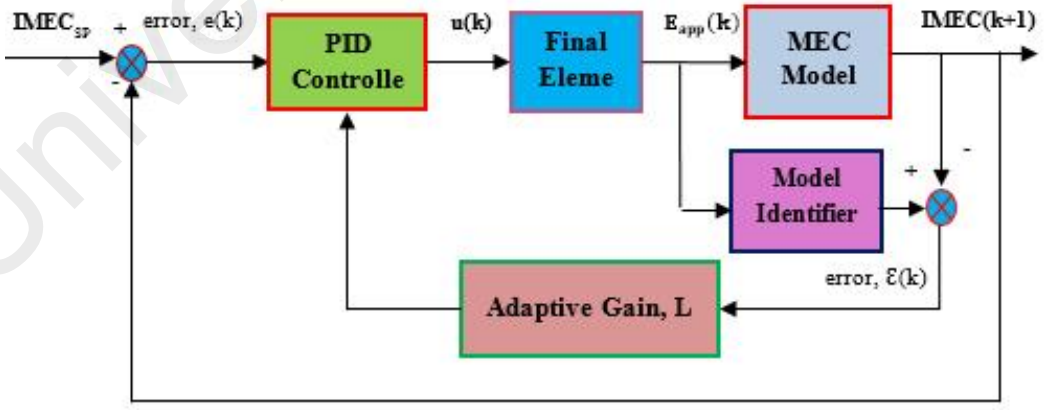

Figure 4.7: Block diagram of PID-Adaptive gain closed loop design

4.2.3 Closed Loop Control studies for set-point tracking study

4.2.3.1 Controller set-point changes with adaptive gain

In this work, a set-point tracking study is performed when the I_{MEC} current was maintained at approximately the nominal optimal operation value of 0.18 A. Figure 4.8 shows the process and controller response when using the *PID*-adaptive gain controllers for set-point tracking performance under nominal operating conditions. The controller performs well and is successful in managing the process to follow the given set point changes to keep up around 0.13 *A*, 0.16 *A* and 0.20 *A*, respectively. However, the *PID* conventional gave a higher overshoot and more oscillations than the *PID*-adaptive gain method. This is also evident in the behavior of the manipulated voltage of the electrode potential applied for both cases.

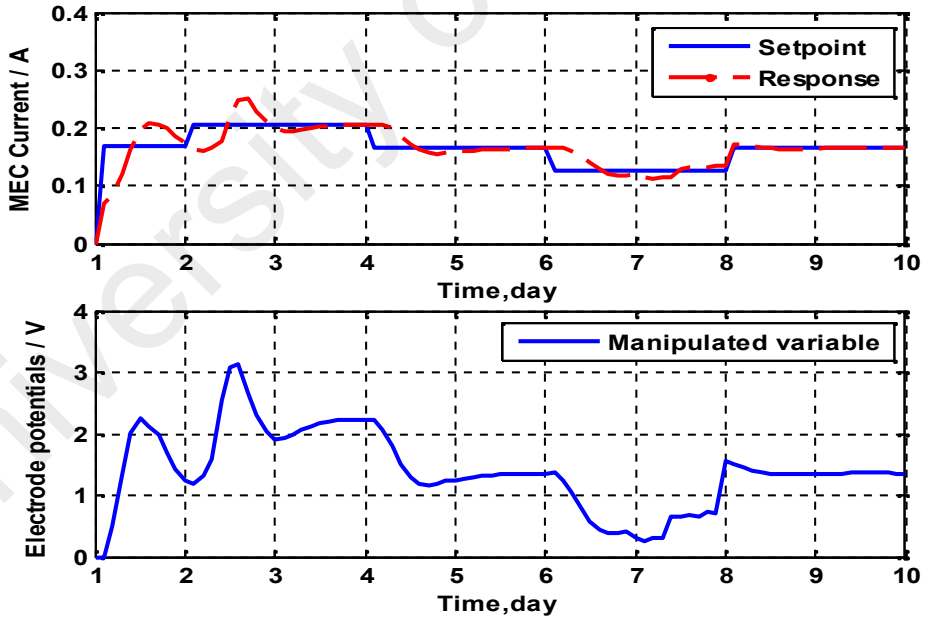

Figure 4.8: *PID*-adaptive gain for set-point tracking study

Figure 4.9 shows the behavior of the hydrogen production rate (Q_{H2}), concentration of hydrogenotrophic microorganism (x_h), concentration of acetoclastic microorganism

(x_m) and concentration of anodophilic microorganisms(x_a) for the *PID*-adaptive gain using the set-point tracking study. In Figure 4.9, the maximum hydrogen production rate increased sharply and reached a peak value of 3.80 l d^{-1}, then changed according to the changing set-point value, then decreased linearly until reaching the steady state value of 1.80 l d^{-1}. It can be seen that there is very close relationship between the electrode potential (volt) and hydrogen production rate (l d^{-1}) in these results, which is in agreement with the previous open-loop results.

From these figures, it can be seen that *PID* with adaptive gain can provide better control of the *MEC* system. It also shows that the controller performs reasonably well when responding to deviation, but it becomes sluggish when responding to large deviations in the process response. However, the controller is capable of following the time-varying characteristic of the process in most conditions.

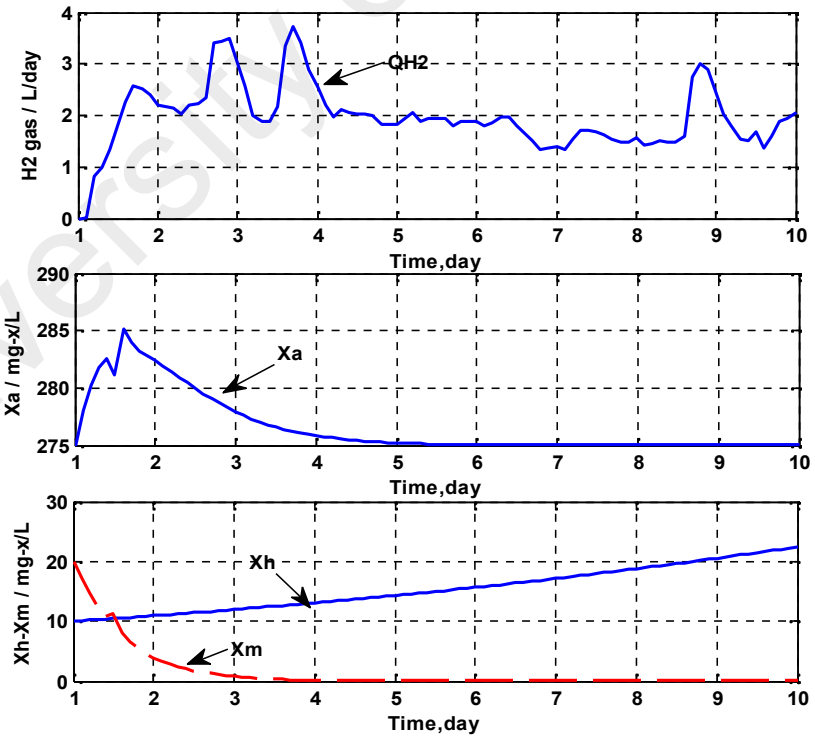

Figure 4.9: The response performance of H_2 production rate, *Xh*, *Xm* and *Xa* for *PID* controller

4.2.3.2 Noise and disturbance rejection

Figure 4.10 shows the *PID*-adaptive gain for tracking set-point changes with disturbances in the system. The disturbance considered in this study was generated through changes in the counter-electromotive force (*V*) as the internal disturbance rejection at nominal value of -0.4 *V*, -0.2 *V* and 0.0 *V*, respectively. Based on these results, the performance of this controller is generally acceptable as shown in Figure 4.10, where the *PID*-adaptive gain controller gave smoother responses in *MEC* system when compared with conventional *PID* controller.

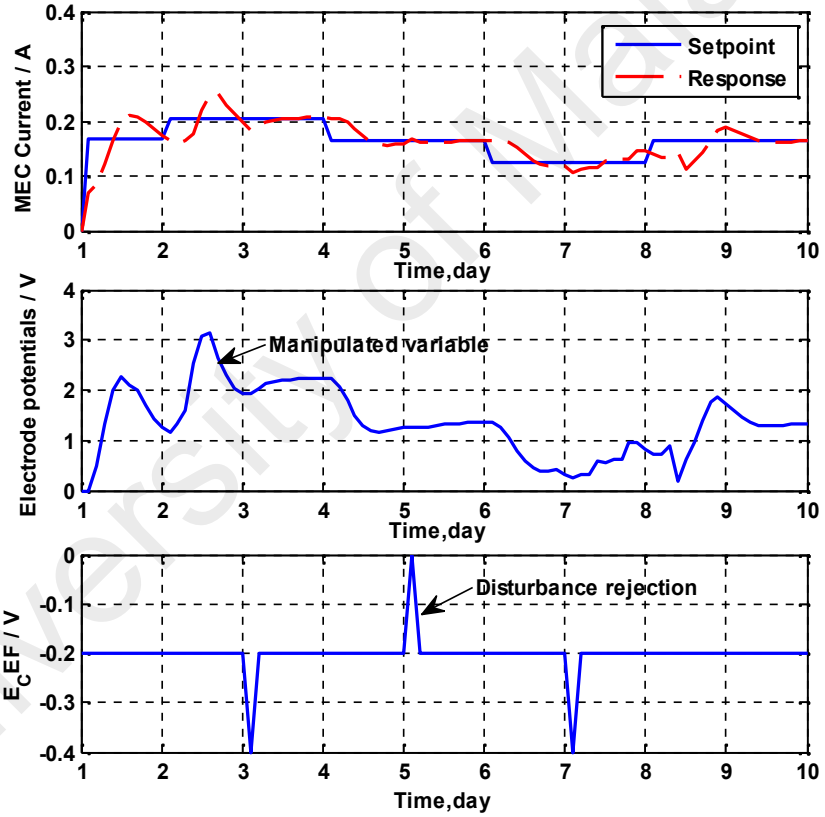

Figure 4.10: The performance of *PID*-adaptive gain for disturbance rejection study

Figure 4.11 shows the performance of the controller when the measurement of the controlled variable is corrupted by noise under nominal operating conditions in the set-point tracking study where the noises are assumed to come from the measurement of the

MEC current in the reactor. From these studies, it can be seen that the *PID*-adaptive gain responses are more stable, with fewer oscillations, compared to the *PID* controller.

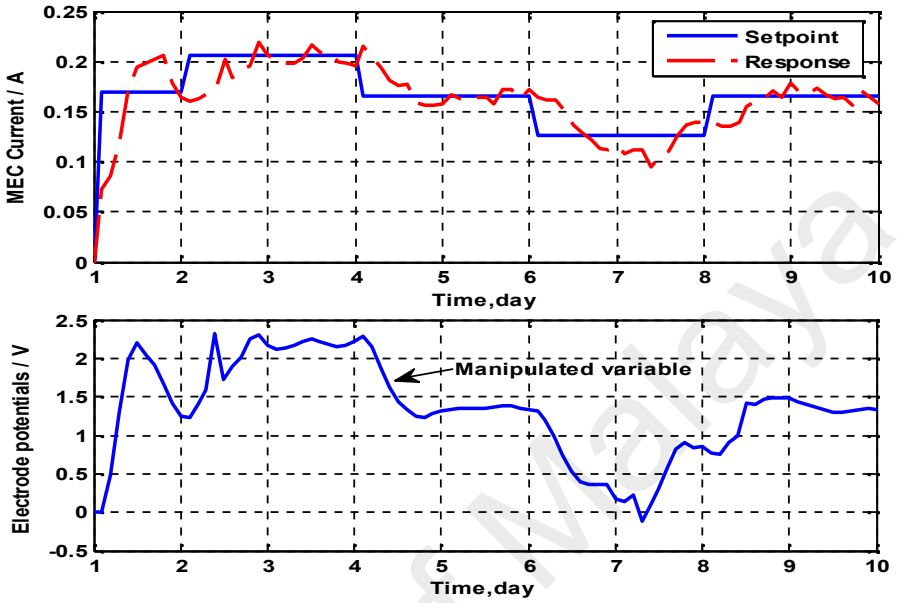

Figure 4.11: The performance of *PID*-adaptive gain for measurement noise

Figure 4.12 shows the performance of control strategy using *PID*-adaptive controller for multiple setpoint tracking study. The controller is corrupted by noise and disturbance rejection under nominal operating conditions. Overall, the controller performs well and is successful in managing the process to follow the given set point changes. From all the results and figures, it can be seen that, despite the fluctuations, the process can roughly be directed by the controllers to follow the set-point changes, and disturbance rejection can be performed satisfactorily. However, the controller is susceptible to noise, leading to severe fluctuations in the controller action as observed in the profiles shown in Figure 4.6 and 4.12.

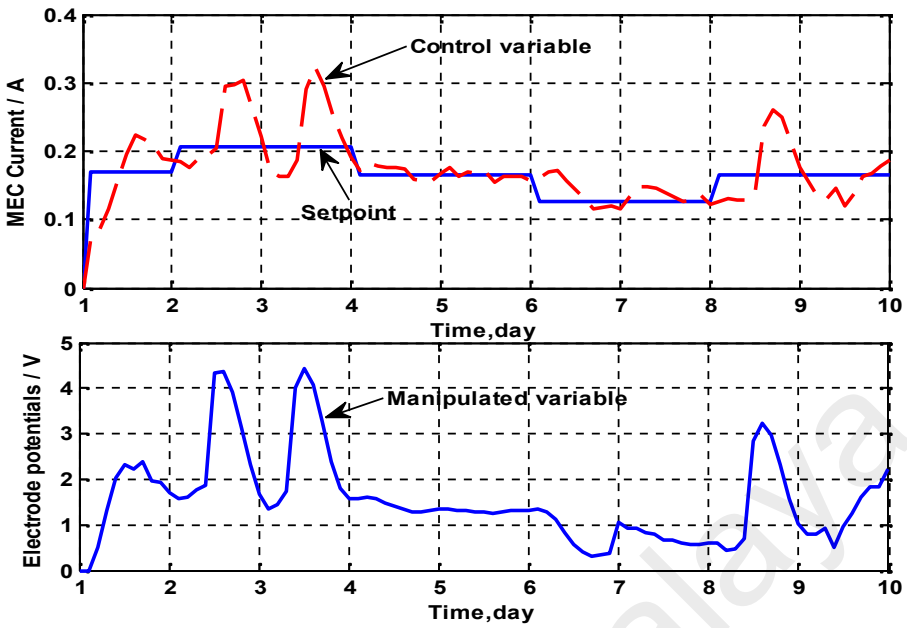

Figure 4.12: *PID*-adaptive gain for measurement noise and disturbance rejection

To minimize overshoot, settling time, steady state error and reference tracking error on the controller, it is require quantification of the performance of the system. For a *PID* controlled system, there are some indications that it can be used to describe the performance of the process, namely Integral Square Error (*ISE*), Integral Absolute Error (*IAE*) and Integral Time Absolute Error (*ITAE*). Table 4.2 shows the comparison of the error in terms on the performance index for *PID*- adaptive controller.

Table 4.2: Integral Square Error (*ISE*), Integral Absolute Error (*IAE*) and Integral Time Absolute Error (*ITAE*) for *PID*-Adaptive controller using set-point changes

Comparison Control Performance for constant study	*ISE*	*IAE*	*ITAE*
Set-point change	0.047292	1.2273	31.9586
Disturbances	0.058517	1.5588	58.8346
Noise	0.048129	1.4038	49.4306
Disturbances and noise	0.064401	1.6945	61.991

In summary, these results show that the *MEC* reactor can be controlled to give optimum current and hydrogen production rate using a *PID* controller. However, the *PID* with adaptive gain was able to give more robust and smoother results than the conventional *PID-ZN* method because the system dynamics are highly nonlinear as shown by the open-loop studies.

*MEC*s present many technological challenges that need to be overcome before their commercial application. For example, the hydrogen-production processes of the *MEC* reactor are very nonlinear and highly complex due to the presence of microbial interactions and highly complex phenomena in the system. Furthermore, the process depends on microbial activity, which shows an irregular correlation between current and voltage. Thus, precise control is required for the *MEC* reactor, so that the amount of current required to produce hydrogen gas can be controlled according to the composition of the substrate in the reactor.

4.3 Neural Network Based Controller

Artificial neural networks (*ANNs*) are simplified models of the central nervous system. They are networks of highly interconnected neural computing elements that have the ability to respond to input stimuli and to learn to adapt to the environment. They go by many names, such as connectionism, parallel distributed processing, neuro-computing, natural intelligent systems, machine learning algorithms, and artificial neural networks. It is an attempt to simulate within specialized hardware or sophisticated software, the multiple layers of simple processing elements called neurons. Each neuron is linked to certain of its neighbors with varying coefficients of connectivity that represent the strengths of these connections. Learning is accomplished by adjusting these strengths to cause the overall network to output appropriate results.

Neural networks have greatest promise in the realm of non-linear control problems. This is implied by their theoretical ability to approximate arbitrary non-linear mappings. Networks may also achieve more modeling than alternative approximation schemes, e.g. based on polynomials. It has a highly parallel structure, which lends itself immediately to parallel implementation. Such an implementation can be expected to achieve a higher degree of fault tolerance and speed of operation than conventional schemes. Furthermore, the elementary processing unit in a neural network has a very simple structure. This also results in an increase of the processing speed.

At present there is a strong interest in the field of neural computation. The recent upsurge in research on neural networks has made it an attractive method for identifying nonlinear processes. Studies of neural networks, e.g. (Bhat & McAvoy, 1990; Hussain, 1999), offer a cost-effective method of developing useful process models. In the absence of reliable sensors for measurement of biomass, substrate and product concentrations, neural network model has shown to be an effective "software sensor" to estimate the bioprocess parameters using available measurements.

Neural networks have been used to perform complex functions in various fields of application including pattern recognition, identification, classification, speech, vision, and control systems. From the control systems viewpoint the ability of neural networks to deal with non-linear systems is perhaps most significant. The networks are used to provide the non-linear systems models required by the techniques for synthesis of non-linear controllers. The neural networks based methods have an immense value for design of non-linear adaptive controllers for dynamical systems with poorly known and difficult dynamics. The learning algorithms are directly applicable as controller strategies for these different to model systems such as the *MEC* reactor systems.

4.3.1 Direct Inverse Neural Network Controller

The basic direct neural network model used for the controller concept refers to the inverse form of the process. Inverse neural network model with feed-forward structure is used directly as elements within the feedback loop. The diagram of the neural network inverse model based control strategy implementation to control the *MEC* current (I_M) controlled in the microbial electrolysis cells fed-batch reactor is shown in Figure 4.13.

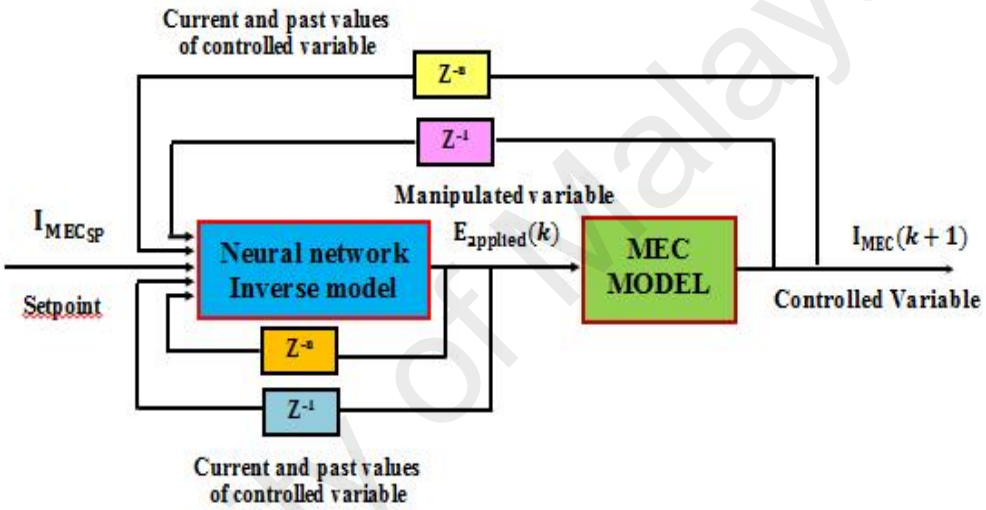

Figure 4.13: Block diagrams for neural network inverse based model control strategy

From the figure, it can be seen that the inverse model acts as the controller and provides the current control action with respect to certain current and past values of the process variables. In this case, the neural network model is trained to predict the required manipulated variable i.e. electrode potentials (E_a) and to bring the process to the set-point i.e. *MEC* current (I_M).

4.4 Design of Neural Networks for Process Control

The NNs controller concept refers to the inverse response of the open loop *MEC* process. The diagram of the controller and control strategy are shown in Figure 4.13. In this case, the neural network model is trained to predict the required manipulated variable, Electrode potential $(E_a \quad)$ with the given desire of set-point, *MEC* current (I_M). Before the neural networks based controllers can be applied, the procedure for obtaining the models i.e. the forward and inverse used in these strategies will have to be performed together with the method of training the controller. These steps will be discussed in the next few sections, before showing the control results.

4.4.1 Input-output Variable Selection

An important issue in constructing a neural network representation of this system is in the choice of inputs (x_n, u) for the model. In particular how many past samples of each of x_1, x_2 and u should be used in order to predict the next value of variables in *MEC*. In keeping up with the model of *MEC*, the current was arbitrarily being selected to be used and one past sample of each of x_1, x_2 and u . The input data to the neural network will subsequently look like $x_n = [x_2(n); x_2(n-1); x_1(n); x_1(n-1); u(n); u(n-1)]$ where the required output is $y_n = x_2(n+1)$. Using the current and one past sample of each variable permits for a limited degree of gradient information. In this case, the neural network model used for the controller is made in an inverse form of the process. Therefore, the selection of input and output variables for the neural network model is in accordance with this method. The inputs and the outputs of the neural network are fed through a moving window approach. The model is made of 16 input and one output nodes, where input nodes consist of data for substrate (S), anodophilic microorganisms (x_a), acetoclastic microorganism (x_m), hydrogenotrophic microorganisms (x_h), oxidized mediator fraction

(M_o), hydrogen production rate (Q_2), MEC current (I_M) and the one output node is electrode potentials (E_a) and past and current data for S i.e. $S_{(t)}$,$S_{(t-1)}$; x_a *i.e.* $x_{a(t)}$,$x_{a(t-1)}$; x_m *i.e.* $x_{m(t)}$,$x_{m(t-1)}$; x_h *i.e.* $x_{h(t)}$, $x_{h(t-1)}$; M_o *i.e.* $M_{o\ (t)}$, $M_{o\ (t-1)}$; I_M *i.e.* $I_{M\ (t)}$, $I_{M\ (t-1)}$,$I_{M\ (t+1)}$; Q_2 *i.e.* $Q_{H2(t)}$, $Q_{H2(t-1)}$ and output node is the electrode potentials (E_a).

The center of the moving window initially is taken to be at the third sampling intervals where each sampling was done at a time step interval, $dt = 0.01$ hour. The forward model was shown on the left and for inverse model shown in the right side of Figure 4.14. The forward model is consists of 16 input nodes, the first six pairs of input (S,x_a,x_m,x_h, M_o , I_M , Q_2 and E_a) matrices, which consist of their current and past values are input into the network. The desired network output is assigned to be the future MEC current,I_M at $t = t + dt$. The output of inverse model is electrode potentials (E_a) at $t = t$ hour.

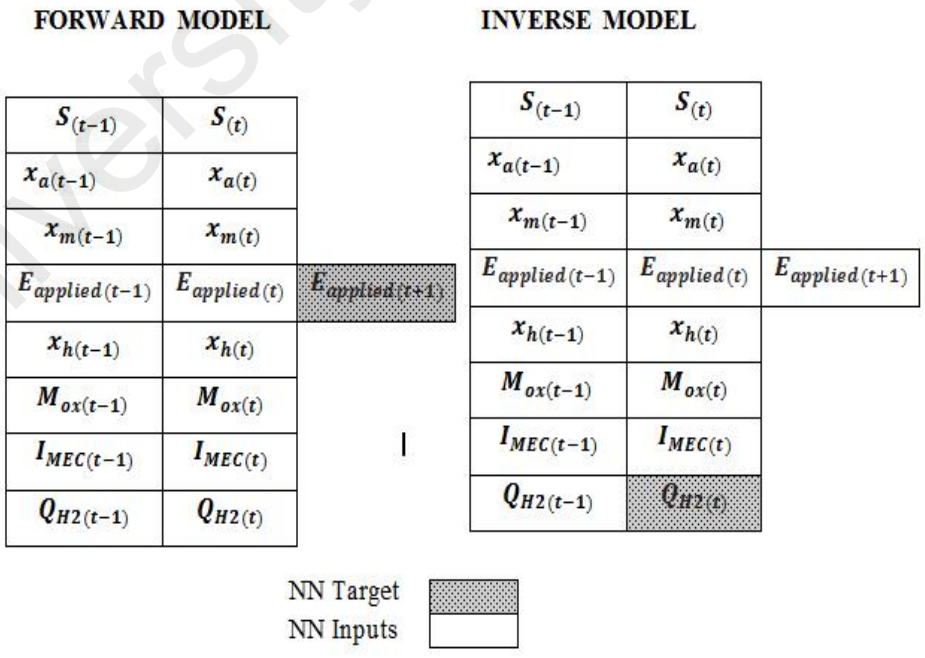

Figure 4.14: Assigned neural network inputs and output

4.4.2 Training and Validation data

The training of a neural network is done in conjunction with the back-propagation algorithm. The back-propagation pass is used to calculate the derivatives and the errors of every neuron in the network. The back-propagation algorithm learns to recognize and reproduce patterns in an iterative process whereby its weights are adjusted in order to minimize a selected error criterion.

Data for training the neural network in the simulation work are obtained by solving the ordinary differential equations (*ODE*) that govern the sequencing batch reactor as discussed in the previous chapter. Two sets of data have been prepared for training the neural network model and one is used for cross validation purposes in order to test the validity of the trained neural network models. The three training data sets are switched between each other during the training session in order to improve system identification by the neural network models (Hussain & Mujtaba, 2001). The training data sets for training neural network control model are shown in Figure 4.15.

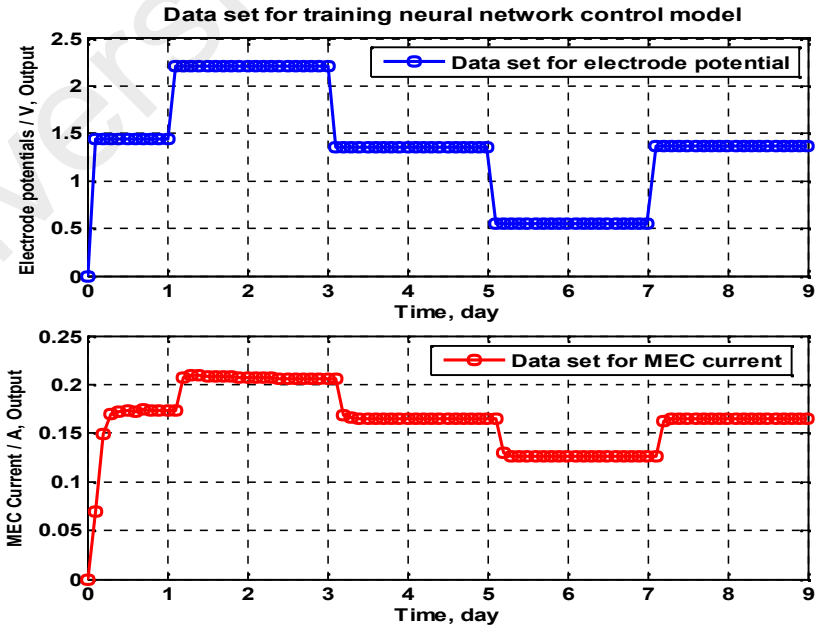

Figure 4.15: Data set for training neural network control model

4.4.3 Procedure for training neural network models.

The procedure for training the neural network models can be summarized as follows:

1. Determine the number of nodes in the hidden layer and the scaling parameters by trial and error method. The hidden nodes are chosen by trial and error where the network having the minimum-trained error with the corresponding hidden nodes will be chosen as the correct number of hidden nodes to be used. The data is scaled down between 0.05 to 0.95 using the following equations:

$$\text{Scale value} = \left\{\frac{a \quad v \quad -\text{m} \quad v}{\text{m} \quad v \quad -\text{m} \quad v}\right\}(0.95 - 0.05) + \min v \tag{4.11}$$

The actual value is given by:

$$\text{Actual value} = \frac{[sc \quad v \quad -m \quad v \quad]\, x\, [m \quad v \quad -m \quad v \quad]}{0.9 \quad -0.0} + m \quad v \tag{4.12}$$

2. The training cycle was repeated with all the sets of input/output pair patterns in data set, and the iteration is stopped when the error rate is small or reaches its defined value. The values of the network weighting coefficients were optimized using the Levenberg-Marquardt method. The performance was measured using the root-mean-squared-error (RMSE). The prediction results were evaluated by the root mean square error that is defined as:

$$R \quad = \sqrt{\left[\frac{1}{N}\sum_{t=1}^{N}(y(t) - \bar{y}(t))^2\right]} \tag{4.13}$$

Where *RMSE* is the number of training data points, $\bar{y}$ is the network prediction, y in the target value, and t is an index of the training data.

4.4.3.1 Forward Modeling

The most commonly used neural network architecture is the multilayer feed forward neural network shown in Figure 4.16. The basic feed forward network performs a nonlinear transformation of the input data in order to approximate the output data. The data from the input neurons is then propagated through the network via the interconnections such that every neuron in a layer is connected to every neuron in the adjacent layers. It is the hidden layer structures, which essentially define the topology of a feed forward network. Each interconnection is associated with it a scalar weight that acts to modify the strength of the signal passing through it. The output of a hidden neuron can be represented as follows:

$$S = \sum_{i-1}^{nh}(b + w_i I_i) \tag{4.14}$$

$$O = \frac{1}{[1+e^{(-S)}]} \tag{4.15}$$

where b is a bias, I_i is the ith input to the hidden neuron, $w_i$is the weight associated with I_i, and O is the hidden neuron output. Eq. (4.15) is known as the sigmoidal neuron activation function and its output is in the range (0, 1). Output layer neurons can also use the sigmoidal activation function. However, for process modeling applications, output layers usually use the linear activation function since it can give a wide range of outputs. Network weights are trained till such a time that the sum of squared network prediction errors is minimized. The prediction results are evaluated by root mean square error (*MSE*).

The forward *NNs* modeling refers to the open loop response of the *MEC* process. The networks have been trained to obtain the weights of every node and map the dynamic response of the input-output open loop dataset. The dataset is collected through a moving window approach. The model is made of 16 input nodes; the input nodes consist of data for substrate (S), anodophilic microorganisms (x_a), acetoclastic microorganism (x_m),

hydrogenotrophic microorganisms (x_h), oxidized mediator fraction (M_o), MEC current (I_M), hydrogen production rate (Q_2) and the single output node is electrode potentials (E_a). The procedure of training a neural network to represent the dynamics of the system is referred to as forward modeling. Forward modeling refers to training the neural network model to predict the plant output, *MEC* current (I_M). In this case, connections between layers, or weights, are changed during training in order to minimize the error between the actual plant output and the predicted output from the neural network model. The architecture of forward neural network model can be seen in Figure 4.16. The input to the network consists of present and past value of S,x_a,x_m,x_h, M_o , I_M , Q_2 and E_a .

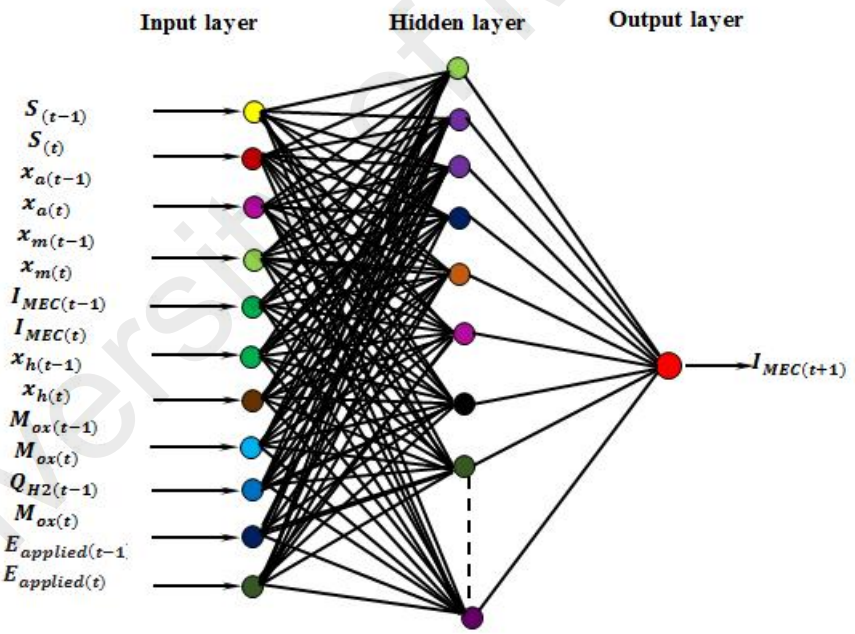

Figure 4.16: The forward model architecture for microbial electrolysis cell

The desired network output is the future *MEC* current ($I_{M\ (t+1)}$) values. Those input and output values are fed into the network in the moving window approach. From these training exercises, the neural network architecture produced is a 16 nodes input layer, 28

nodes of hidden layer and a 1 output layer system. The activation function utilized is the sigmoidal function in both the hidden and output layer. The forward model can be expressed mathematically as a function of inputs to the model as shown below:

$$I_{M\ (t+1)} = f\left(\begin{matrix} S_{(t)}, S_{(t-1)}, x_{a(t)}, x_{a(t-1)}, x_{m(t)}, x_{m(t-1)}, x_{h(t)}, x_{h(t-1)}, Q_{H2(t)}, Q_{H2(t-1)}, M_{o\ (t)}, M_{o\ (t-1)}, \\ I_{M\ (t)}, I_{M\ (t-1)}, E_{a\ (t)}, E_{a\ (t-1)} \end{matrix}\right) \quad (4.16)$$

The network is said to be properly trained when it satisfies the performance criteria with an *RMSE* of less then 0.001.

The validation result for the forward model can be seen in Figure 4.17. The results show that the neural network model has been properly trained to predict the forward dynamics of the system.

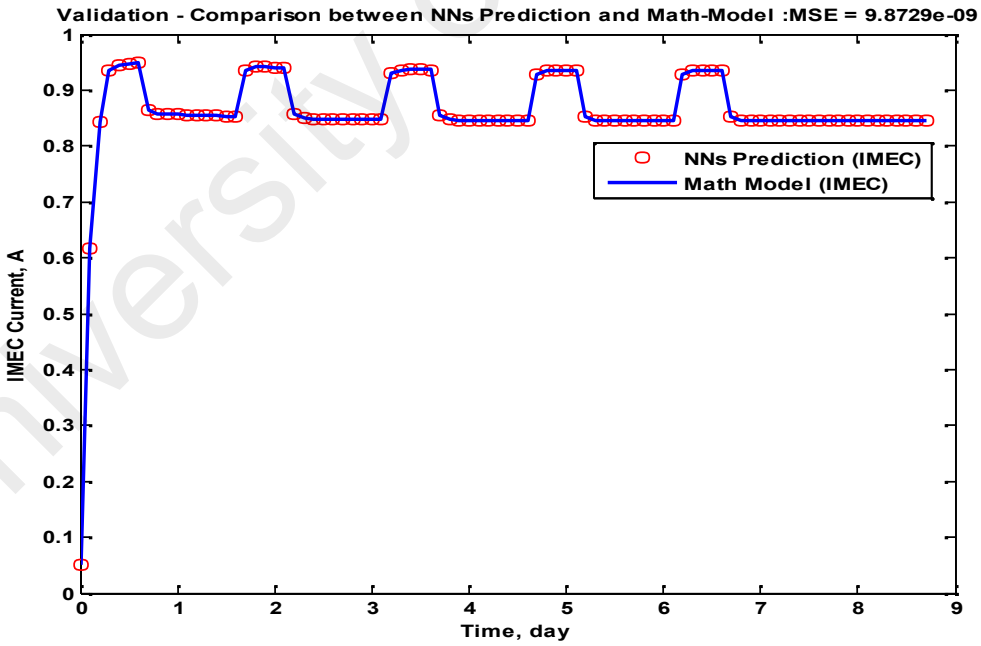

Figure 4.17: Forward model of *MEC* current for Neural Networks Prediction

General regression neural network (*GRNN*) is a neural network architecture that can solve the problem of function approximation using the standard regression multivariate

quadratic equations. *GRNN* is able to estimate the linear or nonlinear regression surface on the independent variables and does not require repetitive training procedures as in the feed forward back-propagation method. *GRNN* has four layers each layer serves as an input layer, layer pattern, the summation layer and output layer. The A layer of hidden neurons are used to hold the input vector, and a neuron output is used as a target value. Figure 4.18 shows the data training, validation and data test for forward model using regression neural network training.

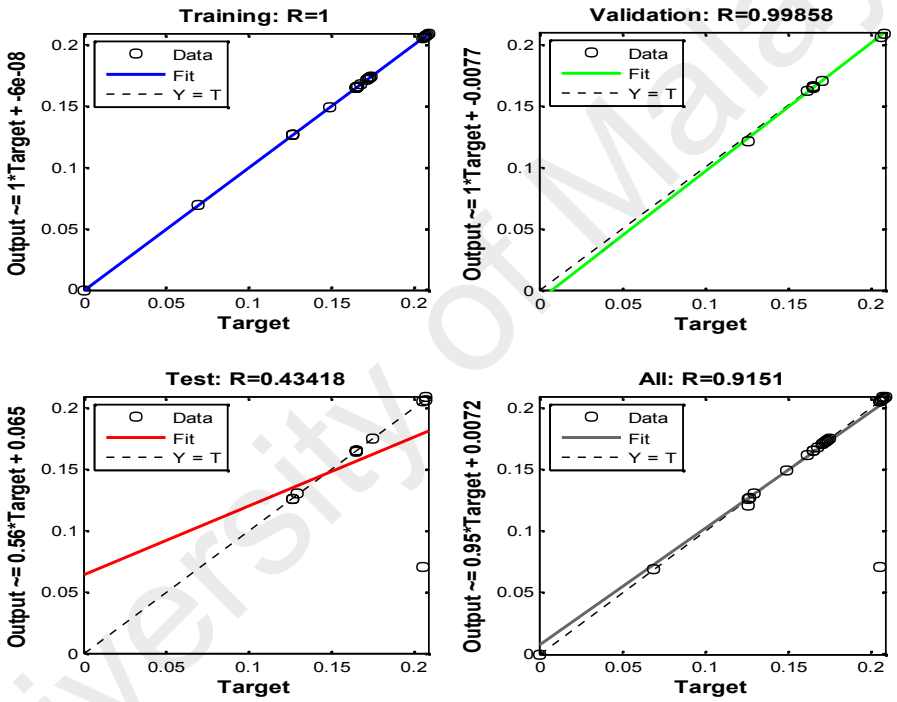

Figure 4.18: Neural Network training regression for forward model

The variable *R* is known as the proportion ofthe variability or sum of squares were used as the coefficient of determination between the model output and measures of the training. Set oftest data is used as an indicator that describes the numerical value of the estimated model.

4.4.3.2 Inverse Modeling

Inverse modeling refers to the training of the neural network in predicting the input to the plant given past data of the inputs and outputs together with the desired output. The inverse model is used directly as the controller within the feedback loop. Similar to the forward modeling methodology two training data sets were used, those were switch from one to the other during training to improve the identification process.

However, inverse *NNs* modelling are the opposite of open loop response which can be used as an ideal controller inside the control system. Inverse model is designed similar to the forward modeling approach. The 16 inputs node and single manipulated output variable has been selected; $S_{(t)}$,$S_{(t-1)}$; x_a *i.e.* $x_{a(t)}$,$x_{a(t-1)}$; x_m *i.e.* $x_{m(t)}$,$x_{m(t-1)}$;x_h *i.e.* $x_{h(t)}$, $x_{h(t-1)}$; M_o *i.e.* $M_{o\ (t)}$, $M_{o\ (t-1)}$; I_M *i.e.* $I_{M\ (t)}$, $I_{M\ (t-1)}$; Q_{H2} *i.e.* $Q_{H2(t)}$,$Q_{H2(t-1)}$ and output node is the electrode potentials (E_a) respectively. The detail network architecture for *NNs* controller development can refer to (Hussain & Mujtaba, 2001).

In determining the inverse model to use as the controller, the network architecture and activation functions that were chosen are similar to the forward model. For this inverse model, the two-layered feed-forward network that has 16 input nodes, 24 hidden nodes and 1 output node is used. The data sets generated from the training and validating, transfer functions and method of training the inverse model used are similar to the forward model. The architecture of the inverse model can be seen in Figure 4.19.

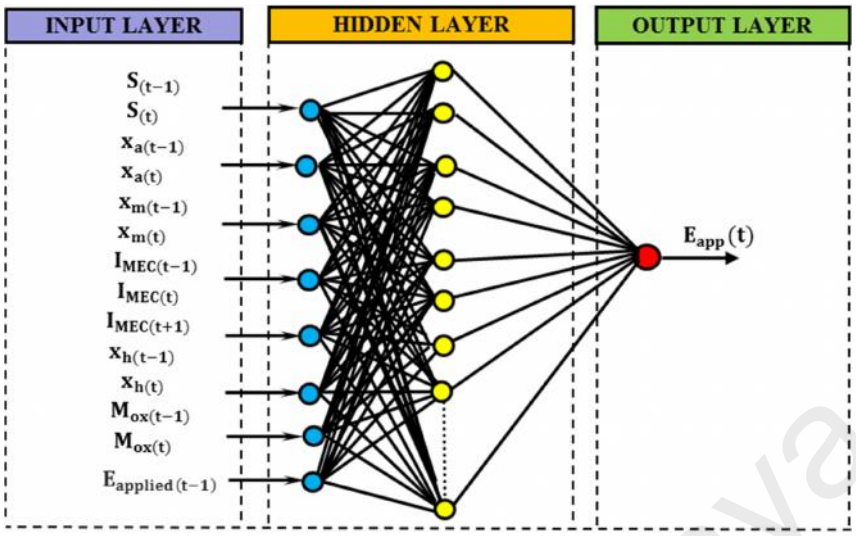

Figure 4.19: The inverse model architecture for *MEC* Reactor

During training the network is fed with the required future value, $I_{M\ (t+1)}$, together with the present and past input and outputs to predict the current input or control action, $E_{a\ (t)}$ as seen in Figure 4.19. The inverse model can be expressed mathematically as a function of inputs to the model as shown below:

$$E_{a\ (t)} = f\left(\begin{matrix} S_{(t)},\ S_{(t-1)},\ x_{a(t)},\ x_{a(t-1)},\ x_{m(t)},\ x_{m(t-1)},\ x_{h(t)},\ x_{h(t-1)},\ Q_{H2(t)},\ Q_{H2(t-1)}, \\ M_{o\ (t)},\ M_{o\ (t-1)},\ I_{M\ (t)},\ I_{M\ (t-1)},\ I_{M\ (t+1)},\ E_{a\ (t-1)} \end{matrix}\right) \quad (4.17)$$

Figure 4.20 show the performance of the inverse model using validation data. From the result, it can be seen that the artificial neural network accurately tracks the dynamics of electrode potentials ($E_{a\ \ \ }$). The results show that the neural network has been adequately trained, with only slight offsets at certain values in order to predict the inverse dynamics of the system and hence ready to be used as a controller in the direct inverse model based process controller for the *MEC* system.

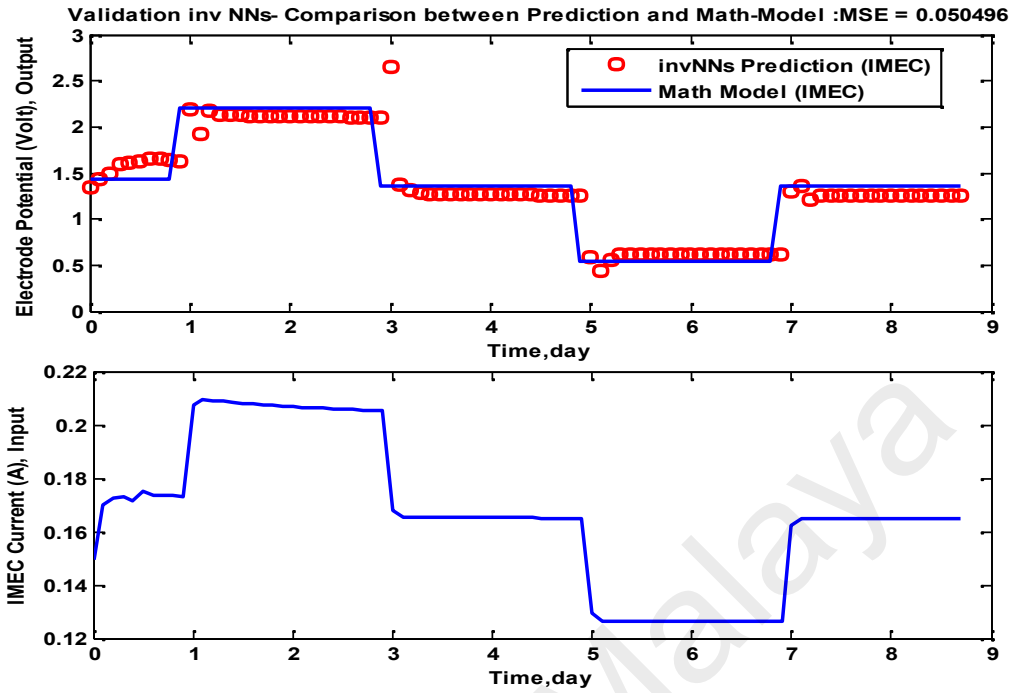

Figure 4.20: Inverse modeling of electrode potentials for training data

In the next sections will be discussed about the performance of the various neural network based controllers. The performance ofthe controller willbe investigated at the nominal operating conditions for multiple set-point tracking under loading disturbance rejection and measurement noise. The disturbances considered in this study generated through potential (V) changes of the counter-electromotive force (E_C) on the *MEC* system, which representing as internal disturbance of the system. The sampling time interval of 0.01 h is chosen in all these simulations.

4.4.4 Direct inverse neural network controller scheme

Direct inverse neural network controller is a control strategy of neural network controller by using the inverse model as a control method. In this control scheme, a neural network inverse models used as a control strategy by feeding it to the appropriate output control parameters to obtain the desired input targets. In the direct inverse neural network controller by using a specific value as set-points, then given to the network together with

the past plant inputs and outputs data to predict the desired current input. In this strategy the basic direct inverse neural network (*DINN*) model is used as the controller for the process and utilized directly as an element within the feedback loop.

Figure 4.21 shows the process and controller response using this strategy for a multiple set-point tracking study under nominal operating condition. It can be seen that the inverse model acts as the controller and provides the current control action with respect to certain current and past values of the process variables. In this case, the neural network model is trained to predict the required manipulated variable, i.e., electrode potential ($E_{a\ (t)}$) and to bring the process to the set point, i.e., *MEC* current (I_M)

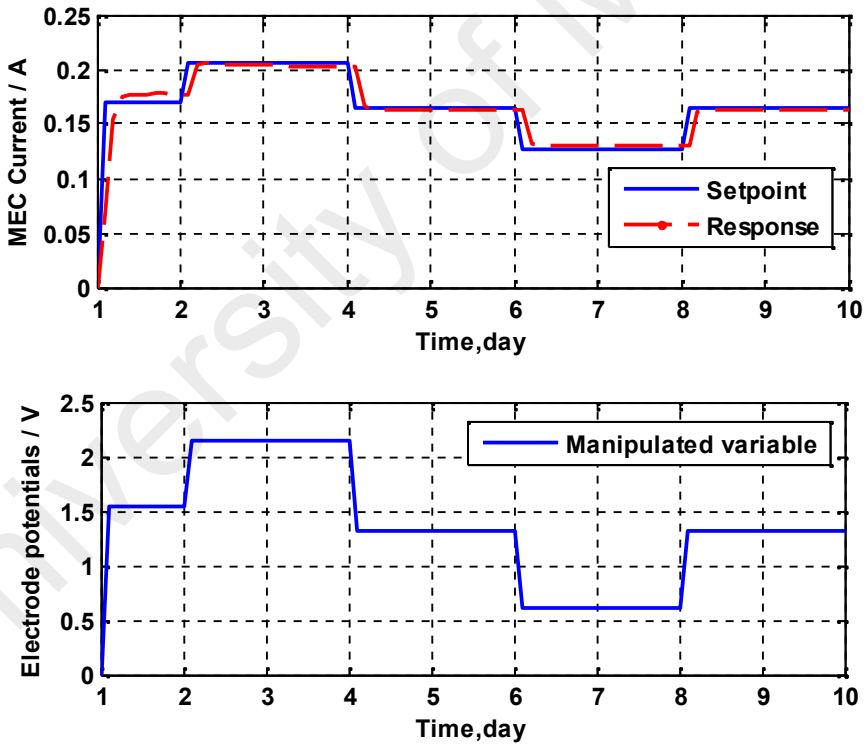

Figure 4.21: Process and controller response of basic *NN* controller with nominal operating condition for multiple set-point tracking study

Figure 4.22 shows the process and controller response of this *NN* controller under disturbance and set-point changes simultaneously. The disturbance considered in this

study was generated by changing potential of the counter-electromotive force (*V*) by decreasing and increasing it by range -0.2 *V* to 0.0 V and -0.2 *V* to -0.4 *V* from the nominal value. From Figure 4.22, it can be seen that the controller performs reasonably when responding to deviation but, it becomes sluggish when responding to large deviations in the process response and the controller does not reject the disturbance completely as noticed in the range t = 3 to 3.2 h, t=5 to 5.2 h, and t=7 to 7.2 h, respectively. Generally, it can be concluded that the disturbances slightly affected the system under *NN* controller strategy with simultaneously set-point changes.

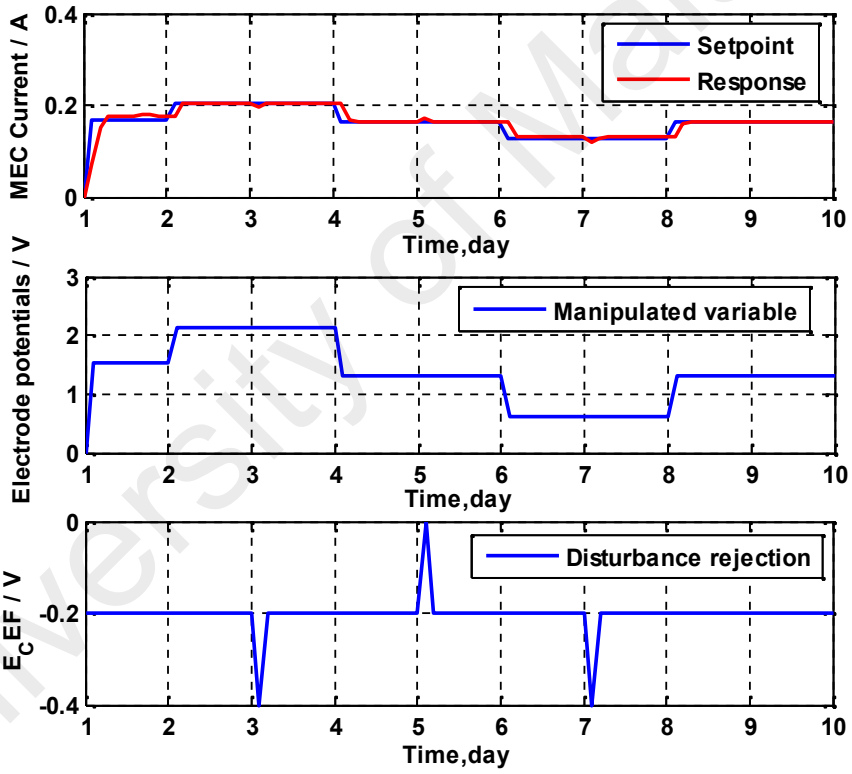

Figure 4.22: Process and controller response of basic *NN* controller for multiple set-points tracking in dealing with disturbance rejection study

Figure 4.23 represents the controller's performance subject to the condition in which the measurement of the controlled variable is corrupted by 10% noises. From this figure, it can be seen that, although the changes in set point can be tracked and the disturbances

can be rejected, the controller action is affected by the noises as significant fluctuations. It can be also noticed in the above-mentioned figure, in spite of disturbance and noisy measurement to the process, the controller is also capable of following the time varying characteristic of the process response and able to track the set-point changes.

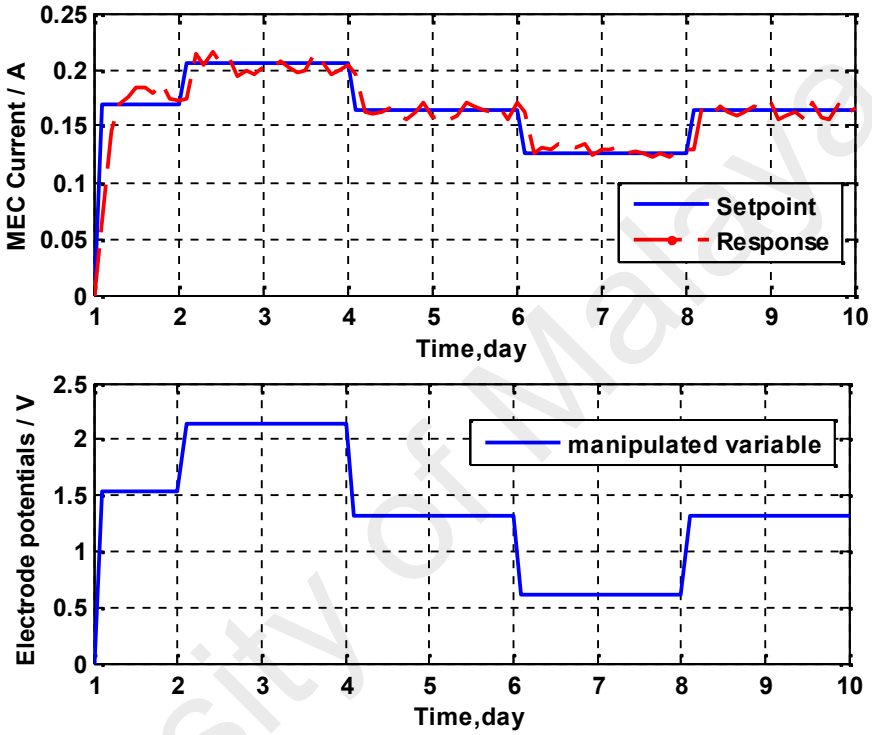

Figure 4.23: Process and controller response of basic *NN* controller for multiple set-points tracking in dealing with measurement noise

Figure 4.24 shows the performance of the controller when the measurement of the controlled variable is corrupted by disturbance and noisy measurement to the process under nominal operating conditions. The noises are assumed to come from the measurement of the *MEC* current in the reactor. However, the disadvantage exhibited by this controller is that the adaptation action works slowly so that the rise time or settling time of the process response is long and these capabilities do not cover a wide control

range. But overall, the performance of this controller is generally acceptable because the controller is successful to bring the process to follow the given set-point changes.

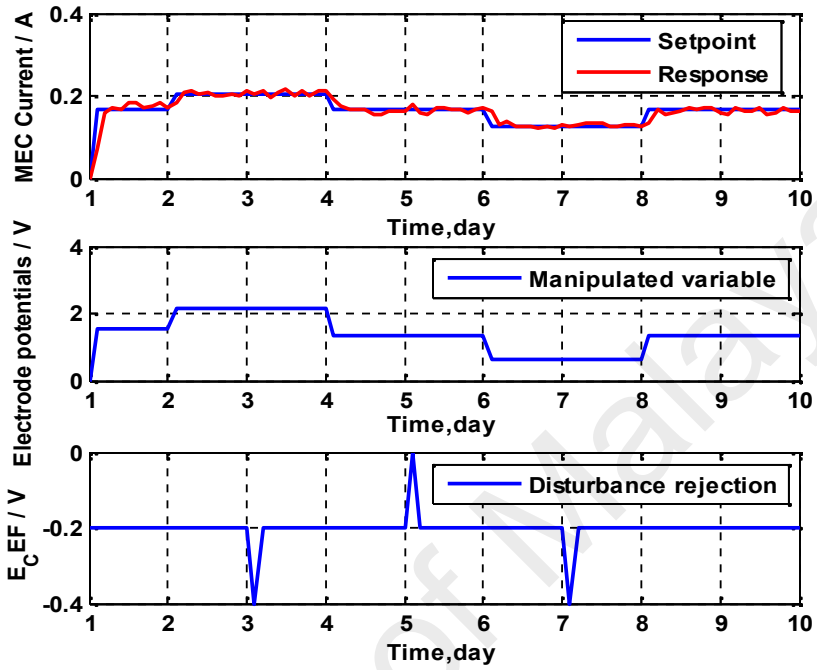

Figure 4.24: Process and controller response of basic *NN* controller for multiple set-points tracking in dealing with disturbance rejection study and measurement noise

Table 4.3 shows the comparison of the error in terms on the integral square error (*ISE*), integral absolute error (*IAE*) and integral time absolute error (*ITAE*) for basic neural network controller.

Table 4.3: Integral Square Error (*ISE*), Integral Absolute Error *(IAE*) and Integral Time Absolute Error (*ITAE*) for Direct Inverse Neural Network Controller performance using set-point changes

Comparison Control Performance for constant study	*ISE*	*IAE*	*ITAE*
Set-point change	0.016042	0.49603	16.2968
Disturbances	0.016945	0.5821	20.2987
Noise	0.019076	0.71676	27.8716
Disturbances and noise	0.019012	0.76699	28.5656

4.5 Internal Model Control (*IMC*) Scheme

In *IMC* the role of system forward and inverse models is emphasized (Garcia & Morari, 1982). In this structure, system forward and inverse models are used directly as elements within the feedback loop. *IMC* has been thoroughly examined with the application of standard robustness and stability analysis. Moreover, *IMC* extends reality to non-linear systems control. A system model is placed in parallel with the real system. The difference between the system and model outputs is used for feedback purposes. This feedback signal is then processed by a controller subsystem in the forward path; the properties of *IMC* using neural networks are straightforward (Hunt & Sbarbaro, 1991).

Some of the control strategy has been applied to control the reactor *MEC* as adaptive *PID* controller (Yahya et al., 2015). However, the conventional control methods cannot provide good damping performance, so that the necessary design Internal Model Control (*IMC*) as one of the control strategy. Development of control strategy is expected to provide satisfactory performance in the *MEC* system. *IMC* design is very suitable for the conditions of the linear process model and nonlinear. *IMC* control models can be applied in bioprocess systems because it has high durability and performance is satisfactory. However, the performance of the *IMC* controller will be less stable when applied to nonlinear processes with various operating conditions. *IMC*-Neural network is an alternative solution and controller design for the open-loop system and is one of the advanced control system based tuning method that has a high programming. Although in practice this method is still very rarely applied among industry.

One alternative approach is to develop black-box models (neural network) from either the data collection process of industrial or experimental work. Data nonlinear dynamics of the process of training the *NN* results are used as models of *IMC*, while the other *NN* training outcome data are used to study the dynamics of the process upside down and

used as a nonlinear *IMC* controller (Kansha et al., 2010). *IMC* algorithm when combined with neural network control method is able to adapt and improve the performance of the *IMC*, so this idea has been widely used in a variety of disciplines. In this study, the application of neural network neural network controller is adopted in the design of *IMC* showed very satisfactory results.

In the internal model control, both the forward and inverse models are used directly as elements within the feedback loop. The network inverse model is utilized in the control strategy, acting as the controller, has to learn to supply at its output, the appropriate control parameter, E_a for the desired targets, $I_{M\ S}$ at its input. The neural network forward model is applied in parallel to compare with the process model and the error between the plant output and the neural net forward model is subtracted from the set point before being feedback into the inverse model. The strategy the schematic of the internal model control is illustrated in Figure 4.25.

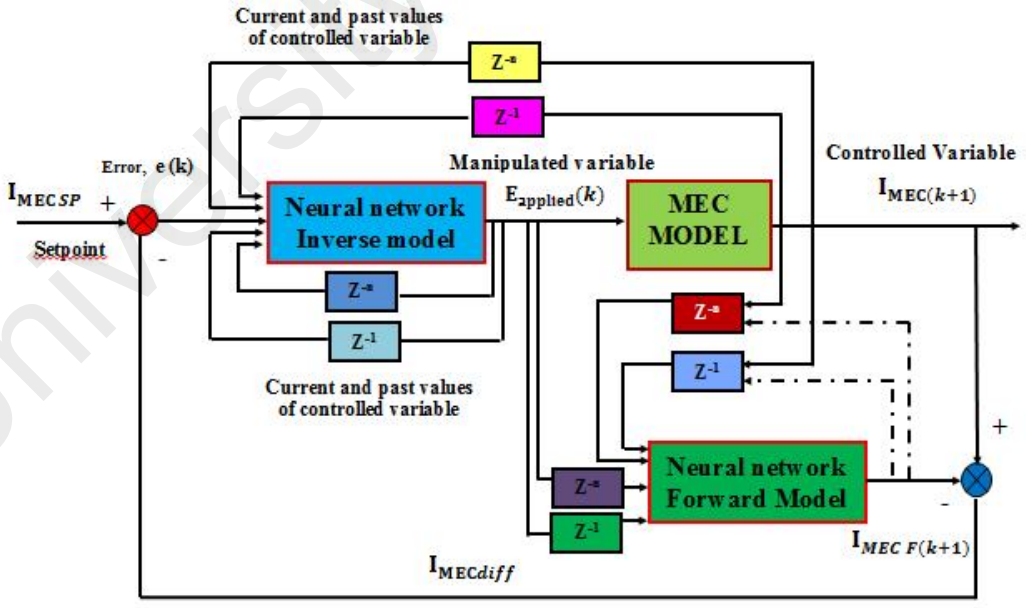

Figure 4.25: Block diagrams for Internal Model-based Control (*IMC*) system of neural network (*NN*) controller

Internal Model-based Control *(IMC*) system of neural network (*NN*) controller is one of the advanced control strategies by combining both forward and inverse models in the control scheme. In the *IMC* system, the inverse model is used as acontroller, while the forward model which represents the dynamic of the process are placed in parallel with the process/ model of a system. Figure 4.26 shows the process and controller response of the *IMC-NN* controller for set-point tracking performance. From the figure, it can be seen that the error between the process output and the neural network forward model is subtracted from the set-point changes before being fed into the inverse model. The controller is successful in managing the process to follow the given set point changes and *IMC-NN* controller is able to give offset free response.

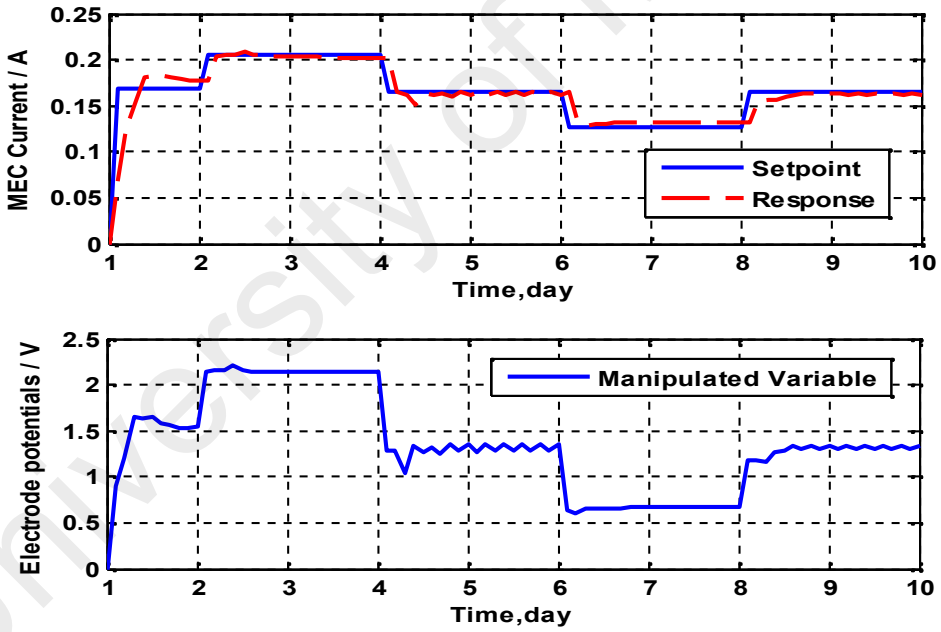

Figure 4.26: Process and controller response of *IMC* for nominal operating condition

Figure 4.27 shows the Internal Model-based Control (*IMC*) system of neural network (*NN*) controller for tracking set-point changes with injected the disturbances in the system. The disturbances rejection test is intended to determine the effect of disturbances

given to the system and to see the controller's ability to reject it. In this test, the disturbance to the system which includes the change of the counter-electromotive force (*V*) by range -0.2 *V* to 0.0 *V* and -0.2 *V* to -0.4 *V* from the initial nominal operating condition of the plant. The results show that the controller is able to bring back the *MEC* current to the set-point in a short time with minimal overshoot and fluctuations.

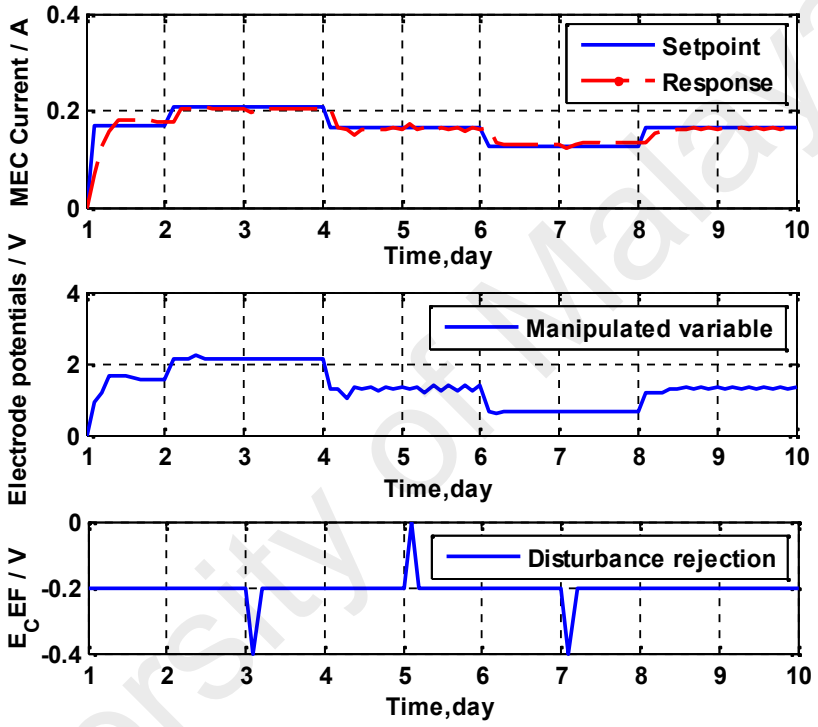

Figure 4.27: Process and controller response of *IMC* for multiple set-points tracking with disturbance rejection study

The random noisy ($\upsilon(k)\neq 0$) which is added to nonlinear system given by the equation added to MEC system. The noise level of a process can be calculated by the equation Signal-to-Noise Ratio (*SNR*) as follows:

$$S = \frac{\sum_{k=1}^{N}(y(k)-\bar{y})^2}{\sum_{k-1}^{N}(v(k)-\bar{v})^2} \tag{4.18}$$

Where $\bar{y}$ and $\bar{v}$ are respectively the output average value and noise value.

Figure 4.28 shows the performance of the process and controller response of *IMC* when the measurement of the controlled variable is corrupted by noise under nominal operating conditions. In this test, the controlled variable is corrupted by 10% noises and the controller action is able to handle the noises although the process is very fluctuating.

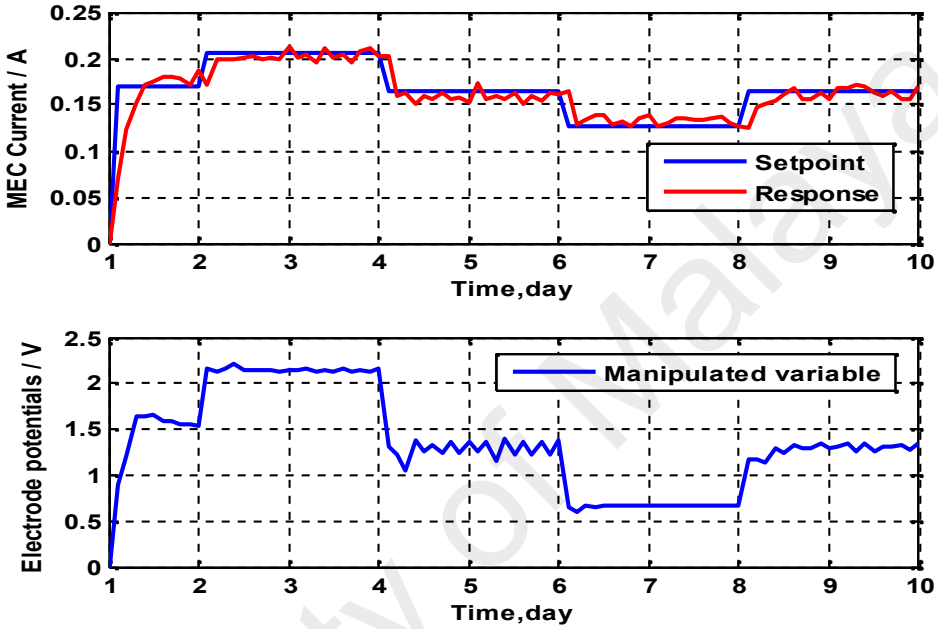

Figure 4.28: Process and controller response of *IMC* for multiple set-point tracking study with measurement noise

Figure 4.29 shows the controller response of *IMC* for disturbance rejection study and measurement noise. The disturbance and noise introduced in the system simultaneously throughout the process to observe the performance of the controller and phenomenon of the process. If observed carefully there are some short comings obtained from the controller such action adaptation works slowly, the rise time or settling time of the process response is rather long. Generally, it can be seen that although the disturbance or noise is given to the process, the controller is able to track the set-point changes and the controller is able to follow the time varying characteristic of the process response.

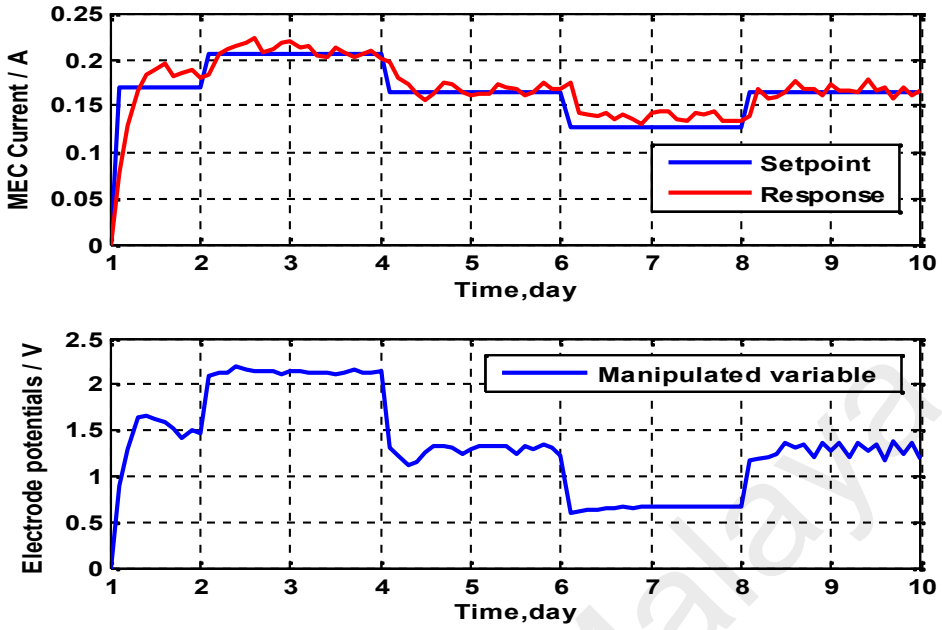

Figure 4.29: Process and controller response of *IMC* for multiple set-point tracking study with disturbance rejection study and measurement noise

To overcome some of the problems in the *IMC* controller and to improve the performance of the process, especially for the treatment of disturbance, noisy measurements, and the delay problem, then one solution is to develop a hybrid technique of neural network controller. Table 4.4 shows the comparison of the error in terms on the integral square error (*ISE*), integral absolute error (*IAE*) and integral time absolute error (*ITAE*) for internal model-based control (*IMC*) system of neural network (*NN*) controller.

Table 4.4: Integral Square Error (*ISE*), Integral Absolute Error *(IAE*) and Integral Time Absolute Error (*ITAE*) for Internal Model-based Control (*IMC*) system of neural network (*NN*) controller using set-point changes

Comparison Control Performance for constant study	*ISE*	*IAE*	*ITAE*
Set-point change	0.019039	0.63646	21.5856
Disturbances	0.019584	0.66506	23.3581
Noise	0.022654	0.85717	32.7788
Disturbances and noise	0.023003	0.92802	34.9735

4.6 Hybrid Neural Network Controller Scheme

The basic principle of artificial neural networks (*ANNs*) is to mimic the working of the human brain nervous system where information between one neuron to other neurons is connected to each other. Each input-output value of inter-connected with a certain numerical weight and between one nodes with other nodes adapt to each other and stored in the inter-unit power of certain connections. Hybrid neural networks (*HNNs*) controller is one of the model control strategy developed by using neural networks and combined with other components such as *PID*, fuzzy logic or Kalman Filter.

In this study, the main focus is to develop a hybrid technique of neural network controller in controlling microbial electrolysis cells in a fed-batch reactor process. Hybrid Neural Network Controller has a better performance when compared with the Direct Inverse Neural Network Controller. Although the inverse neural network controller using neural black-box models have been widely used in applications of biochemical processes (Thibault et al., 1990), but still have many short comings such as still having a high overshoot. And the controller performance is still slow when responding to large deviations in the response process. One solution to overcome this problem is to develop Hybrid Neural Network Controller. The hybrid scheme is consists of a basic neural

network (*NN*) controller and a proportional integral derivative (*PID*) controller. The schematic of the hybrid controller is illustrated in Figure 4.30.

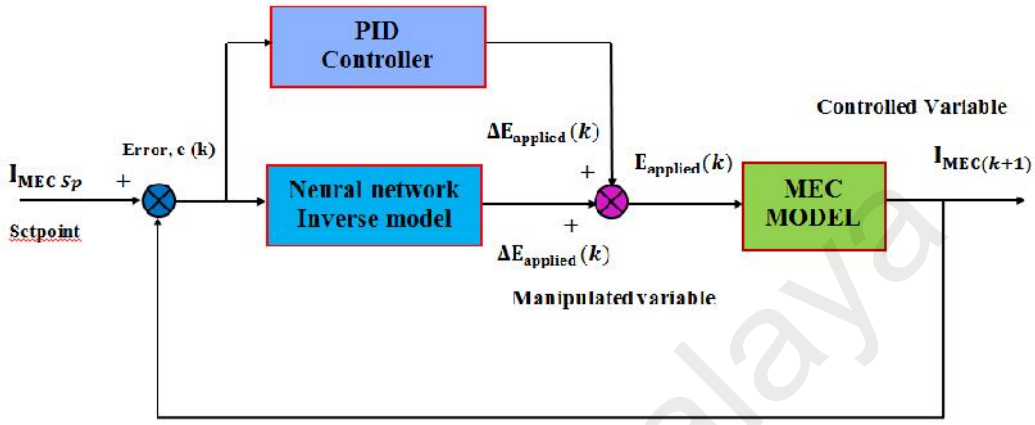

Figure 4.30: Block diagrams for hybrid control system of neural network (*NN*) controller combination with proportional integral derivative (*PID*) controller

The actual control action in this control system is the combination of the two controllers. The combination is arranged in parallel manner as shown in Figure 4.30 above. Here, the role of the *PID* controller is to compensate for the possible sluggish control action resulting from the basic neural network controller.

Consider the following *PID* control law:

$$\Delta E_a \quad _t = k_c\left(e_t + \frac{\Delta t}{k_I}\sum_{i=1}^{t} e_i - \frac{k_d}{\Delta t}(e_t - e_{t-1})\right) \tag{4.19}$$

where k_c, k_I and k_d are proportional, integral and differential constants, respectively. In the implementation, the value of k_c, k_I and k_d, above were scheduled according to linear segments based on the reference variable of electrode potentials (E_a). The control law of this hybrid controller is formulated as follows:

$$E_a \quad _{(t+1)} = E_a \quad _t + \Delta E_a \quad ^P_{(t+1)} + \Delta E_a \quad ^N_{(t+1)} \tag{4.20}$$

Where ΔE_a $^{P}_{(t+1)}$ is the output of *PID* controller and ΔE_a $^{N}_{(t+1)}$ is the output of the basic neural network controller.

Figure 4.31 shows the process and controller response of multiple setpoint tracking study for *HNN* controller with nominal operating condition. It can be seen that the Hybrid *PID*-neural network model-based controller performs reasonably well when responding to deviation and the controller is also capable of following the time-varying characteristic of the process in most conditions.

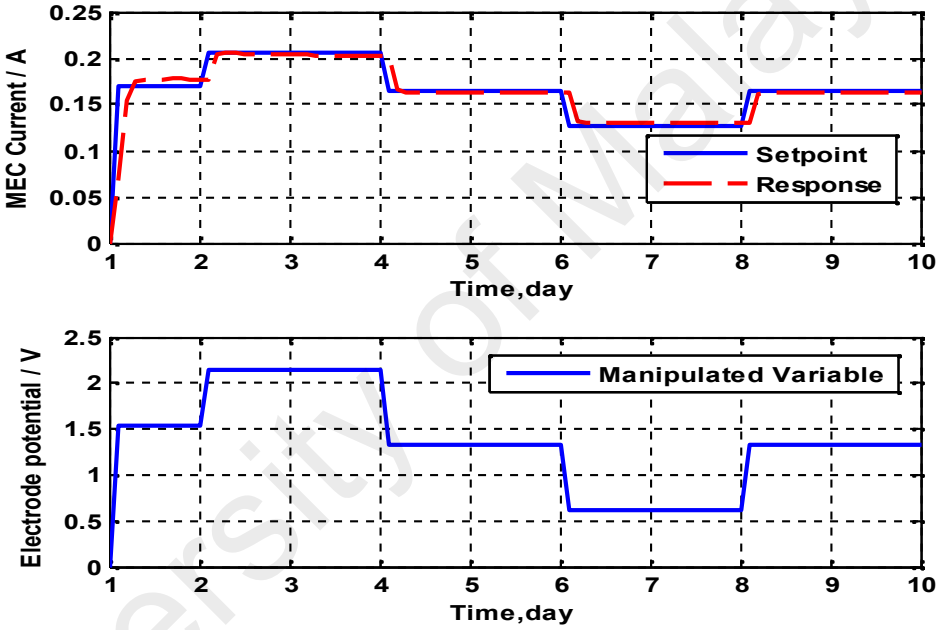

Figure 4.31: Process and controller response of set-point tracking performance for *HNN* controller with nominal operating condition

Figure 4.32 shows the *HNN* model-based controller for multiple setpoint tracking with disturbance rejection study in the *MEC* system. From the figure, it can be seen that the variation in disturbance was generated by changing the counter-electromotive force (nominal value of -0.20 *V*). Based on these results, the performance of this controller is generally acceptable and the *HNN* model-based controller gave smoother responses in the *MEC* system.

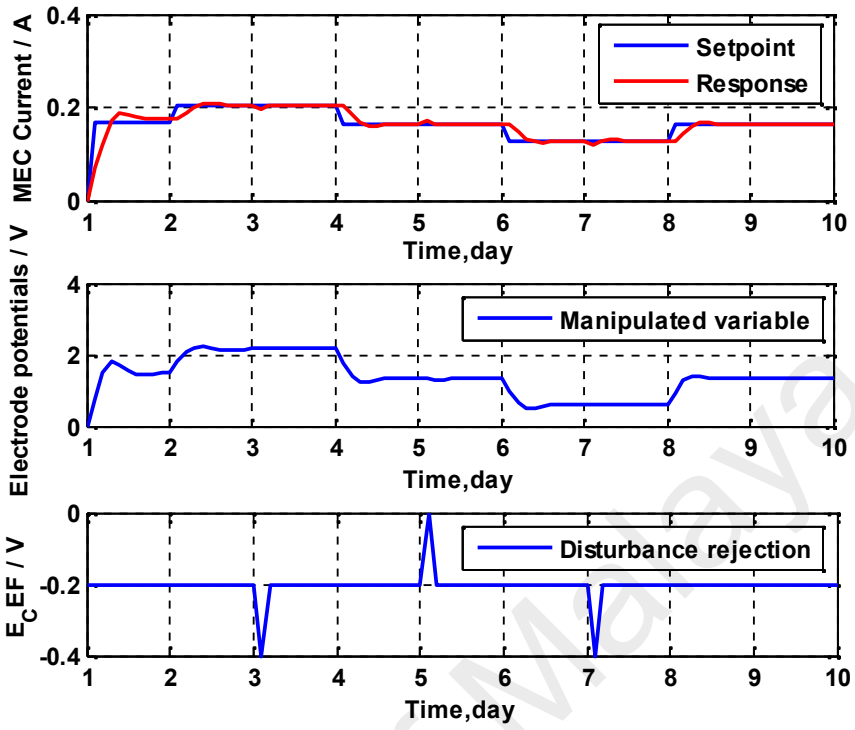

Figure 4.32: Process and controller response of set-point tracking performance for *HNN* controller with disturbance rejection study

Figure 4.33 shows the performance of the *HNN* controller when the noises are assumed to come from the measurement of the *MEC* current in the reactor. From these studies, it can be seen that the *HNN* controller responses are still stable, acceptable and stillable to bring *MEC* current closely to the set point with a small overshoot, oscillations and offset although the controlled variable is corrupted by noise.

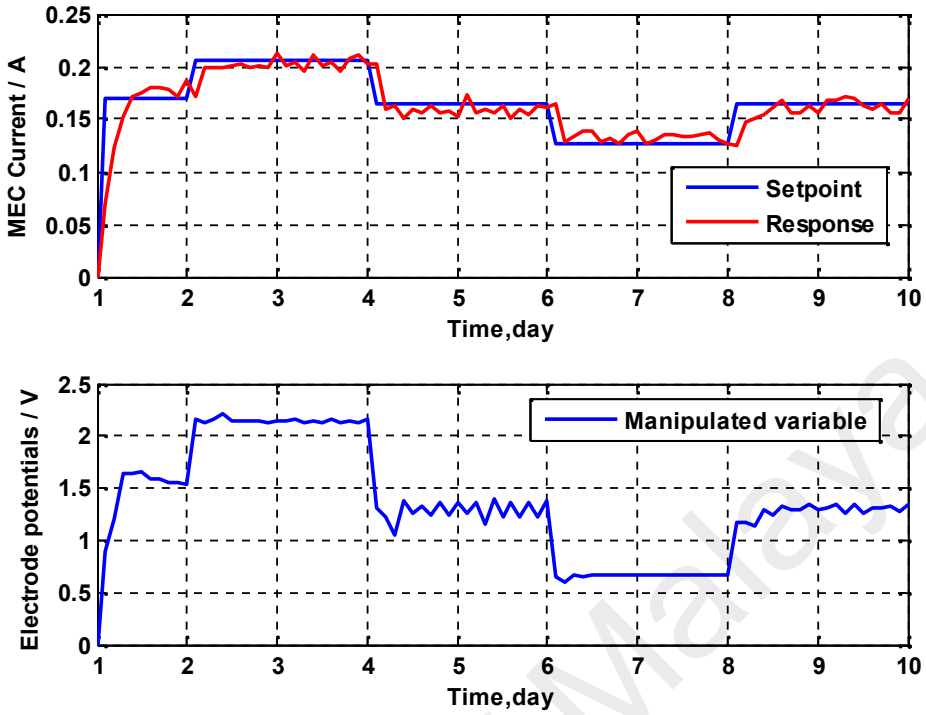

Figure 4.33: Process and controller response of set-point tracking performance for *HNN* controller with measurement noise

Figure 4.34 shows the *HNN* controller response of set-point tracking study for the disturbance and noise test. From the figure shows that the occurrence of fluctuation and oscillations due to the presence of disturbance and noise in the *MEC* process, so *HNN* controller cannot control well to the *MEC* current value according to the desired set-point. But overall, from observation it can be seen that the level of resistance *HNN* controller due to the influence of fluctuation and oscillations in the *MEC* process is still within the range of permissible and the controller performance is better when compared with other control strategies.

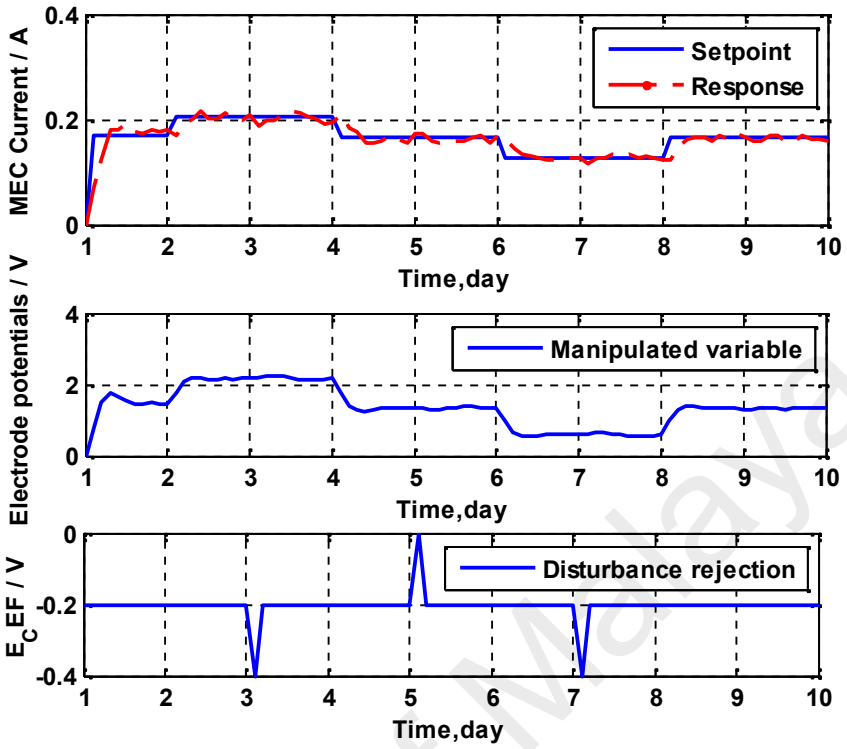

Figure 4.34: Process and controller response of set-point tracking performance for *HNN* controller with disturbance rejection study and measurement noise

When compared with other controllers, the hybrid neural network (*HNN*) is a more powerful and flexible controller because it was able to overcome tracking set-point changes, load disturbance and interrupted of noise in a more efficient manner. This proves its ability and capability to operate in future in real plant of *MEC* reactor, in which the hybrid neural network (*HNN*) based controller has never used before. Table 4.5 shows the comparison of the integral square error (*ISE*), integral absolute error (*IAE*) and integral time absolute error (*ITAE*) for hybrid neural network (*HNN*) controller.

Table 4.5: Integral Square Error (*ISE*), Integral Absolute Error *(IAE*) and Integral Time Absolute Error (*ITAE*) for hybrid technique of neural network controller using set-point changes

Comparison Control Performance for constant study	*ISE*	*IAE*	*ITAE*
Set-point change	0.020488	0.58176	17.6339
Disturbances	0.020559	0.62782	20.2174
Noise	0.022149	0.77702	28.1243
Disturbances and noise	0.024363	0.83611	29.2277

In summary, these results show that the comparative study on the *MEC* reactor with various simulation tests have been conducted involving conventional *PID*, adaptive *PID*, direct inverse neural network (*DINN*), Internal Model Control (*IMC*) and hybrid neural network based model (*HNN*) controller. Neural network is an effective technique and a powerful tool to be used in modelling of complex processes, unknown systems and control strategy. Neural network are able to cope with non-linear process between input and output variables without the requirement of explicit mathematical correlation. This comparison shows that *HNN* provides the best control performance in terms of nominal and *MEC* model mismatch cases. Overall this indicates that the hybrid neural network based model (*HNN*) controller gives better results in terms of lower error and faster response time. *HNN* controller gives fast settling time in the response, less overshoots, minimal offset and able to keep the performance for any variation of disturbance and noise. Thus, *NN* controller performances are surpassing the other types of controller and perform better in all the analyzed cases. To determine the performance of all controllers, each respective performance can be seen on Table 4.1 to Table 4.5 in previous Chapter 4 to highlight respective performance comparison of each strategy in terms on *ISE, IAE* and *ITAE*.

CHAPTER 5: ON-LINE MODEL VALIDATION AND CONTROL STRATEGY FOR MICROBIAL ELECTROLYSIS CELLS REACTOR

5.1 Introduction

In this chapter will be presented in detail about the on-line implementation of control strategies for biohydrogen production in microbial electrolysis cell reactor system. In general, the discussion in this chapter will be divided into three parts. The first part will be discussed about the experimental reactor design and operation, instrumentation and hardware specifications that are required for on-line measurement. In the second part will be presented about a general description of the specification of substrate used in the *MEC* reactor, inoculum preparation and secondary cultivation and experimental pretreatment and analysis methods.And the last section will be discussed on start-up process value and noise filtering, open-loop validation models for microbial electrolysis cell (*MEC*), Process and Instrumentation Diagram (*P&ID*), online signal flow diagram, closed-loop control for the online system, *PI* Closed loop control for online system and implementation of neural network control strategy. Performance comparison between the PI controller and the Neural Network controller on an on-line test that involves some set-point change and disturbance rejection will be reviewed and discussed in this chapter.

5.2 Design of Microbial Electrolysis Cell Experinmental Setup

This research will be presented strategy for *MEC* reactor control on a pilot plant-scale reactor. Most research has been done but generally still at the lab-scale, using a pilot-scale plant is expected to make the process conditions closer to the real plant. The *MEC* for

reactor design used in this research is to design relevant closed-loop dynamic and develop an advanced control strategy to regulate the *MEC* process.

To achieve good control performance at *MEC* reactor will require an appropriate pilot plant design. Besides using low-cost materials and a sustained period of time, it should also be noted that other parameters is very important as electrode potential, current, reactor temperature, *pH* and turbidity. Selection of appropriate materials for the design of the pilot plant could also provide a better quality in the performance of the control. The time delay can be present during the process is underway, and it will create instability in the model and the control system. If the pilot plant is designed well, then this delay time can be reduced to a minimum.

5.2.1 *MEC* Reactor

The *MEC* pilot plant is located at pilot laboratory of Chemical Engineering Department, University of Malaya. Figure 5.1, show pilot plant design, instrument and process of MEC reactor for experimental setup.

Characteristics of the pilot scale reactor used herein were designed using a “single membrane-less chamber”. The *MEC* reactor is made of *PVC* clear container products with a thickness of 12 mm and has a 10 liter capacity. Then the reactor was connected to two tanks with the size of each 5 liter. The first tank that serves as a supply for the substrate and the second serves as an effluent tank. Because the design of the reactor using a "single membrane-less chamber" type so that the cathode and anode installed in series without separated by membranes.

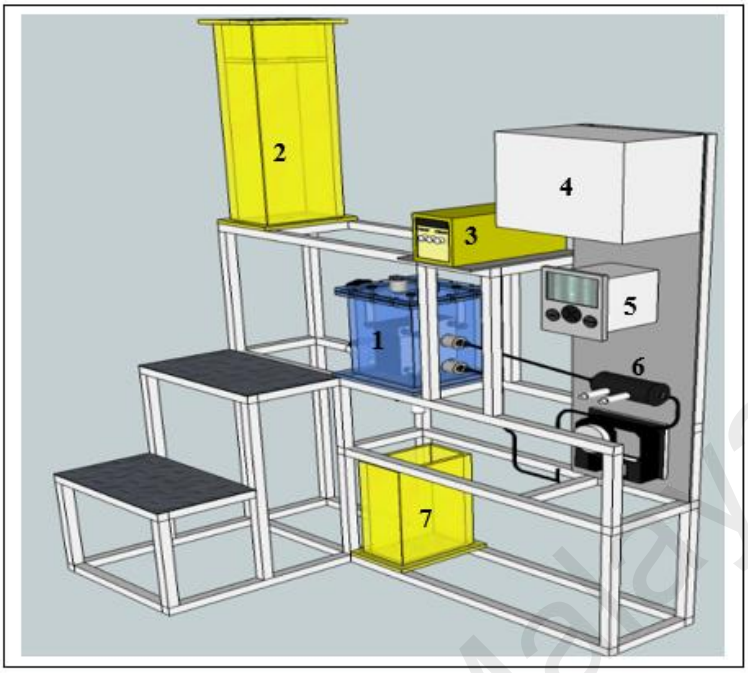

1-MEC reactor, 2-Wastewater Tank, 3-Power Supply, 4-Control Panel, 5-AquaPro Display for pH & Turbidity Sensor, 6-Pump, 7-Effluent Tank.

Figure 5.1: Detailed process plant schematic and instrumentation process for *MEC* fed-batch reactor setup

Cathode and anode materials used in this study were a stainless steel plate. The distance of space between the cathode and anode plate each about 2 mm. Cathode and anode material is made of stainless steel plate (*SS* 304) with a size of 150 mm x 150 mm x 2mm. The amount of each of the cathode and anode used in this system is 10 units (Figure 5.2).

1-MEC reactor (12 mm *PVC* clear container), 2-Reactor and SS304 Plate, 3-Cathode and anode parallel plate design, 4-Upper cover of the *MEC* reactor

Figure 5.2: Schematic description and design of apparatus for *MEC* set-up in Fed-batch Reactor

MEC reactor consists of seven inlets and outlets of flow. Two flow inlets located on the left side of the reactor, which one is used as a substrate supply and the other one serves to supply the nitrogen gas in the reactor. At the top of the reactor consists of two points, one serves as a collection of outlets for gas flow H_2 and one point again function as a *pH* regulator and flow inlets nutrients to bacteria. While on the right side of the reactor consists of a two-point function as inlets and outlets of flow from the reactor to the pH and turbidity sensors. At the bottom of the reactor there is a stream outlet for liquid waste disposal. A detailed description of the design of equipment for *MEC* set-up in Fed-batch reactor can be seen in Appendix 1.

5.2.2 *pH* and turbidity sensor

pH sensor is a type of measuring instrument used to measure the degree of acidity or alkalinity of a liquid that is connected to an electronic device that measures and displays the *pH* value. The working principle of the *pH* sensor is based on the electro-chemical potential that occurs between the liquid contained in the sensor probe in the form of glass electrode (glass electrode) by measuring the amount of hydrogen ions or potential of hydrogen in solution. Glass electrode can be damaged due to dirt or sludge filled of liquid in the reactor. Buffer calibration check is required to keep the value of the error can be minimized. To optimize the performance of *MEC* reactor, the catholyte *pH* is one of the parameters that need to be considered. Previous research has shown that the production of hydrogen can level at *pH* 5 to *pH* 9 (Call & Logan, 2008; Rene A Rozendal et al., 2008).

Turbidity testing instrument turbidity meter is a fluid which is expressed as a ratio of the reflected light intensity of the light received by the sensor. Turbidity can be seen from the insolubility concentration and the presence of particles in liquids measured in Nephelometric Turbidity Units (*NTU*). In palm oil mill effluent (*POME*), high turbidity value that can be caused by dissolved particles such as organic material, small particles and microorganisms. In the *MEC*, the turbidity value can be used as indicators and quality control to ensure the efficiency and performance of the reactor.

In this study, for *pH* and turbidity sensors are equipped using AquaPro. One of the advantages of the device is to have color graphics display and *USB* data port to transfer measurement data at various environmental conditions (Figure 5.3). AquaPro digital sensor is an on-line liquid analytical measurement that are not only capable of measuring *pH* and turbidity but also capable of a wide range of other parameters such as *ORP*, *DO*, conductivity, ozone, suspended solids, free chlorine and others. When viewed from the

specification tool, AquaPro able to measure the *pH* value from *pH* = 0-14 and turbidity = 0-4000 *NTU*, while the current outputs can be configured for 0 to 20 mA and 4 to 20 mA in both linear and log formats.

1-pH and turbidity sensor, 2-Flowrate meter setting pump, 3-Graphics display and USB data port of AquaPro sensor

Figure 5.3: AquaPro equipment for *pH* and turbidity sensors

5.2.3 Power Supply

In the *MEC* process, so that hydrogen gas can form in the reactor, it would require a supply of energy or voltage from a source outside the system. Voltage monitoring is required continuously and it is sent to the reactor circuit *MEC* that obtained from a power supply. The main function of the power supply is to convert one form of electric energy in the form of voltage alternating current (*AC*) and then drain into a series diode and convert it into direct current (*DC*). In MEC reactor, additional voltage is supplied from a power supply connected to the negative terminal (anode) and the positive terminal (cathode) and then sends a current of the second terminal hardware to the computer via the "Data Acquisition". The amount of current and voltage in the reactor was continuously monitored and controlled automatically using a computer program. In this study, a power supply with the brand "New *PL* and *PL-P* Series" with voltage ranges from 0*V* to 15 *V*

with 10 m*V* resolution and current ranges of 0-5 *A* with 1 mA resolution are used. Power supply is also equipped with "Digital Bus Interface *RS232, USB* and *LAN*" (Figure 5.4).

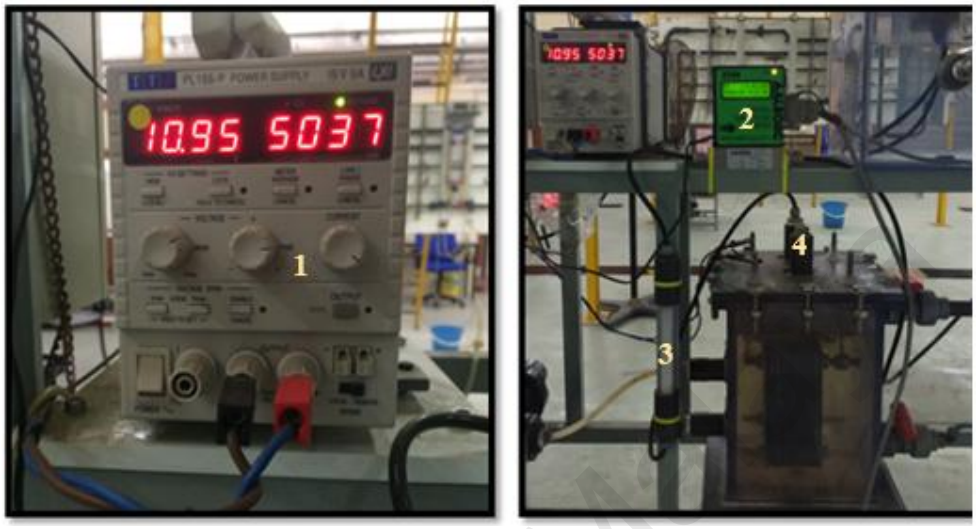

1-New PL and PL-P series power supply, 2-Digital Mass Flow meter, 3-Silica gel for hydrogen gas dryer, 4-Outlet flow for hydrogen gas.

Figure 5.4: Description and design of apparatus for power supply and mass flow meter

5.2.4 Digital mass flow meter

Digital mass flow meter is one of the measuring instruments used to measure the flow velocity or flow rate and total mass or volume of liquid or gas. In the digital mass flow meter equipped with a sensor and indicator function to read the parameters of the flow of a gas or liquid that is displayed the form of data or numbers. And then the data is forwarded to produce electricity or signals that can be used as a control input system. In this experiment, *XFM* series Mass Flow Meters are used to measure the flow rate of hydrogen gas produced from *MEC* reactor and controlled continuously using computer software. This instrument comes with calibrated 0-5 *VDC* or 4-20 mA output signals and optional local connection 2x16 characters *LCD* (Figure 5.5). The workings of this measure is the first flow of gas entering the Mass Flow transducer is split by shunting a small portion of the flow through the capillary tube stainless steel sensor, then the flow

rate measured in the sensor tube is directly proportional to the total flow through the transducer. The resulting output signal is a function of the amount of heat carried by the gases to indicate mass flow rate based molecules.

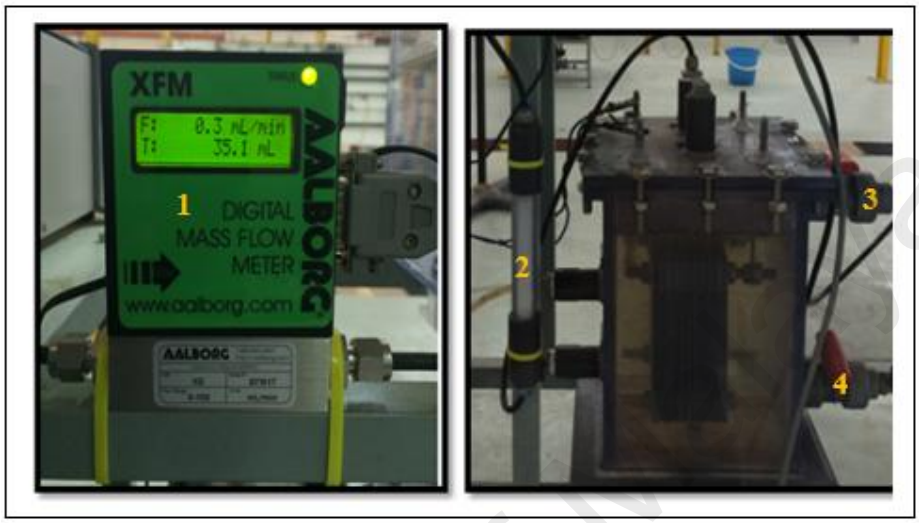

1-Digital Mass Flow meter, 2-Silica gel for hydrogen gas dryer, 3-Inlet-valve flow from *pH* and turbidity sensor, 4-Outlet-valve flow to flow meter pump.

Figure 5.5: Design of apparatus for mass flow meter and hydrogen gas dryer

5.2.5 Data Acquisition (*DAQ*) Display

To maximize the performance of *MEC* pilot plant, it is necessary to observe, measure and controls every variable in the process continuously. Each value measurement of process variables such as current, voltage, hydrogen production rate, pH and turbidity is still in the form of analog signals. Data acquisition or *DAQ* is a data acquisition system that is able to convert from analog signal to digital data, or better known as analogue-to-digital transformers (*ADC*), and converting digital data into analogue signals, known as digital-to-analogue transformers (*DAC*) (Figure 5.6).

At the end of this decade, *DAQ* has been widely recognized for laboratory automation, industrial monitoring and control. Usually the device is connected to a *PC* to perform the

functions of measurement and control instrumentation applications. *DAQ* module used in this work is National Instruments *USB-6009*.

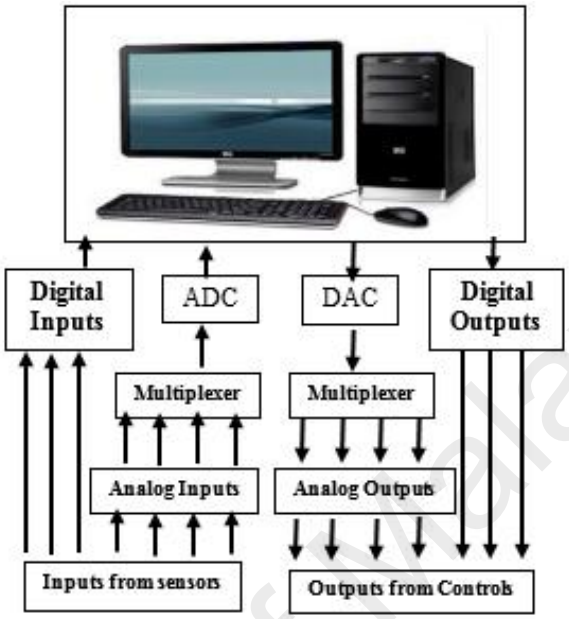

Figure 5.6: Simplified block diagram of *DAQ* for *ADC* and *DAC*.

The data acquisition has eight analog input (*AI*) channels, two analog output (*AO*) channels, 12 digital input / output (*DIO*) channels, and the 32-bit counter when using a full speed *USB* interface (Figure 5.7).

Figure 5.7: Design of National Instruments *USB-6009* for data acquisition (*DAQ*)

5.3 Substrates used in *MEC* reactor

Substrate is one of the most important parameters for *MEC* reactor, as well as serve as a source of fuel but also used as a nutrient for the growth of cells in *MEC* reactor. *MEC* microbial growth process in the reactor involves a metabolic process starts from transport nutrients from the medium into the cells, then the conversion of nutrients into energy and cell constituents, chromosome replication, increasing the size and age of cell growth and cell division in the reactor. In *MEC* reactor, the substrate is not only integral effect on the composition of the bacterial communities in the biofilm anode, but also affects the overall performance of *MEC* include coulombic efficiency (*CE*), the ratio of the electron and current efficiency (Darus, 2011).

Hydrogen gas fuel can be produced from a variety of substrates are non-fermentable and fermentable organics. One of the non-fermented organic substrates most widely used in *MEC* is the end product of the fermentation general and dark fermentation is acetic acid. (Jeremiasse et al., 2010) reported on several studies conducted that acetate is one

substrate that gives the best performances to *MEC* with the level of hydrogen production rate of 50 m^3 H_2/m^3 day and nearing the theoretical value of around 4 mol H_2/mol of acetic (Call & Logan, 2008).

The most popular substrate of fermentable organics is bio-ethanol or carbohydrate polymers such as cellulose, hemicellulose and aromatic polymers (lignin). Biomass wastes generated from various industrial sectors of agriculture and forestry for example stovers corn, bagasse, straw, saw mill and paper mill waste are other examples of substrate fermentable organics. Because of the abundant lignocellulosic materials from agricultural and forestry residues, making raw materials from biomass has become very popular and promising for cost-effective energy production. The main problem is the efficiency of hydrogen production is lower than the hydrogen production from volatile fatty acids (*VFAs*). This is because of lignocellulosic biomass cannot be used directly by microorganisms in the *MEC* reactor, and must be first converted into monosaccharides or other compounds that lower molecular weight (Cheng & Logan, 2007b).

The first time the introduction of *MEC* technology, the researchers only use simple substrates such as acetate and glucose for yielding hydrogen gas. Then in the last few years, the use subtract as a raw material to produce hydrogen gas has expanded in the remaining liquid waste disposal. One of the most interesting is the hydrogen gas can be produced from a wide variety of sewage containing organic materials such as domestic wastewater, industrial effluent fermentation and food processing wastewater, winery wastewater, potato processing wastewater, dairy manure wastewater, wastewaters from molasses and others. Domestic wastewater has a dual function, as well as serves as a substrate to produce hydrogen gas, can also function as wastewater treatment. By using the *MEC* process, the value of *BOD* and *COD* can be reduced to the range of 87-100%

and is capable of producing a maximum coulombic efficiencies up to 26% at a voltage of 0.41 V and the hydrogen recovery was 42% at a voltage of 0.5 V (Ditzig et al., 2007).

5.4 Inoculum preparation and cultivation medium

In this study, the substrate and seed sludge used were obtained from an aerobic digester of a palm oil mill treatment plant at east oil mill. Sime Darby plantation, Carey Island, Selangor, Malaysia. The characteristics of sludge consist of 33 g/L volatile suspended solids (*VSS*), 65.1 g/L total solid (*TS*), pH 7.2 and 1,350 mg/L alkalinity as CaCO3. To eliminate dissolved oxygen in the substrate and seed sludge, both samples are thoroughly cleaned using nitrogen gas and stored in the dark at 4 ^{o}C for five days.

The steps inoculum preparation and cultivation medium is as follows: the first process of cultivation media by using a solution of sucrose, 5 g / l, which weighed as much as 5 grams of sucrose, then dissolved in a liter of aquades and and stored in a refrigerator. The next step to make 1 liter of nutrient solution and then stored in dark bottles to avoid contact with light. The composition of each liter of nutrient stock solution containing 2.0 g of NH_4HCO_3, 1.0 g of KH_2PO_4, 0:01 g of $MgSO_4.7H_2O$, 0.001 g of NaCl, 0.001 g of $Na_2MoO_4.2HO$, 0.001 g of $CaCl_2.2H_2O$, 0.0015 g of $MgSO_4.7H_2O$, 0.00278 g of $FeCl_2$, which was slightly modified from Lay (Fan et al., 2002). Take a sucrose solution of 90 ml at no.1 and input into the baker duran 100 ml, set up in five bottles, the bottle should be tightly closed. Then take 10 ml of nutrient solution at no.2 and insert it into each bottle. Prepare a solution of pH regulator ie NaOH 3 M and H_2SO_4 3 M, each of 500 ml. Then the sample at no. 3 and no. 4 mixed and measured *pH* value, prepare some media at *pH* 5.5 by adding a *pH* regulator solution that has been prepared. Note: Keep a few bottles with the original *pH* value. Then take the sludge as much as 5 grams and insert it into the media which has been set at *pH* 5.5. Place the inoculum no.7 into sacker with rotation at 150 rpm for 3x24 hour and test the generated hydrogen gas. The volume of biogas was

determined using glass syringes. Finally, take 10% palm oil mill effluent (10 ml) of inoculum volume (100 ml) and mix it into a solution no.8, then in sacker again for 24 hour and do testing hydrogen gas production. The reactors were incubated at 36 ±1 ºC and mixed on an orbital shaker rotated at 150 rpm to provide better contact among substrates, nutrients and microorganisms.

5.5 Start-up process value and noise filtering

Almost all industrial processes, especially in bioprocess plant, the results of the online real data are always disrupted by noise. Basically, the noise in the *MEC* plant process is known as noise input and output noise. For input noise associated with the process noise or disturbance, while the noise at the output is associated with noise measurement. The presence of noise in the process of making the plant becomes volatile and very dangerous when the plant is operated. Noise that interfere *MEC* process can be anticipated by using one of the robust controllers such as Neural Network Model-Based Controller. The presence of measurement noise can degrade the performance of *MEC* reactor.

In this section will be described in detail related to real noise disturbance on the measurement data. The main problem why real measurement data becomes inaccurate, it is because the resulting noise is recorded along with real data from the *MEC*. Noise can be defined as a disorder or waves that interfere with the signal from the measurement data. Noise comes at a time of recording real data from *MEC* processes both in the form of random error or gross error. With the noise in the plant this process led to real data from MEC process becomes very difficult to interpret.

Figure 5.8 is an example of real data for closed loop online system that has been disrupted by noise. It shows that the relationship between the hydrogen production rate, *MEC* current and electrode potential. The purpose of this study is how to maintain the level of hydrogen production rate in the reactor continuously. One way to maintain the

level of hydrogen production rate is by controlling the amount of supply current in a reactor.

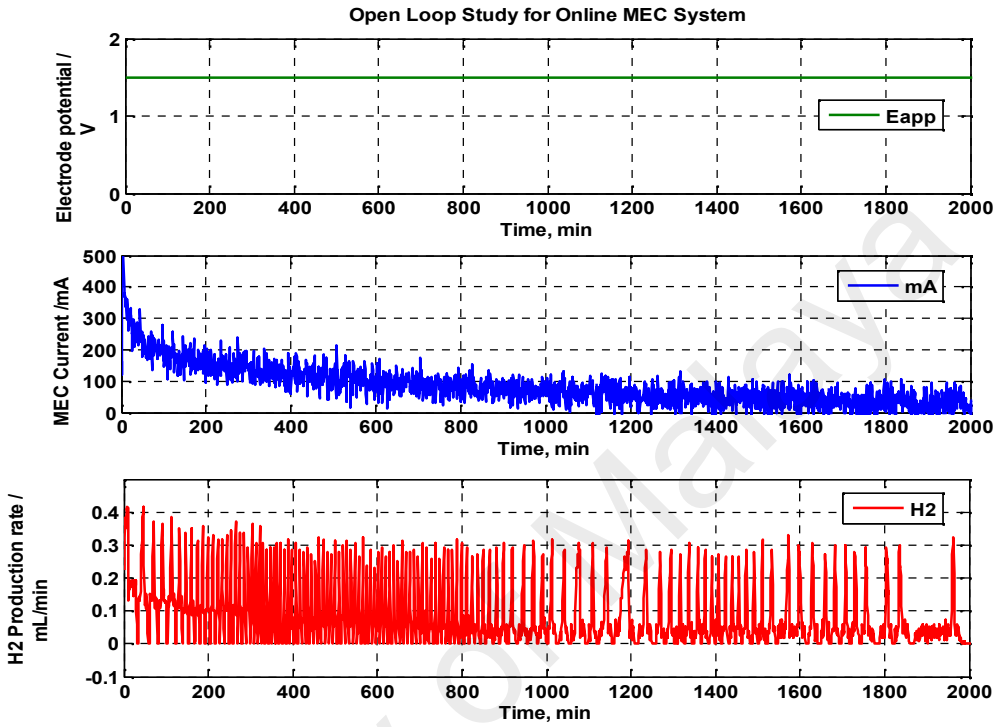

Figure 5.8: The *MEC* process and open loop online system for constant set-point studies

To control the amount of current in a reactor optimally, then the supply voltage applied to the system must be maintained at a certain value. In Figure 5.8 shows that although there are some amount of voltage supplied to the reactor at a constant value that is 1.8 V, but the movement of MEC currents and the rate of formation of hydrogen gas are varied and tend to fluctuations. This is because both of these parameters have been affected by the signal from the noise.

Figure 5.9 shows that the measurement values of the *MEC* process is operated in closed loop online system for multiple set-point studies. The hydrogen production rate, as well as determined by the concentration of the substrate in the reactor, also largely determined by the supply voltage from outside. From the results of the study indicated that the effect

of the number of supply voltages and currents are applied to the *MEC* reactor is very determining the level of hydrogen production rate.

The amount of voltage supplied to the reactor *MEC* is varied and gradually increased starting at 1.5 V, 1.8 V to 2 V. From Figure 5.9 it appears that when the voltage was raised to 2 V, the current movement in the reactor rose sharply and very fluctuation that reached its peak value at 0.5 A. And then the movement of currents in the system continuously varies by the amount of voltage supply to the reactor. It indicates that the effect of noise in the system is very dominant, so this is one of the factors causing the declining performance of *MEC* reactor. Because almost all parameters in the system were disrupted by noise, the movement of currents in the reactor is very difficult to predict. Time-varying median filter method is the one right solution to reduce noise in the *MEC* process.

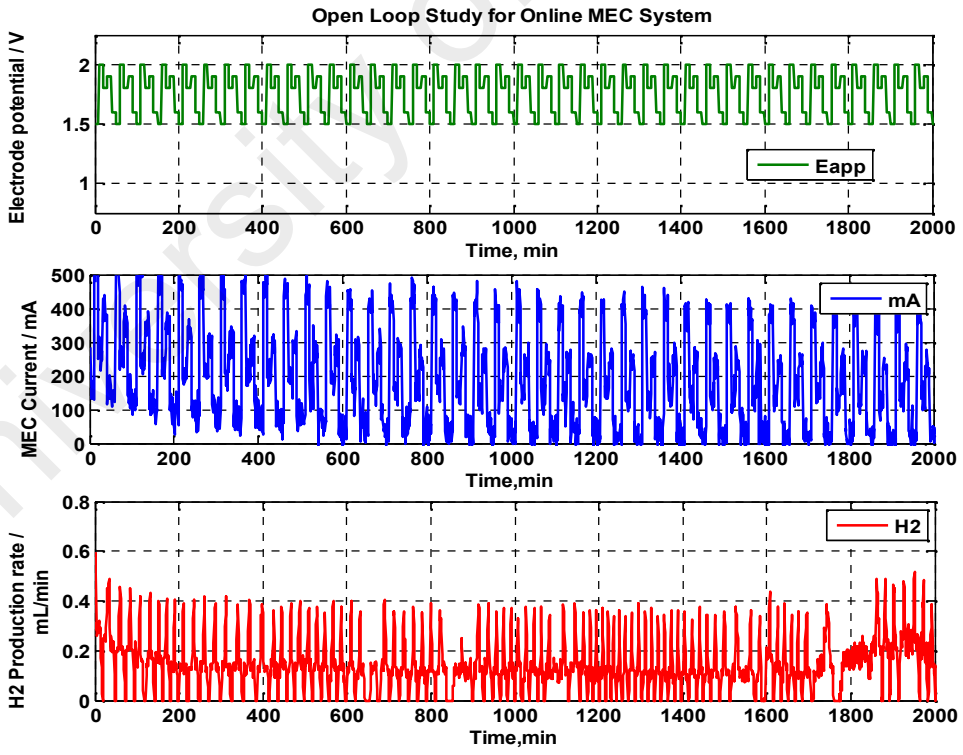

Figure 5.9: The *MEC* process and open loop online system for multiple set-point studies

In data processing, the noise in the measurement data can be eliminated or reduced by using filtering techniques. In Figure 5.10 describes a comparison between the raw data from the measurement results prior to filtering with the raw data after filtering. From Figure 5.10 shows that the “Butherworth Lowpass filter method ", able to reduce the noise in the measurement data with excellent performance.

Filter is a process of separation of the signals of certain frequencies to be desired from the real data and discard unneeded signals. The purpose of filtering is to produce valid data. This technique is very effective to recover the signal from the noise that interferes with plant processes.

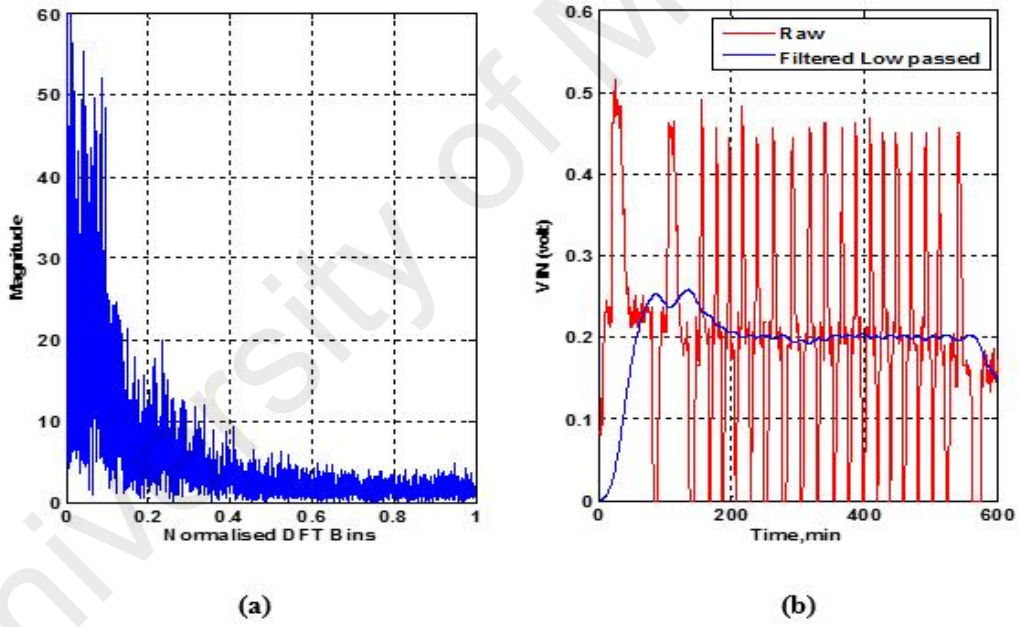

Figure 5.10: (a) Fourier transform for frequency analysis and (b) Comparison for raw and filtered signals

In this study, the filtering techniques used are “Butherworth Lowpass filter method”. A number of real data from experimental work then analyzed and processed using computing program MATLAB (Appendix 2). Lowpass filter is one method that has been used effectively to reduce noise and is very well known among engineers.

Figure 5.11 shows the performance of *MEC* process after the raw data is screened from the influence of noise. In the Figure shows that the electrode potential is supplied to the reactor and kept at a constant value of 1.8 volts. In the figure 5.11 shows that the correlation between the current and the hydrogen production rate in the reactor.

The bubbles of hydrogen gas produced in the reactor are strongly influenced by the amount of current flow to the voltaic elements. The hydrogen production rate tends to follow the trend of current flow in the reactor. As seen in Figure 5.11 that when the *MEC* current rise in the value of 225 mA, the hydrogen gas production also increased to 0.2 mL/min. Conversely, when the *MEC* current in the reactor decreases slowly until steady state conditions, the rate of hydrogen gas production also decreased following the trend of the *MEC* current.

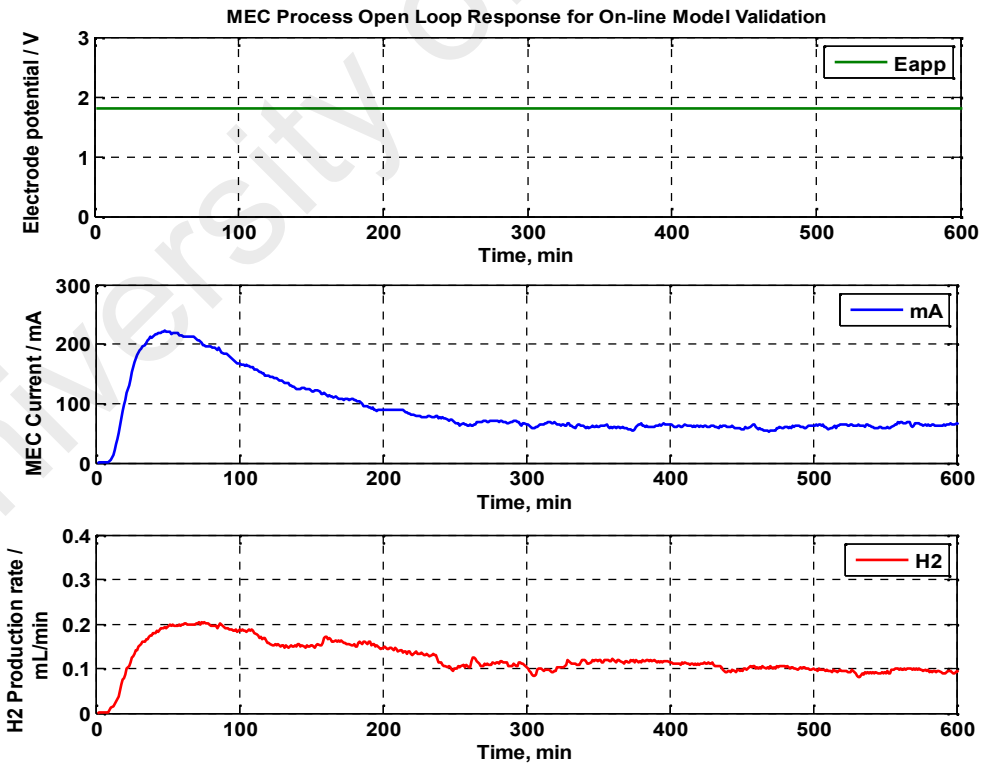

Figure 5.11: The *MEC* proses performance after using filtering techniques for constant set-point studies

Figure 5.12 shows the performance of *MEC* process after filtering data from the influence of noise. These tests are conducted for multiple set-point studies with the number of electrode potential supplied to the reactor is raised varied and gradual. In the first stage electrode potential is increased from 1.5 *V* to 2 *V*, then decreased gradually from 2 *V* to 1.8 *V* and 1.5 *V*. Total supply electrode potential into the reactor continuously varies every 15 minutes.

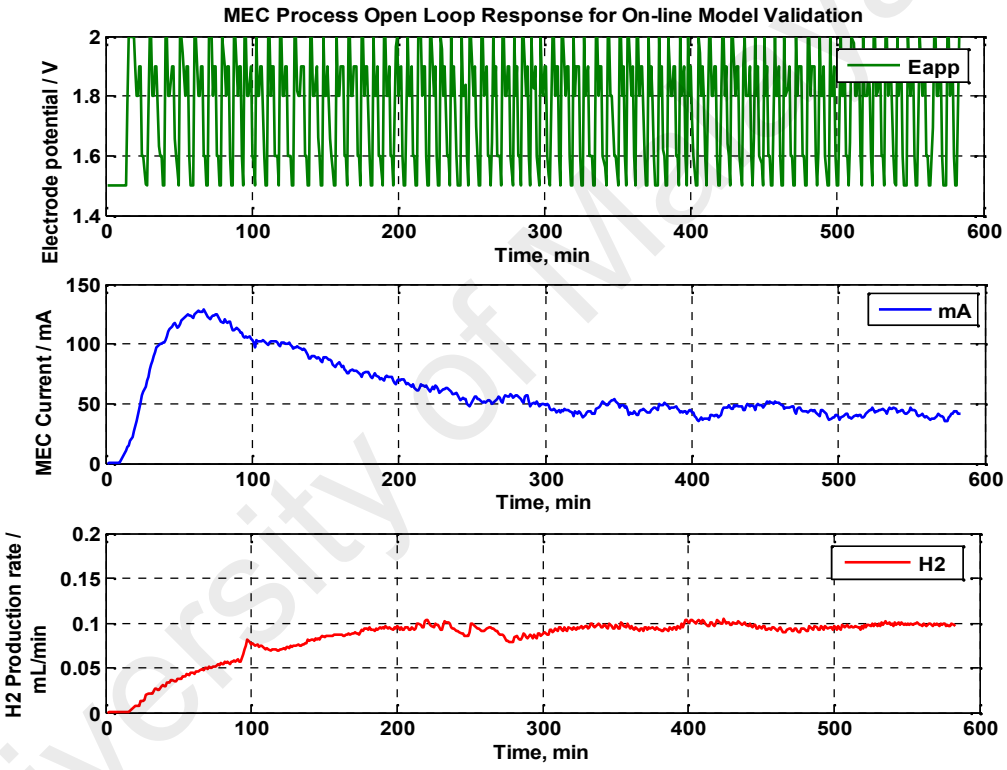

Figure 5.12: The *MEC* proses performance after using filtering techniques for multiple set-point studies

In Figure 5.12, it can see that although the amount of electrode potential supplied to the reactor is constantly changing with time, but no significant effect on the movement of current flow and the rate of hydrogen production system. This is because the performance of *MEC* reactor and the rate of hydrogen gas production, as well as determined by the supply of energy from the outside but is also determined by other factors such as the

amount of substrate, *pH* and temperature in the reactor. However, various studies literature states that the rate of hydrogen gas production in the *MEC* system is very dominant influenced by the amount of electrode potential supplied to the reactor.

5.6 Model Validation for microbial electrolysis cell (*MEC*)

MEC mathematical model is a representation or formalization of *MEC* systems. With modeling studies will facilitate in determining the information and mechanisms of various kinds of interaction processes. And will assist in the calculation of scale-up and also facilitate the optimization study or control. To ensure a simulation of a model that will be designed to produce a precise simulation, it is necessary to verify and validate the output of the simulation models.

Model validation is needed to test whether the model simulations obtained really an accurate representation of the real system or the real plant. Plant test is needed to confirm the validity of the model and other important things that arise from the study models. A model is said to be valid if the comparison between the outputs of simulation with experimental systems have no significant differences.

Figure 5.13 represents a comparison between the mathematical models and on-line real data on the *MEC* Process. The purpose of validation of the model output is to see whether the model is able to more accurately reflect or represent of the real system. The mathematical model used here is a modified version of the Pinto model so that it can represent the actual process conditions of a real system or on a pilot plant scale.

There are several modifications and assumptions made at the Pinto model and then adapted to the pilot plant scale. The formation of biofilm in the reactor is limited only two Layer. The first layer (Layer 1) is called the biofilm anodic and second layer (Layer 2) called biofilm cathode. The microorganisms in the anode compartment is assumed to be

perfectly and homogeneously distributed in each layer. To approach to the real conditions of the process, then in simulating the models, there are several on-line data is entered into the model equations. Reactor assumed a volume of 5 liters and takes place in fed-batch system, while the substrate concentration, *pH* and temperature of the reactor is controlled and maintained at a certain value.

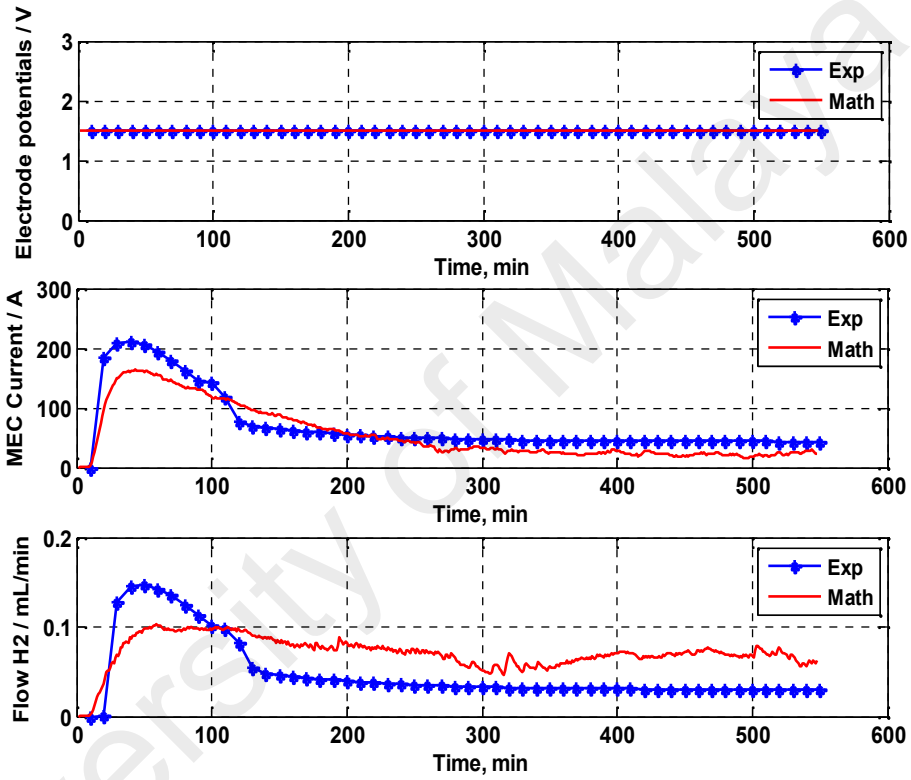

Figure 5.13: Comparison response performance between mathematical model and on-line real data for *MEC* proses

Figure 5.13 above shows that the model is able to represent on the real system of the pilot plant. It can also be concluded that in general the *MEC* model is able to predict the value of current and hydrogen production rate of the data signal pilot plant. So that these models can be used in the study of optimization, control and *MEC* reactor design on a larger scale.

5.7 Piping and Instrumentation Diagram (*P&ID*)

Piping and Instrumentation Diagram (*P&ID*) is a process flow diagram that describes a system that can provide more information about equipment and instruments used in a process. At *MEC* plant, an overview of *P&ID* is needed to get the right information about the whole process and operation of the *MEC* system.

The *P&ID* for the *MEC* plant that includes pipelines, Instrumentation, equipment, valves and fittings, measuring element, flow direction, controller, and the final element.The following will explain several critical components used in the control setup online at *MEC* plant. For the control system has 4 elements of the process, the measuring element, controller, and the final element. A detailed description of the *P&ID* for *MEC* plant can be seen in the Figure 5.14.

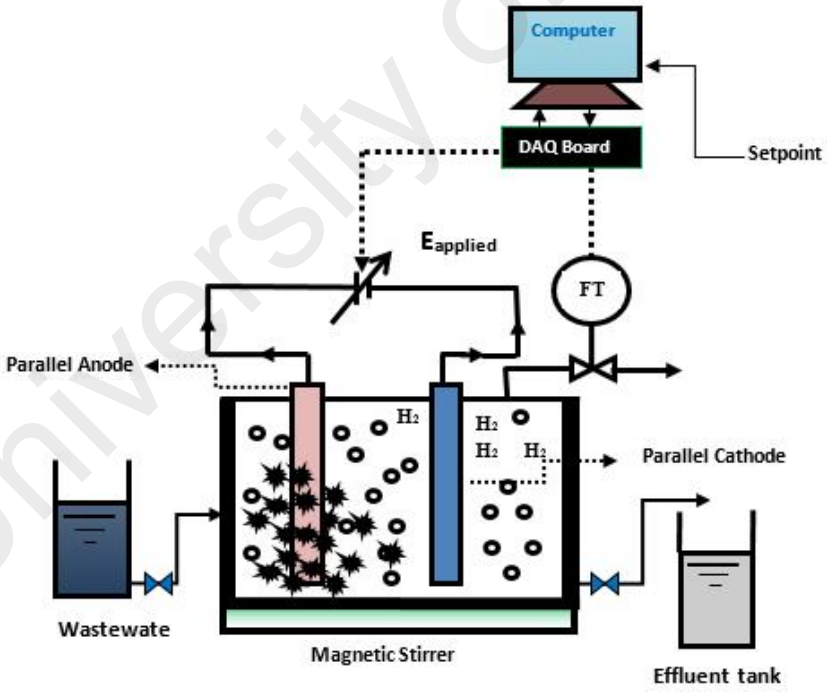

Figure 5.14: *P&ID* for close-loop online control of *MEC* plant

In online control setup, a digital domain has being carried out in this study. The digital domain can be formulated as in equation below.

$$y(k) = y(ht) = f(x, u) \tag{5.1}$$

Where $y(k)$the output of process (hydrogen production litre/hour), k is the time unit that corresponding to sampling time and unit time. As refer to Figure 5.14, flow transmitter for Hydrogen production rate has been selected as measurement element that can produced signal from 4 to 20 mA. Voltage regulator is the final element that can be used to regulate the voltage supply to reactor in range of 0 to 15 Volts. The behaviour of the system differs significantly as the value of applied voltage is changed and given a significant influence on hydrogen production rate.It is demonstrated that the rate of hydrogen production could be maximized without excessive energy consumption by minimizing the apparent resistance of the MEC. Figure 5.15 shows signal flow diagram feedback control system.

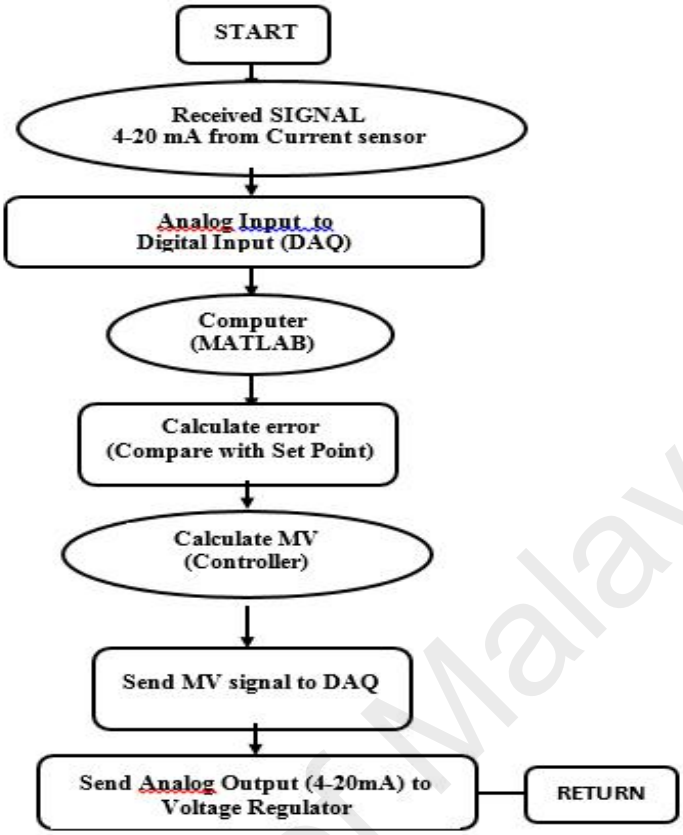

Figure 5.15: Signal flow diagram for feedback control system

5.8 PI Closed loop control for online system

The online control implementation has to done in digital domain wherein the close loop system, computer with *DAQ* is used. The control strategy like neural network and *PID* controller that discussed in Chapter 4 are implemented in computer platform (MATLAB/Simulink). In order for computer to understand the signal from the plant, *DAQ* hardware is needed. This hardware consists of analogue-input and analogue-output converter. After the signal conversion, computer are able to give a command to process reactor via voltage regulator while, it can receives how much hydrogen produces at certain time. Figure 5.16 shows the close-loop for PI online system that being carried out for this study.

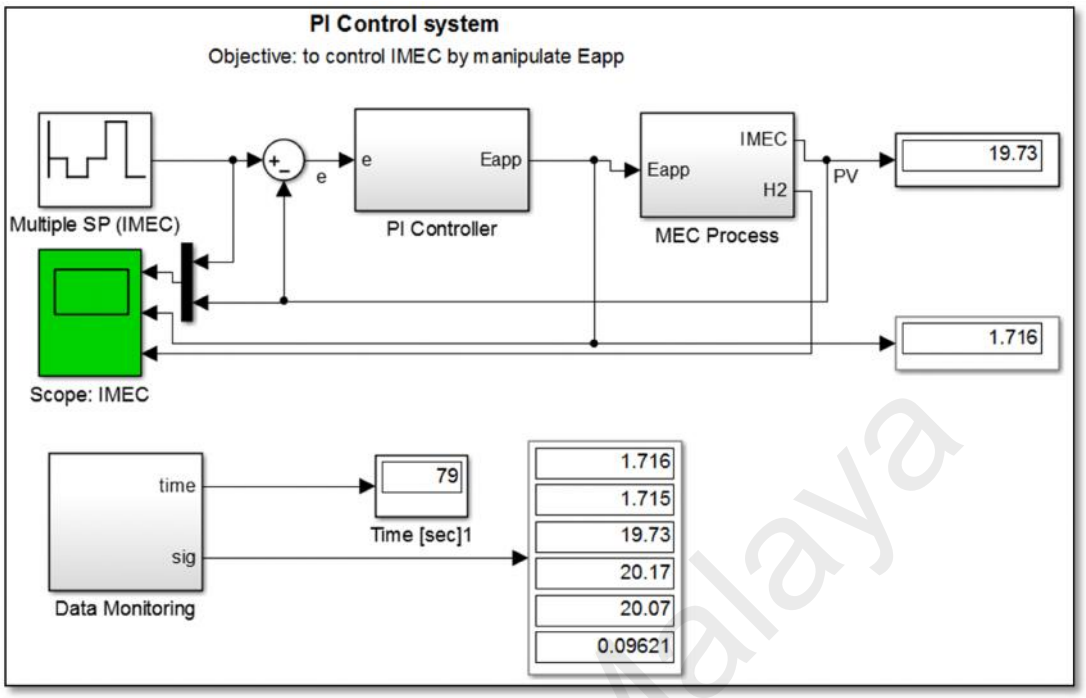

Figure 5.16: PI Closed loop control for online system using multiple set-point tracking study

Figure 5.17 shows the process and *PI* controller response for closed-loop control on online system using constant set-point study. The controllers have worked well and satisfactorily manage the process when changes in the set point value of 40 mA to 30 mA. It also shows that the change in electrode potential is following the change of trend in the current MEC system, while H_2 production rate continues to rise gradually until the end of the process. In Figure 5.17 shows the behavior of the MEC current and the hydrogen production rate, it is a representation of Figure 5.12. From the figure, it can be seen that the hydrogen production rate increased sharply at the beginning of the period up to 230 minutes and then continued to decrease slowly until the end of the period.

Generally, it can be concluded that the controller is able to follow the changes in the characteristics of time even though there is a delay when the large deviations in the process. From the figure, it shows that although the controller is still slow in responding,

especially early in the process, but the overall controller is still able to manage the process despite the change of set-point value.

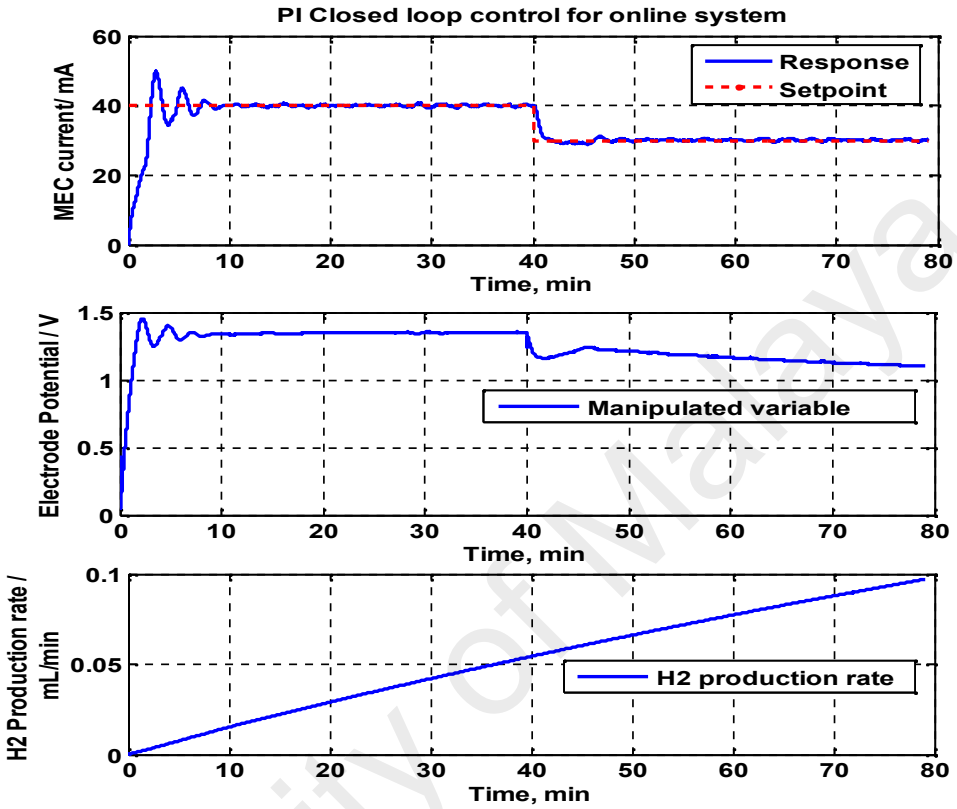

Figure 5.17: PI controller for online system using constant set-point study

Figure 5.18 shows the process and *PI* controller response to an online system for multiple set-point tracking. In this process set-point value varied with time starting at 40 mA, 20 mA, 25 mA, 35 mA and 20 mA, respectively. From Figure 5.18 it can be seen that the performance of the *PI* controller is very good in responding to *MEC* process. In the picture also shows that the value of overshoot and oscillation is greater at the beginning of the process and then slowly decreased and reached a stable condition at the end of the process. The hydrogen production rate in the system is increasing gradually until it reaches the peak value of 0.17 mL / min at 200 minutes. From Figure 5.18, it can

be concluded that although there are still fluctuations in the process, but overall the PI controller has excellent performance and satisfying to manage the process despite at the condition of multiple setpoint changes.

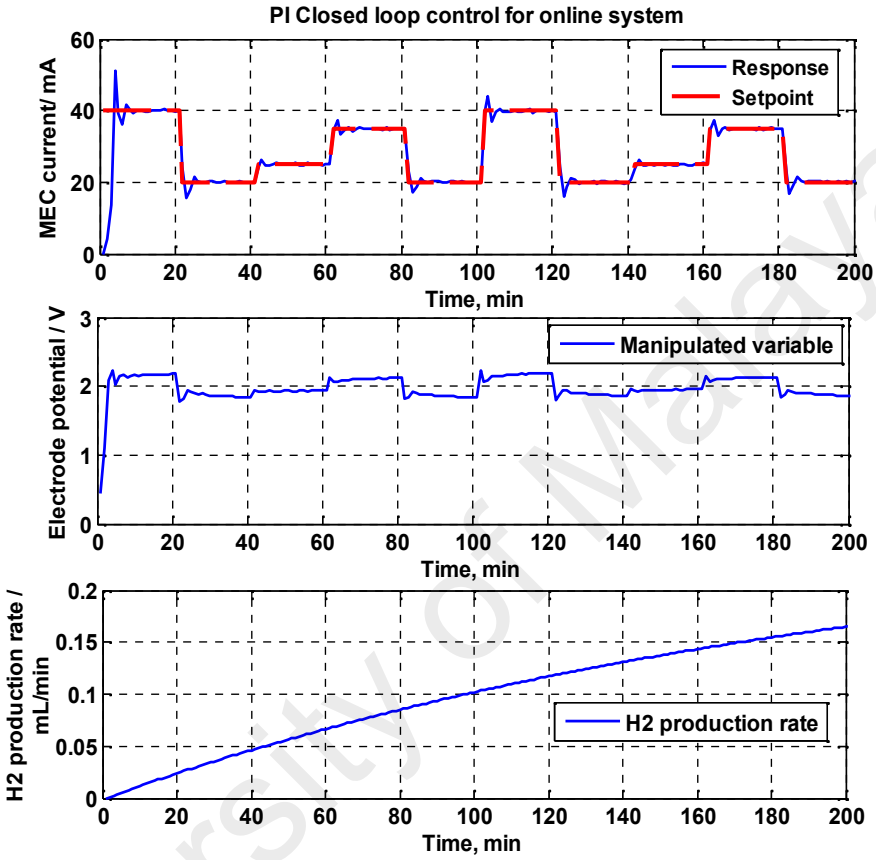

Figure 5.18: PI controller for online system using multiple set-point tracking study

5.9 Neural Network Inverse Controller Close-loop for online control system

In this part, the design and development of the neural network based controllers for online control system are presented. Prior to considering an advanced control method to the process, it is important to assess the controllability of the system using conventional control methods. Therefore, before it is discussed in detail about neural network based controller then has been discussed in advance of the performance of the PI controller.

The design of basic neural network controller which covers direct inverse neural network on the online system will be studied. Inverse neural network model with feed-forward structure is used as the controller in this case. The control method proposed utilizes feed forward neural networks in the direct inverse neural network control method.

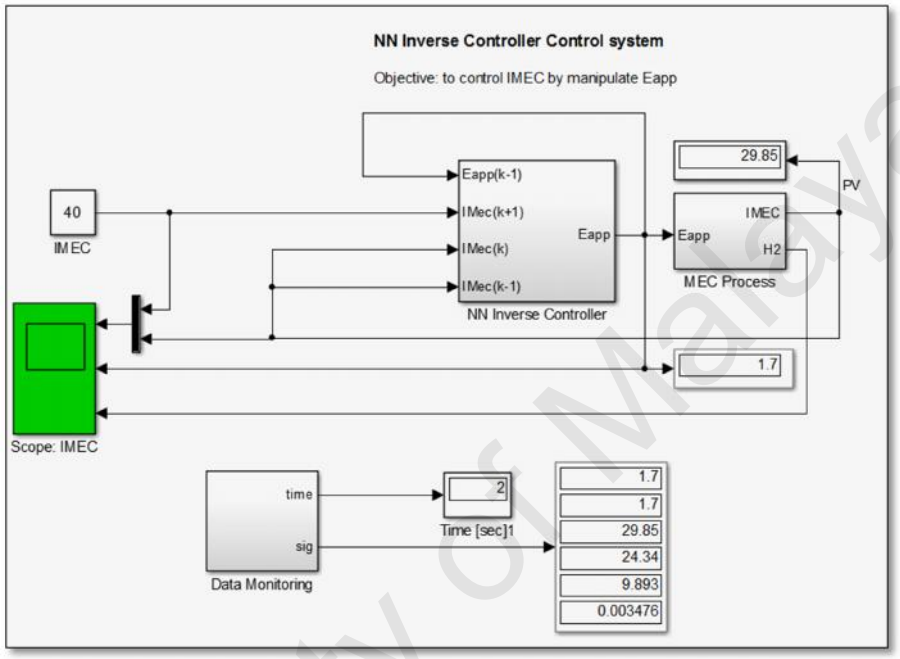

Figure 5.19: Structure of Neural Network closed-loop block diagram for on-line *MEC* control strategy

The proper control strategy is developed by using the neural network based inverse model for set point tracking and disturbance rejection tests. The models were chosen in an effort to identify the one that best represent the system. The development includes the selection of input-output variable for the model, the data used for training and validation, and neural network model formulation. The design and performance of neural network controller for the basic schemes are discussed in this study. Figure 5.19 shows the block diagram of the closed loop on-line control system for Neural Network Inverse Controller strategy in *MEC* reactor.

Figure 5.20 shows the open-loop test which is used as input and output data for training Neural Network controller. Variable input and output data, which is used as a neural network model and then the data is fed through a moving window approach.

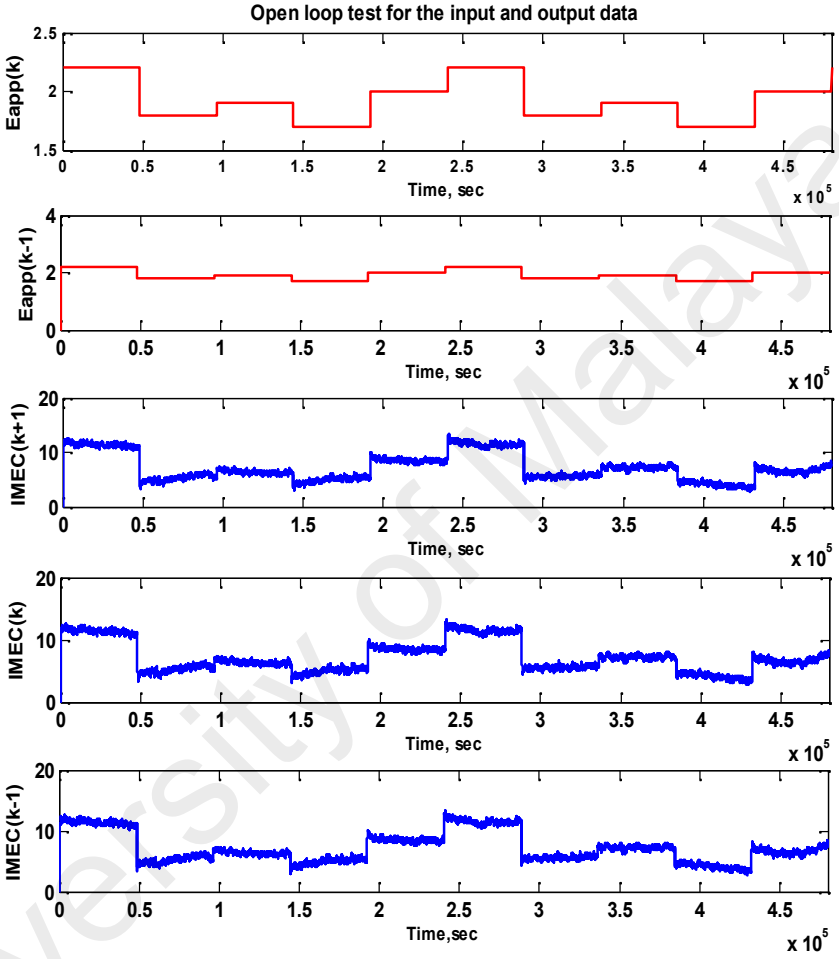

Figure 5.20: Open loop test to the input and output data set for training Neural Network controller

Neural network models are used as input and output data sets for training neural network controller in on-line control system is made up of 4 inputs and one output node. Input and output nodes consist of past and current data from the electrode potential and current *MEC*. The past and current data is used as input nodes of a neural network model of electrode potential i.e. $E_{a\ (k)}$, $E_{a\ (k-1)}$ and of the *MEC* current i.e.

$I_{M\ (k-1)}, I_{M\ (k)}$. While current data from current MEC used as an output node i.e. $I_{M\ (k+1)}$.

Figure 5.21 shows the input and output data sets are used for training inverse Neural Network. One data set of electrode potential and current MEC was obtained from open-loop test on the on-line system. Then the data set is used to train the neural network model.In neural network-based controller using the inverse model refers to the inverse form of the process as a control strategy.For the network architecture and activation functions, the inverse model has two-layered feed-forward network with 4 input, 8 hidden nodes and 1 output node.

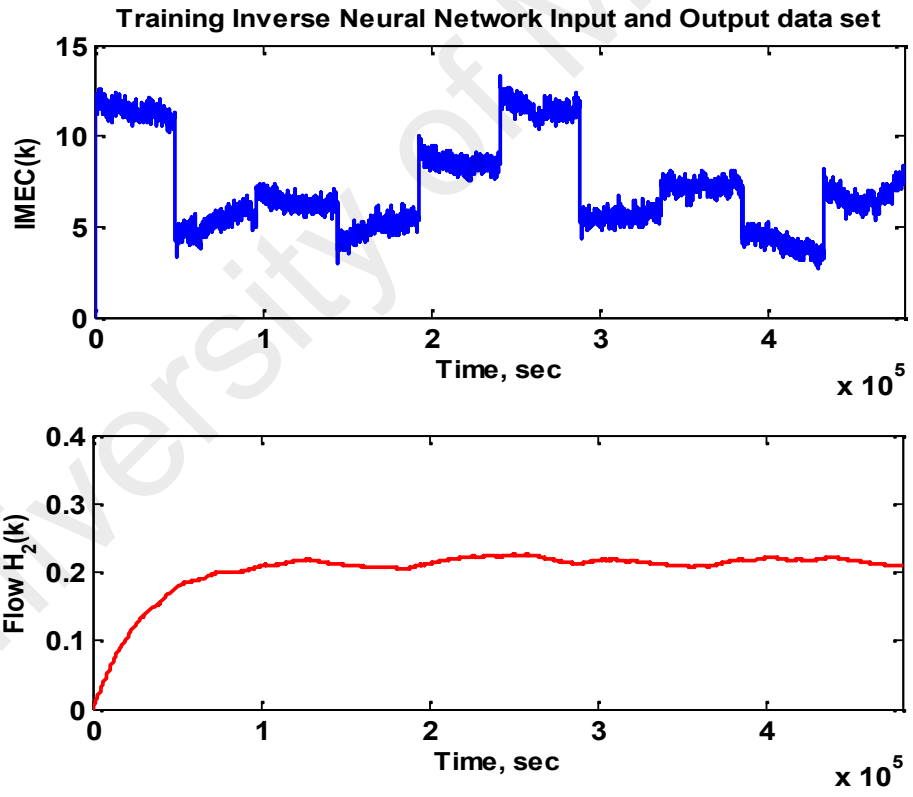

Figure 5.21: Data set of training neural network control model for online control system

Figure 5.22 shows that the inverse neural network training model used for neural network-based controller on the online system. To get the best value from the inverse neural network training, the training cycle should be repeated in order to get the value of a small error in the input and output of data sets.

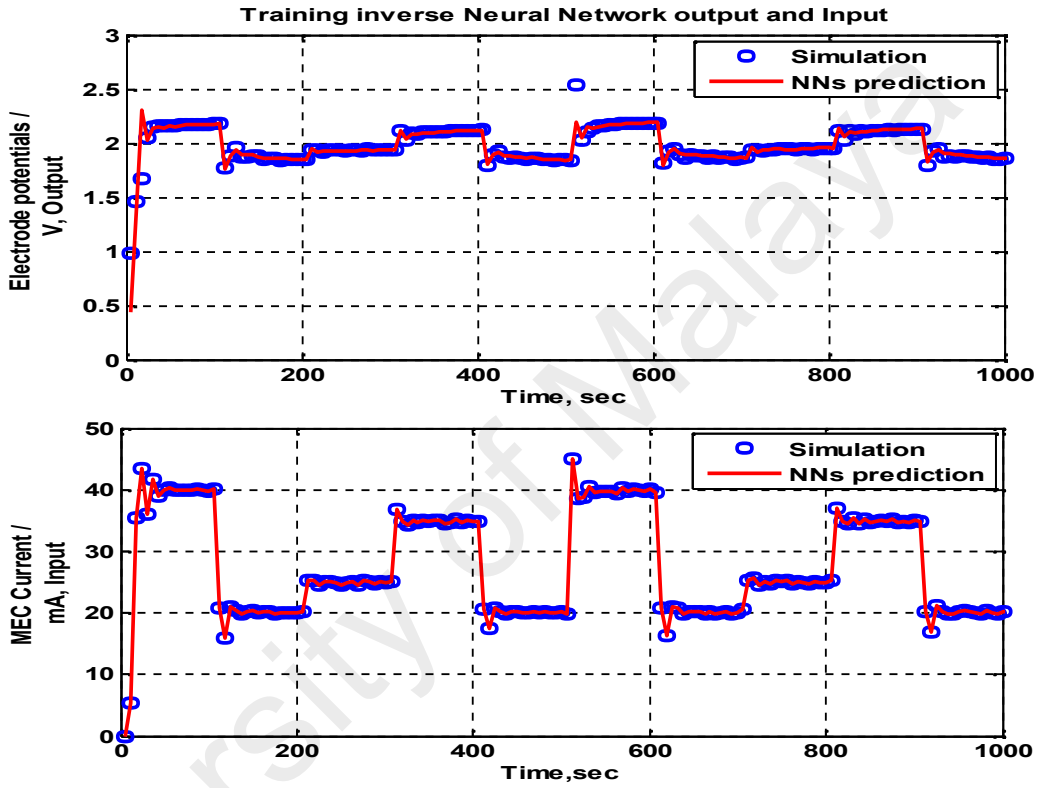

Figure 5.22: Training Inverse Neural Network model for online control system

From Figure 5.22, it can be seen that the artificial neural network is able to accurately track the trend dynamics of electrode potential and *MEC* current in the system.From the results of training artificial neural network can be concluded that the inverse neural network model that has been obtained is very suitable for use in the neural network-based controller on the online system.

Figure 5.23 show that the performance of the neural network controller and comparison with PID controller for online control system. Training inverse neural network shown in Figure 5.22 with a feed-forward structure is then used as a controller. From Figure 5.23, it can be seen that the neural network controller is able to accurately track the trend dynamics of electrode potential and current MEC in the system.

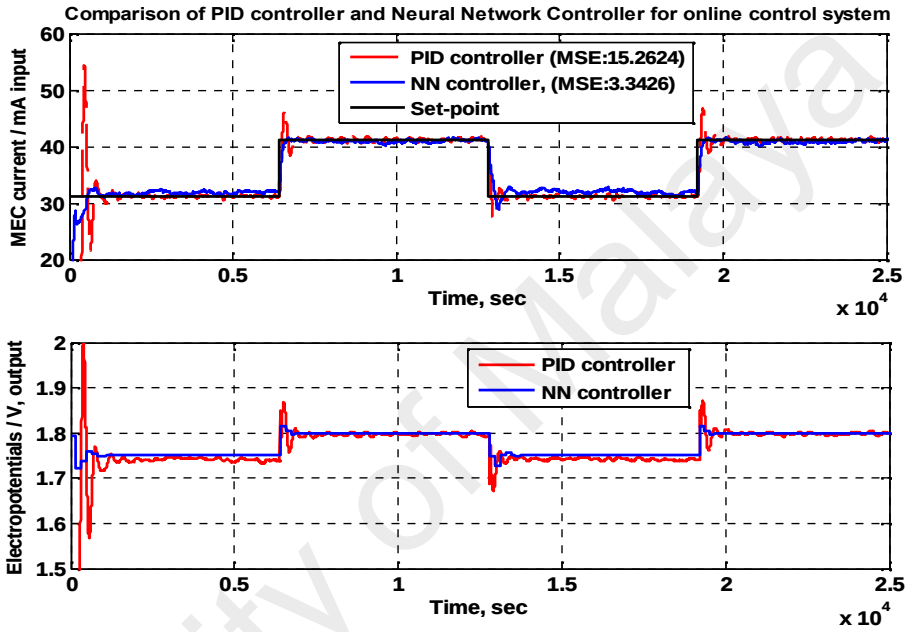

Figure 5.23: Neural network controller for online system using multiple set-point tracking study

Figure 5.24 shows detailed view about the performance of the neural network controller for online system in the time period of 6200 seconds to 8000 seconds. From the Figure 5.24, it can be seen that the performance of the neural network controller is better at responding to the set point compared to the tuned PID process controller. The neural network controllers have out performed and successfully regulate the MEC process when changes in the set point value of 32 to 42 mA are introduced in the system.

The figure also highlights the comparison of the error in terms of the performance index for the PID and neural network controllers. MSE value of the neural network

controller is 2.63, much smaller than the MSE value of the PID controller which is 4.95. It significantly suggested that the performance of the neural network controller is much better than the PID controller can offer.

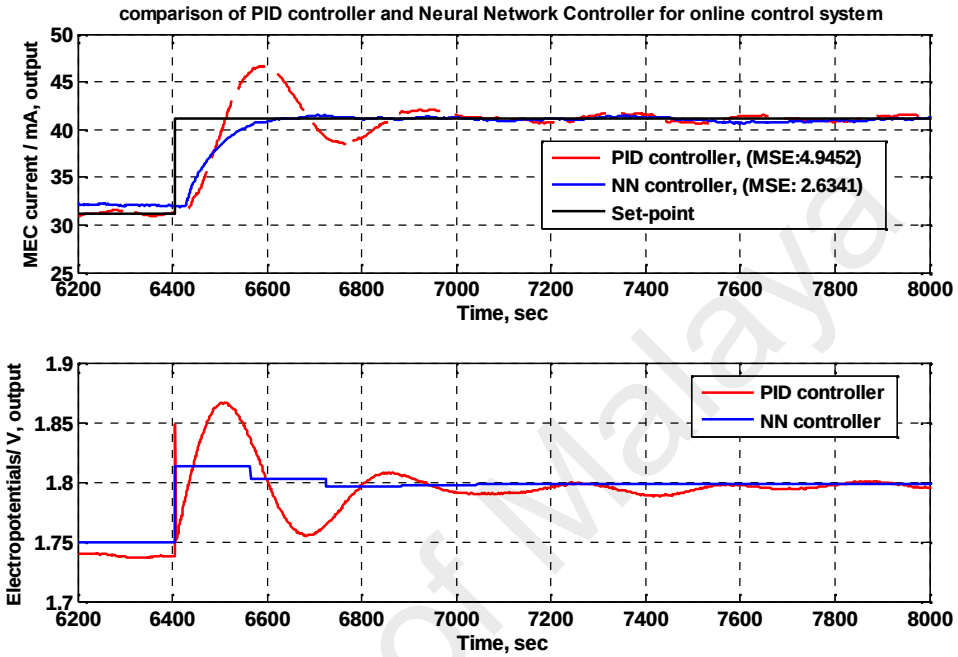

Figure 5.24: The performance of the neural network controller for online system in the time period 6200 seconds to 8000 seconds.

In summary, from the online performance comparison of the two tested controllers, results showed and concluded that the neural network controller able to provide a good control performance when responding to irregularities and were able to follow the time-varying characteristics of the MEC process. Neural network controller has respectively smaller overshoots, oscillations and offset compared to the tuned PID controller. Therefore, the neural network controller is concluded to be more efficient and able to cope with changes in the set-point, load disturbance and noise from the process with better and more efficient.

CHAPTER 6: CONCLUSIONS AND RECOMMENDATIONS FOR FUTURE WORK

6.1 Conclusions and summary of work

In this work, studies involving modeling, optimization and control of an integrated approach to the design of the MEC reactor have been discussed in detail. An explanation of the MEC model describing substrate consumption and biomass growth behavior as anodophilic, hydrogenotrophic and acetoclastic microorganisms has also studied. MEC models that have been modified from the Pinto model and then using the computer program codes have been developed in Matlab development environment. From the overall discussion of the thesis, the author can conclude several important conclusions as follows;

i. The mathematical MEC model has been successfully used to predict the hydrogen production by improving the internal and external parameters. For example: substrate concentration(S); hydrogenotrophic microorganism (X_h) ; anodophilic (x_a) and acetoclastic (x_m) microorganism; the electrode potentials (E_a); I_{MEC} current and the maximum growth rate ($\mu_{m\ ,a}$).

ii. The optimum parameters of anodophilic microorganisms obtained at 425 mg/l, the electrode potential at 0.8 V, and MEC current at 0.16 A gave the maximum hydrogen production rate of 1.17 L/day.

iii. From the validation between MEC mathematical models and experimental work, the value of Current MEC Model validation is obtained with fitness R^2 = 92.9% and Hydrogen Model with R^2 = 92.7%.

iv. The hybrid neural network based model (HNN) controller provides better control of the MEC system compared with others controller. HNN controller gives fast settling time in the response, less overshoots, minimal offset and able to give good performance for any variation of disturbance and noise.

6.2 Major Contribusions of this work

In general, the results of this work have provided some important contributions in several aspects related to the *MEC* process. All the important things that have been studied in this thesis include modeling, optimization and on-line implementation of advanced control strategies for biohydrogen production in *MEC* reactor system. Here are some of the significant contribution that has been done in this work includes the following:

i. The author has collected all the important information from various studies in the literature relating to the production of biohydrogen gas, mathematical models and control strategies of the *MEC*.
ii. The *MEC* model chosen and used in the simulation is the *MEC* model that has been developed by Pinto. Then the model is modified in accordance with the *MEC* reactor design. Modifications models include several aspects such as Fed-batch process operations, the phase of biofilm growth, metabolic activities, and the reactor size. The simulation model is written in a computer program code using Matlab software. Data from the simulation of the dynamic process of open loop has been collected and analyzed for purposes of control system design.
iii. Response surface methods (*RSM*) were used to identify the parameters that have a significant influence on the hydrogen production rate. As for some important parameters that are relevant then tested using statistical analysis, namely: initial concentration of microorganisms anodophilic, electrode potentials, counter-electromotive force and current *MEC*.

iv. A pilot plant for *MEC* reactor together with its control loop has been designed to implement the simulation work. The results of model simulations were then validated by on-line data from the *MEC* experimental work.

v. Control strategies have been designed to regulate the *MEC* process and a closed loop system has been described in detail. As several control strategies that have been developed include conventional *PID* algorithm, adaptive *PID* controller, direct inverse neural network (*DINN*) controller, Internal Model Control (*IMC*) and hybrid neural network based model (*HNN*) control strategies. The purpose of the implementation of advanced controller is to control the *MEC* current in reactor and keep the potential energy supply from outside the system so that the gas biohydrogen can be produced continuously.

6.3 Recommendations and future work

The following will present a number of new research that can be studied and analyzed about the *MEC* reactor. The possibility of several important recommendations related to the reactor design, modified model and development of control strategies. Some of the important works in the future that can be done are proposed as follows:

i. To improve the performance of *MEC* reactor, new strategies that *MxC* cogeneration unit is proposed. These strategies shall apply the concept of a combination of *MFC* and *MEC* reactor. This strategy has many advantages, because in addition to producing the hydrogen gas in the same time as well as to treat wastewater. Another advantage is the current produced from *MFC* reactors can be used directly as the voltage applied to the *MEC* reactor, so that there is not need for any external source of energy supply.

ii. To improve the design of the pilot plant, a new model based Model *MxC* can be developed and further improved. As for the approach to the real process it is

necessary to modify an existing model by adding some new parameters such as the effects of *pH*, and temperature konduktivity reactor. These parameters are very important because it has a direct influence on the performance of *MxC* reactor such as the mechanism of electron transfer, substrate consumption kinetics and reactor internal resistance.

iii. To improve further the performance of *MEC* reactor, it is necessary to develop more sophisticated control strategies such as hybrid models and fuzzy logic controller, neuro-fuzzy control strategy, sliding mode control, and genetic algorithm control model-based controller.

REFERENCES

Adams, M. W., & Stiefel, E. I. (1998). Biological hydrogen production: not so elementary. *Science, 282*(5395), 1842-1843.

Aelterman, P., Rabaey, K., Pham, H. T., Boon, N., & Verstraete, W. (2006). Continuous electricity generation at high voltages and currents using stacked microbial fuel cells. *Environmental science & technology, 40*(10), 3388-3394.

Akkerman, I., Janssen, M., Rocha, J., & Wijffels, R. H. (2002). Photobiological hydrogen production: photochemical efficiency and bioreactor design. *International Journal of Hydrogen Energy, 27*(11), 1195-1208.

Amend, J. P., & Shock, E. L. (2001). Energetics of overall metabolic reactions of thermophilic and hyperthermophilic Archaea and Bacteria. *FEMS microbiology reviews, 25*(2), 175-243.

Arcand, Y., Chavarie, C., & Guiot, S. R. (1994). Dynamic modelling of the population distribution in the anaerobic granular biofilm. *Water Science and Technology, 30*(12), 63-73.

Argun, H., Kargi, F., Kapdan, I. K., & Oztekin, R. (2008). Biohydrogen production by dark fermentation of wheat powder solution: effects of C/N and C/P ratio on hydrogen yield and formation rate. *International Journal of Hydrogen Energy, 33*(7), 1813-1819.

Åström, K. J., & Hägglund, T. (2006). *Advanced PID control*: ISA-The Instrumentation, Systems and Automation Society.

Azwar, M., Hussain, M., & Abdul-Wahab, A. (2014). Development of biohydrogen production by photobiological, fermentation and electrochemical processes: A review. *Renewable and Sustainable Energy Reviews, 31*, 158-173.

Barbosa, M. J., Rocha, J. M., Tramper, J., & Wijffels, R. H. (2001). Acetate as a carbon source for hydrogen production by photosynthetic bacteria. *Journal of biotechnology, 85*(1), 25-33.

Bard, A. J., & Faulkner, L. R. (2001). Fundamentals and applications. *Electrochemical Methods, 2nd ed.; Wiley: New York*.

Bard, A. J., Parsons, R., & Jordan, J. (1985). *Standard potentials in aqueous solution* (Vol. 6): CRC press.

Basak, N., & Das, D. (2007). The prospect of purple non-sulfur (PNS) photosynthetic bacteria for hydrogen production: the present state of the art. *World Journal of Microbiology and Biotechnology, 23*(1), 31-42.

Benemann, J. (1996). Hydrogen biotechnology: progress and prospects. *Nature biotechnology, 14*(9), 1101-1103.

Benemann, J., Polle, J., Huesemann, M., Yu, J., Brune, D., Weissman, J., & Kyle, D. (2004). *A novel photobiological hydrogen production process.* Paper presented at the Proceedings of the 13th International Congress of Photosynthesis.

Bhat, N., & McAvoy, T. J. (1990). Use of neural nets for dynamic modeling and control of chemical process systems. *Computers & Chemical Engineering, 14*(4-5), 573-582.

Bleijlevens, B., Buhrke, T., Van der Linden, E., Friedrich, B., & Albracht, S. P. (2004). The auxiliary protein HypX provides oxygen tolerance to the soluble [NiFe]-hydrogenase of Ralstonia eutropha H16 by way of a cyanide ligand to nickel. *Journal of Biological Chemistry, 279*(45), 46686-46691.

Blokesch, M., Paschos, A., Theodoratou, E., Bauer, A., Hube, M., Huth, S., & Böck, A. (2002). Metal insertion into NiFe-hydrogenases. *Biochemical Society Transactions, 30*(4), 674-680.

Bond, D. R., Holmes, D. E., Tender, L. M., & Lovley, D. R. (2002). Electrode-reducing microorganisms that harvest energy from marine sediments. *Science, 295*(5554), 483-485.

Bond, D. R., & Lovley, D. R. (2003). Electricity production by Geobacter sulfurreducens attached to electrodes. *Applied and environmental microbiology, 69*(3), 1548-1555.

Boon, N., Aelterman, P., Clauwaert, P., De Schamphelaire, L., Vanhaecke, L., De Maeyer, K., . . . Rabaey, K. (2008). Metabolites produced by Pseudomonas sp. enable a Gram-positive bacterium to achieve extracellular electron transfer. *Applied microbiology and biotechnology, 77*(5), 1119-1129.

Brentner, L. B., Peccia, J., & Zimmerman, J. B. (2010). Challenges in developing biohydrogen as a sustainable energy source: implications for a research agenda. *Environmental science & technology, 44*(7), 2243-2254.

Cai, M., Liu, J., & Wei, Y. (2004). Enhanced biohydrogen production from sewage sludge with alkaline pretreatment. *Environmental science & technology, 38*(11), 3195-3202.

Call, D., & Logan, B. E. (2008). Hydrogen production in a single chamber microbial electrolysis cell lacking a membrane. *Environmental science & technology, 42*(9), 3401-3406.

Casalot, L., & Rousset, M. (2001). Maturation of the [NiFe] hydrogenases. *Trends in microbiology, 9*(5), 228-237.

Chen, C.-Y., Yang, M.-H., Yeh, K.-L., Liu, C.-H., & Chang, J.-S. (2008). Biohydrogen production using sequential two-stage dark and photo fermentation processes. *International Journal of Hydrogen Energy, 33*(18), 4755-4762.

Chen, H.-C., Yokthongwattana, K., Newton, A. J., & Melis, A. (2003). SulP, a nuclear gene encoding a putative chloroplast-targeted sulfate permease in Chlamydomonas reinhardtii. *Planta, 218*(1), 98-106.

Chen, W.-H., Chen, S.-Y., Khanal, S. K., & Sung, S. (2006). Kinetic study of biological hydrogen production by anaerobic fermentation. *International Journal of Hydrogen Energy, 31*(15), 2170-2178.

Chen, X., Chen, G., & Yue, P. L. (2002). Investigation on the electrolysis voltage of electrocoagulation. *Chemical Engineering Science, 57*(13), 2449-2455.

Cheng, S., & Logan, B. E. (2007a). Ammonia treatment of carbon cloth anodes to enhance power generation of microbial fuel cells. *Electrochemistry Communications, 9*(3), 492-496.

Cheng, S., & Logan, B. E. (2007b). Sustainable and efficient biohydrogen production via electrohydrogenesis. *Proceedings of the National Academy of Sciences, 104*(47), 18871-18873.

Claassen, P., Van Lier, J., Contreras, A. L., Van Niel, E., Sijtsma, L., Stams, A., . . . Weusthuis, R. (1999). Utilisation of biomass for the supply of energy carriers. *Applied microbiology and biotechnology, 52*(6), 741-755.

Clauwaert, P., Van der Ha, D., Boon, N., Verbeken, K., Verhaege, M., Rabaey, K., & Verstraete, W. (2007). Open air biocathode enables effective electricity generation with microbial fuel cells. *Environmental science & technology, 41*(21), 7564-7569.

Cooney, M., Maynard, N., Cannizzaro, C., & Benemann, J. (2007). Two-phase anaerobic digestion for production of hydrogen–methane mixtures. *Bioresource technology, 98*(14), 2641-2651.

Darus, L. (2011). Effect of substrate concentration to anode chamber performance in microbial electrolysis cell. *Indo J Biotech, 16*, 53-59.

Das, D., & Veziroğlu, T. N. (2001). Hydrogen production by biological processes: a survey of literature. *International Journal of Hydrogen Energy, 26*(1), 13-28.

Dasgupta, C. N., Gilbert, J. J., Lindblad, P., Heidorn, T., Borgvang, S. A., Skjanes, K., & Das, D. (2010). Recent trends on the development of photobiological processes and photobioreactors for the improvement of hydrogen production. *International Journal of Hydrogen Energy, 35*(19), 10218-10238.

Dey, C., & Mudi, R. K. (2009). An improved auto-tuning scheme for PID controllers. *ISA transactions, 48*(4), 396-409.

Ditzig, J., Liu, H., & Logan, B. E. (2007). Production of hydrogen from domestic wastewater using a bioelectrochemically assisted microbial reactor (BEAMR). *International Journal of Hydrogen Energy, 32*(13), 2296-2304.

Fan, K.-S., Kan, N.-r., & Lay, J.-j. (2006). Effect of hydraulic retention time on anaerobic hydrogenesis in CSTR. *Bioresource technology, 97*(1), 84-89.

Fan, Y., Sharbrough, E., & Liu, H. (2008). Quantification of the internal resistance distribution of microbial fuel cells. *Environmental science & technology, 42*(21), 8101-8107.

Fang, H. H., & Liu, H. (2002). Effect of pH on hydrogen production from glucose by a mixed culture. *Bioresource technology, 82*(1), 87-93.

Forestier, M., King, P., Zhang, L., Posewitz, M., Schwarzer, S., Happe, T., . . . Seibert, M. (2003). Expression of two [Fe]-hydrogenases in Chlamydomonas reinhardtii under anaerobic conditions. *European Journal of Biochemistry, 270*(13), 2750-2758.

Freguia, S., Rabaey, K., Yuan, Z., & Keller, J. (2007). Non-catalyzed cathodic oxygen reduction at graphite granules in microbial fuel cells. *Electrochimica Acta, 53*(2), 598-603.

Frey, M. (2002). Hydrogenases: hydrogen-activating enzymes. *ChemBioChem, 3*(2-3), 153-160.

Garcia, C. E., & Morari, M. (1982). Internal model control. A unifying review and some new results. *Industrial & Engineering Chemistry Process Design and Development, 21*(2), 308-323.

Ghirardi, M. L., Zhang, L., Lee, J. W., Flynn, T., Seibert, M., Greenbaum, E., & Melis, A. (2000). Microalgae: a green source of renewable H 2. *Trends in biotechnology, 18*(12), 506-511.

Ginkel, S. V., Sung, S., & Lay, J.-J. (2001). Biohydrogen production as a function of pH and substrate concentration. *Environmental science & technology, 35*(24), 4726-4730.

Golbert, J., & Lewin, D. R. (2004). Model-based control of fuel cells::(1) regulatory control. *Journal of Power Sources, 135*(1), 135-151.

Gyöngy, I., & Clarke, D. (2006). On the automatic tuning and adaptation of PID controllers. *Control Engineering Practice, 14*(2), 149-163.

Hallenbeck, P. C., & Benemann, J. R. (2002). Biological hydrogen production; fundamentals and limiting processes. *International Journal of Hydrogen Energy, 27*(11), 1185-1193.

Hallenbeck, P. C., & Ghosh, D. (2009). Advances in fermentative biohydrogen production: the way forward? *Trends in biotechnology, 27*(5), 287-297.

Hallenbeck, P. C., Kochian, L. V., Weissman, J. C., & Benemann, J. R. (1978). *Solar energy conversion with hydrogen-producing cultures of the blue-green alga, Anabaena cylindrica.* Paper presented at the Biotechnol. Bioeng. Symp.;(United States).

Happe, T., & Kaminski, A. (2002). Differential regulation of the Fe-hydrogenase during anaerobic adaptation in the green alga Chlamydomonas reinhardtii. *European Journal of Biochemistry, 269*(3), 1022-1032.

Harwood, C. S., Wall, J., & Demain, A. (2008). *Nitrogenase-catalyzed hydrogen production by purple nonsulfur photosynthetic bacteria.* Paper presented at the Bioenergy.

Hawkes, F., Dinsdale, R., Hawkes, D., & Hussy, I. (2002). Sustainable fermentative hydrogen production: challenges for process optimisation. *International Journal of Hydrogen Energy, 27*(11), 1339-1347.

Hawkes, F. R., Hussy, I., Kyazze, G., Dinsdale, R., & Hawkes, D. L. (2007). Continuous dark fermentative hydrogen production by mesophilic microflora: principles and progress. *International Journal of Hydrogen Energy, 32*(2), 172-184.

He, Z., & Angenent, L. T. (2006). Application of bacterial biocathodes in microbial fuel cells. *Electroanalysis, 18*(19-20), 2009-2015.

Hillmer, P., & Gest, H. (1977). H2 metabolism in the photosynthetic bacterium Rhodopseudomonas capsulata: H2 production by growing cultures. *Journal of Bacteriology, 129*(2), 724-731.

Hu, H., Fan, Y., & Liu, H. (2008). Hydrogen production using single-chamber membrane-free microbial electrolysis cells. *Water research, 42*(15), 4172-4178.

Hunt, K., & Sbarbaro, D. (1991). *Neural networks for nonlinear internal model control.* Paper presented at the IEE Proceedings D-Control Theory and Applications.

Hussain, M. A. (1999). Review of the applications of neural networks in chemical process control—simulation and online implementation. *Artificial intelligence in engineering, 13*(1), 55-68.

Hussain, M. A., & Mujtaba, I. (2001). *Application of neural networks and other learning technologies in process engineering*: World Scientific.

Isaksson, A., & Hagglund, T. (2002). Editorial-pid control. *IEE Proceedings-Control Theory and Applications, 149*(1), 1-2.

Jeremiasse, A. W., Hamelers, H. V., Saakes, M., & Buisman, C. J. (2010). Ni foam cathode enables high volumetric H 2 production in a microbial electrolysis cell. *International Journal of Hydrogen Energy, 35*(23), 12716-12723.

Kansha, Y., Jia, L., & Chiu, M.-S. (2010). Adaptive IMC controller design using linear multiple models. *Journal of the Taiwan Institute of Chemical Engineers, 41*(4), 446-452.

Kato Marcus, A., Torres, C. I., & Rittmann, B. E. (2007). Conduction-based modeling of the biofilm anode of a microbial fuel cell. *Biotechnology and Bioengineering, 98*(6), 1171-1182.

Kawagoshi, Y., Hino, N., Fujimoto, A., Nakao, M., Fujita, Y., Sugimura, S., & Furukawa, K. (2005). Effect of inoculum conditioning on hydrogen fermentation and pH effect on bacterial community relevant to hydrogen production. *Journal of Bioscience and Bioengineering, 100*(5), 524-530.

Khan, M. J. H., Hussain, M. A., & Mujtaba, I. M. (2014). Polypropylene production optimization in fluidized bed catalytic reactor (FBCR): Statistical modeling and pilot scale experimental validation. *Materials, 7*(4), 2440-2458.

Kotay, S. M., & Das, D. (2008). Biohydrogen as a renewable energy resource—prospects and potentials. *International Journal of Hydrogen Energy, 33*(1), 258-263.

Kraemer, J. T., & Bagley, D. M. (2008). Optimisation and design of nitrogen-sparged fermentative hydrogen production bioreactors. *International Journal of Hydrogen Energy, 33*(22), 6558-6565.

Lay, J. J. (2000). Modeling and optimization of anaerobic digested sludge converting starch to hydrogen. *Biotechnology and Bioengineering, 68*(3), 269-278.

Lee, Y. J., Miyahara, T., & Noike, T. (2002). Effect of pH on microbial hydrogen fermentation. *Journal of Chemical Technology and Biotechnology, 77*(6), 694-698.

Levin, D. B., Pitt, L., & Love, M. (2004). Biohydrogen production: prospects and limitations to practical application. *International Journal of Hydrogen Energy, 29*(2), 173-185.

Li, C., & Fang, H. H. (2007). Fermentative hydrogen production from wastewater and solid wastes by mixed cultures. *Critical Reviews in Environmental Science and Technology, 37*(1), 1-39.

Lin, C. Y., & Chang, R. C. (1999). Hydrogen production during the anaerobic acidogenic conversion of glucose. *Journal of Chemical Technology and Biotechnology, 74*(6), 498-500.

Liu, H., & Fang, H. (2003). Hydrogen production from wastewater by acidogenic granular sludge. *Water Science and Technology, 47*(1), 153-158.

Liu, H., Grot, S., & Logan, B. E. (2005). Electrochemically assisted microbial production of hydrogen from acetate. *Environmental science & technology, 39*(11), 4317-4320.

Liu, H., Hu, H., Chignell, J., & Fan, Y. (2010). Microbial electrolysis: novel technology for hydrogen production from biomass. *Biofuels, 1*(1), 129-142.

Liu, H., & Logan, B. E. (2004). Electricity generation using an air-cathode single chamber microbial fuel cell in the presence and absence of a proton exchange membrane. *Environmental science & technology, 38*(14), 4040-4046.

Liu, H., Ramnarayanan, R., & Logan, B. E. (2004). Production of electricity during wastewater treatment using a single chamber microbial fuel cell. *Environmental science & technology, 38*(7), 2281-2285.

Logan, B. (2004). Biologically extracting energy from wastewater: biohydrogen production and microbial fuel cells. *Environ. Sci. Technol, 38*(9), 160-167.

Logan, B., Cheng, S., Watson, V., & Estadt, G. (2007). Graphite fiber brush anodes for increased power production in air-cathode microbial fuel cells. *Environmental science & technology, 41*(9), 3341-3346.

Logan, B. E. (2009). Exoelectrogenic bacteria that power microbial fuel cells. *Nature Reviews Microbiology, 7*(5), 375-381.

Logan, B. E., Call, D., Cheng, S., Hamelers, H. V., Sleutels, T. H., Jeremiasse, A. W., & Rozendal, R. A. (2008). Microbial electrolysis cells for high yield hydrogen gas production from organic matter. *Environmental science & technology, 42*(23), 8630-8640.

Logan, B. E., Hamelers, B., Rozendal, R., Schröder, U., Keller, J., Freguia, S., . . . Rabaey, K. (2006). Microbial fuel cells: methodology and technology. *Environmental science & technology, 40*(17), 5181-5192.

Logan, B. E., & Regan, J. M. (2006). Electricity-producing bacterial communities in microbial fuel cells. *Trends in microbiology, 14*(12), 512-518.

Maness, P.-C., Yu, J., Eckert, C., & Ghirardi, M. L. (2009). Photobiological hydrogen production-prospects and challenges. *Microbe Magazine, 4*(6, June 2009).

Marcus, A. K., Torres, C. I., & Rittmann, B. E. (2011). Analysis of a microbial electrochemical cell using the proton condition in biofilm (PCBIOFILM) model. *Bioresource technology, 102*(1), 253-262.

Miyake, J., Mao, X.-Y., & Kawamura, S. (1984). Photoproduction of hydrogen from glucose by a co-culture of a photosynthetic bacterium and Clostridium butyricum. *Journal of Fermentation Technology, 62*(6), 531-535.

Miyake, J., Miyake, M., & Asada, Y. (1999). Biotechnological hydrogen production: research for efficient light energy conversion. *Journal of biotechnology, 70*(1), 89-101.

Miyake, J., Tomizuka, N., & Kamibayashi, A. (1982). Prolonged photo-hydrogen production by Rhodospirillum rubrum. *Journal of Fermentation Technology, 60*(3), 199-203.

Miyamoto, K., Hallenbeck, P. C., & Benemann, J. R. (1979). Nitrogen fixation by thermophilic blue-green algae (cyanobacteria): temperature characteristics and potential use in biophotolysis. *Applied and environmental microbiology, 37*(3), 454-458.

Mohan, S. V., Babu, V. L., & Sarma, P. (2007). Anaerobic biohydrogen production from dairy wastewater treatment in sequencing batch reactor (AnSBR): effect of organic loading rate. *Enzyme and Microbial Technology, 41*(4), 506-515.

Mohan, S. V., Bhaskar, Y. V., Krishna, P. M., Rao, N. C., Babu, V. L., & Sarma, P. (2007). Biohydrogen production from chemical wastewater as substrate by selectively enriched anaerobic mixed consortia: influence of fermentation pH and substrate composition. *International Journal of Hydrogen Energy, 32*(13), 2286-2295.

Moletta, R., Verrier, D., & Albagnac, G. (1986). Dynamic modelling of anaerobic digestion. *Water research, 20*(4), 427-434.

Mosey, F. (1983). Mathematical modelling of the anaerobic digestion process: regulatory mechanisms for the formation of short-chain volatile acids from glucose. *Water Science and Technology, 15*(8-9), 209-232.

Mueller, F., Brouwer, J., Kang, S., Kim, H.-S., & Min, K. (2007). Quasi-three dimensional dynamic model of a proton exchange membrane fuel cell for system and controls development. *Journal of Power Sources, 163*(2), 814-829.

Nandi, R., & Sengupta, S. (1998). Microbial production of hydrogen: an overview. *Critical reviews in microbiology, 24*(1), 61-84.

Nath, K., & Das, D. (2004). Improvement of fermentative hydrogen production: various approaches. *Applied microbiology and biotechnology, 65*(5), 520-529.

Nath, K., Muthukumar, M., Kumar, A., & Das, D. (2008). Kinetics of two-stage fermentation process for the production of hydrogen. *International Journal of Hydrogen Energy, 33*(4), 1195-1203.

Noike, T., Ko, I., Yokoyama, S., Kohno, Y., & Li, Y. (2005). Continuous hydrogen production from organic waste. *Water Science and Technology, 52*(1-2), 145-151.

Noren, D., & Hoffman, M. (2005). Clarifying the Butler–Volmer equation and related approximations for calculating activation losses in solid oxide fuel cell models. *Journal of Power Sources, 152*, 175-181.

O'Dwyer, A. (2009). *Handbook of PI and PID controller tuning rules* (Vol. 57): World Scientific.

Oh, Y.-K., Park, M. S., Seol, E.-H., Lee, S.-J., & Park, S. (2003). Isolation of hydrogen-producing bacteria from granular sludge of an upflow anaerobic sludge blanket reactor. *Biotechnology and Bioprocess Engineering, 8*(1), 54-57.

Ozmihci, S., Kargi, F., & Cakir, A. (2011). Thermophilic dark fermentation of acid hydrolyzed waste ground wheat for hydrogen gas production. *International Journal of Hydrogen Energy, 36*(3), 2111-2117.

Picioreanu, C., Katuri, K., Head, I., van Loosdrecht, M. C., & Scott, K. (2008). Mathematical model for microbial fuel cells with anodic biofilms and anaerobic digestion. *Water Science and Technology, 57*(7), 965-971.

Picioreanu, C., van Loosdrecht, M. C., Curtis, T. P., & Scott, K. (2010). Model based evaluation of the effect of pH and electrode geometry on microbial fuel cell performance. *Bioelectrochemistry, 78*(1), 8-24.

Pinto, R., Srinivasan, B., Escapa, A., & Tartakovsky, B. (2011). Multi-population model of a microbial electrolysis cell. *Environmental science & technology, 45*(11), 5039-5046.

Pinto, R., Srinivasan, B., Manuel, M.-F., & Tartakovsky, B. (2010). A two-population bio-electrochemical model of a microbial fuel cell. *Bioresource technology, 101*(14), 5256-5265.

Pinto, R. P., Srinivasan, B., & Tartakovsky, B. (2011). A unified model for electricity and hydrogen production in microbial electrochemical cells. *IFAC Proceedings Volumes, 44*(1), 5046-5051.

Plambeck, J. (1995). Hydrogen electrodes, oxygen electrodes, and pH. *Published online at (http://www. psigate. ac. uk/newsite/reference/plambeck/chem2/1995, 2104*.

Popat, S. C., Ki, D., Rittmann, B. E., & Torres, C. I. (2012). Importance of OH− transport from cathodes in microbial fuel cells. *ChemSusChem, 5*(6), 1071-1079.

Quarmby, J., & Forster, C. (1995). A comparative study of the structure of thermophilic and mesophilic anaerobic granules. *Enzyme and Microbial Technology, 17*(6), 493-498.

Quéméneur, M., Hamelin, J., Benomar, S., Guidici-Orticoni, M.-T., Latrille, E., Steyer, J.-P., & Trably, E. (2011). Changes in hydrogenase genetic diversity and proteomic patterns in mixed-culture dark fermentation of mono-, di-and tri-saccharides. *International Journal of Hydrogen Energy, 36*(18), 11654-11665.

Rabaey, K., & Verstraete, W. (2005). Microbial fuel cells: novel biotechnology for energy generation. *Trends in biotechnology, 23*(6), 291-298.

Rauch, W., Vanhooren, H., & Vanrolleghem, P. A. (1999). A simplified mixed-culture biofilm model. *Water research, 33*(9), 2148-2162.

Redwood, M. D., Paterson-Beedle, M., & Macaskie, L. E. (2009). Integrating dark and light bio-hydrogen production strategies: towards the hydrogen economy. *Reviews in Environmental Science and Bio/Technology, 8*(2), 149-185.

Rodríguez, J., Kleerebezem, R., Lema, J. M., & van Loosdrecht, M. (2006). Modeling product formation in anaerobic mixed culture fermentations. *Biotechnology and Bioengineering, 93*(3), 592-606.

Rousset, M., & Cournac, L. (2008). *Towards hydrogenase engineering for hydrogen production.* Paper presented at the Bioenergy.

Rozendal, R. A., Hamelers, H. V., Euverink, G. J., Metz, S. J., & Buisman, C. J. (2006). Principle and perspectives of hydrogen production through biocatalyzed electrolysis. *International Journal of Hydrogen Energy, 31*(12), 1632-1640.

Rozendal, R. A., Hamelers, H. V., Rabaey, K., Keller, J., & Buisman, C. J. (2008). Towards practical implementation of bioelectrochemical wastewater treatment. *Trends in biotechnology, 26*(8), 450-459.

Rozendal, R. A., Jeremiasse, A. W., Hamelers, H. V., & Buisman, C. J. (2007). Hydrogen production with a microbial biocathode. *Environmental science & technology, 42*(2), 629-634.

Sagnak, R., Kargi, F., & Kapdan, I. K. (2011). Bio-hydrogen production from acid hydrolyzed waste ground wheat by dark fermentation. *International Journal of Hydrogen Energy, 36*(20), 12803-12809.

Sasikala, K., Ramana, C. V., & Rao, P. R. (1991). Environmental regulation for optimal biomass yield and photoproduction of hydrogen by Rhodobacter sphaeroides OU 001. *International Journal of Hydrogen Energy, 16*(9), 597-601.

Seibert, M., King, P. W., Posewitz, M. C., Melis, A., Ghirardi, M. L., Wall, J., . . . Demain, A. (2008). *Photosynthetic water-splitting for hydrogen production.* Paper presented at the Bioenergy.

Shamsuzzoha, M., & Skogestad, S. (2010). The setpoint overshoot method: A simple and fast closed-loop approach for PID tuning. *Journal of Process Control, 20*(10), 1220-1234.

Shi, X.-Y., & Yu, H.-Q. (2005). Response surface analysis on the effect of cell concentration and light intensity on hydrogen production by Rhodopseudomonas capsulata. *Process Biochemistry, 40*(7), 2475-2481.

Shin, H.-S., Youn, J.-H., & Kim, S.-H. (2004). Hydrogen production from food waste in anaerobic mesophilic and thermophilic acidogenesis. *International Journal of Hydrogen Energy, 29*(13), 1355-1363.

Stal, L. J., & Krumbein, W. E. (1985). Oxygen protection of nitrogenase in the aerobically nitrogen fixing, non-heterocystous cyanobacterium Oscillatoria sp. *Archives of microbiology, 143*(1), 72-76.

Su, H., Cheng, J., Zhou, J., Song, W., & Cen, K. (2009). Combination of dark-and photo-fermentation to enhance hydrogen production and energy conversion efficiency. *International Journal of Hydrogen Energy, 34*(21), 8846-8853.

Taguchi, F., Yamada, K., Hasegawa, K., Taki-Saito, T., & Hara, K. (1996). Continuous hydrogen production by Clostridium sp. strain no. 2 from cellulose hydrolysate in an aqueous two-phase system. *Journal of Fermentation and Bioengineering, 82*(1), 80-83.

Tamagnini, P., Axelsson, R., Lindberg, P., Oxelfelt, F., Wünschiers, R., & Lindblad, P. (2002). Hydrogenases and hydrogen metabolism of cyanobacteria. *Microbiology and Molecular Biology Reviews, 66*(1), 1-20.

Tamburic, B., Zemichael, F. W., Crudge, P., Maitland, G. C., & Hellgardt, K. (2011). Design of a novel flat-plate photobioreactor system for green algal hydrogen production. *International Journal of Hydrogen Energy, 36*(11), 6578-6591.

Tao, Y., Chen, Y., Wu, Y., He, Y., & Zhou, Z. (2007). High hydrogen yield from a two-step process of dark-and photo-fermentation of sucrose. *International Journal of Hydrogen Energy, 32*(2), 200-206.

Ter Heijne, A., Hamelers, H. V., De Wilde, V., Rozendal, R. A., & Buisman, C. J. (2006). A bipolar membrane combined with ferric iron reduction as an efficient cathode system in microbial fuel cells. *Environmental science & technology, 40*(17), 5200-5205.

Thauer, R. K., Jungermann, K., & Decker, K. (1977). Energy conservation in chemotrophic anaerobic bacteria. *Bacteriological reviews, 41*(1), 100.

Thibault, J., Van Breusegem, V., & Chéruy, A. (1990). On-line prediction of fermentation variables using neural networks. *Biotechnology and Bioengineering, 36*(10), 1041-1048.

Torres, C. I., Marcus, A. K., Parameswaran, P., & Rittmann, B. E. (2008). Kinetic experiments for evaluating the Nernst− Monod model for anode-respiring bacteria (ARB) in a biofilm anode. *Environmental science & technology, 42*(17), 6593-6597.

Uyar, B., Eroglu, I., Yücel, M., & Gündüz, U. (2009). Photofermentative hydrogen production from volatile fatty acids present in dark fermentation effluents. *International Journal of Hydrogen Energy, 34*(10), 4517-4523.

Van Ginkel, S. W., Oh, S.-E., & Logan, B. E. (2005). Biohydrogen gas production from food processing and domestic wastewaters. *International Journal of Hydrogen Energy, 30*(15), 1535-1542.

Vignais, P., & Colbeau, A. (2004). Molecular biology of microbial hydrogenases. *Current issues in molecular biology, 6*(2), 159-188.

Vignais, P. M., Billoud, B., & Meyer, J. (2001). Classification and phylogeny of hydrogenases. *FEMS microbiology reviews, 25*(4), 455-501.

Wang, J., & Wan, W. (2008). Comparison of different pretreatment methods for enriching hydrogen-producing bacteria from digested sludge. *International Journal of Hydrogen Energy, 33*(12), 2934-2941.

Woodward, J., Orr, M., Cordray, K., & Greenbaum, E. (2000). Biotechnology: enzymatic production of biohydrogen. *Nature, 405*(6790), 1014-1015.

Wykoff, D. D., Davies, J. P., Melis, A., & Grossman, A. R. (1998). The regulation of photosynthetic electron transport during nutrient deprivation in Chlamydomonas reinhardtii. *Plant physiology, 117*(1), 129-139.

Yahya, A. M., Hussain, M. A., Wahab, A., & Khairi, A. (2015). Modeling, optimization, and control of microbial electrolysis cells in a fed-batch reactor for production of renewable biohydrogen gas. *International Journal of Energy Research, 39*(4), 557-572.

Yang, Y.-P., Wang, F.-C., Chang, H.-P., Ma, Y.-W., & Weng, B.-J. (2007). Low power proton exchange membrane fuel cell system identification and adaptive control. *Journal of Power Sources, 164*(2), 761-771.

Yokoi, H., Maki, R., Hirose, J., & Hayashi, S. (2002). Microbial production of hydrogen from starch-manufacturing wastes. *biomass and bioenergy, 22*(5), 389-395.

Zhang, H., Bruns, M. A., & Logan, B. E. (2006). Biological hydrogen production by Clostridium acetobutylicum in an unsaturated flow reactor. *Water research, 40*(4), 728-734.

Zhang, Y., Merrill, M. D., & Logan, B. E. (2010). The use and optimization of stainless steel mesh cathodes in microbial electrolysis cells. *International Journal of Hydrogen Energy, 35*(21), 12020-12028.

Zong, W., Yu, R., Zhang, P., Fan, M., & Zhou, Z. (2009). Efficient hydrogen gas production from cassava and food waste by a two-step process of dark fermentation and photo-fermentation. *biomass and bioenergy, 33*(10), 1458-1463.

LIST OF PUBLICATIONS AND PAPERS PRESENTED

A. Publication (Academic Journal)

1. **Azwar**, Mohd Azlan Hussain and Ahmad Khairi Abdul Wahab. Modeling, optimization, and control of microbial electrolysis cells in a fed-batch reactor for production of renewable biohydrogen gas. International Journal of Energy Research (**wileyonlinelibrary.com**).Volume 39, Issue 4, pages 557-572, 25 March 2015 **(ISI-CitedPublication).**

2. **Azwar**, M.A.Hussain, A.K. Abdul Wahab and M.F. Zanil. A Comparative study between Neural Networks (NN)-based and Adaptive-PlD Controllers for the Optimal Bio-Hydrogen Gas Production in Microbial Electrolysis Cell Reactor. Computer Aided Chemical Engineering. **Elsevier,** Volume 37, pages 1529-1534. (**ISI-Cited Publication**)

3. **Azwar**, Mohd Azlan Hussain and Ahmad Khairi Abdul Wahab. Development of Biohydrogen Production by Photobiological, Fermentation and Electrochemical Processes: a Review. Renewable & Sustainable Energy Reviews, **Elsevier**, Volume 31, pages 158-173. 2014 **(ISI-Cited Publication)**.

4. **Azwar**, Mohd Azlan Hussain and Ahmad Khairi Abdul Wahab. The Effect of Internal Parameters on Biohydrogen Production in Batch Microbial Electrolysis Cell Reactor. ICREGA'14- Renewable Energy: Generation and Applications, Edited by Mohammad O. Hamdan, Chapter 2, pages 11-22, ISSN 2352- 2534, **Springer** Cham Heidelberg New York Dordrecht London. 2014**(SCOPUS-Cited Publication)**.

5. **Azwar**, Ahmad Khairi Abdul-Wahab, Mohamed Azlan Hussain. 2013. Optimal Production of Biohydrogen Gas via Microbial Electrolysis, Cells (MEC) in a ControlledBatch Reactor System, Chemical Engineering Transactions, Vol. 32, ISBN 978-88-95608-23-5, ISSN: 1974-9791 **(SCOPUS-Cited Publication).**

6. **Azwar**, Mohd Azlan Hussain and Ahmad Khairi Abdul Wahab. Design of Neural Network Model-Based Controller in a Fed-Batch Microbial Electrolysis Cell Reactor for Bio-Hydrogen Gas Production. In prepration to be submitted to "International Journal of Hydrogen Energy".**Elsevier (ISI-Cited Publication)**.

B. Paper Presented

1. **Azwar**, M.A.Hussain, A.K. Abdul Wahab and M.F. Zanil, Comparison of PID and Neural Network Model-based Controller inaFed-batchMicrobial Electrolysis Cell Reactor for Optimal Bio-hydrogenGas Production, Proceeding of Chemeca 20l4,Perth.Western Australia **(SCOPUS- Cited Publication)**

2. **Azwar**, Mohd Azlan Hussain and Ahmad Khairi Abdul Wahab, Modeling and Simulation of Biohydrogen Production via Microbial Electrolysis Cells (MECS) in Batch Reactor, The Proceedings of The 6th International Conference on Process System Engineering,ID-178, 25-27 June 2013, PWTC, Kuala Lumpur. **(SCOPUS-Cited Publication)**

3. **Azwar**, A.K. Abdul Wahab and M.A. Hussain. Tuning Rules of a PID Controller for Optimal Production of Biohydrogen Gas in Fed-Batch Microbial Electrolysis Cells Reactor. National Colloquium on Process Control, Oct 1st, 2013 (NCPC'2013), USM Penang. **(Non-SCOPUS Cited Publication)**

4. **Azwar,** Ahmad Khairi Abdul Wahab, Mohd. AzlanHussain, Mathematical modelling of microbial electrolysis cells (MEC) in batch reactor for biohydrogen production: Preliminary study, Book of Abstracts, the 4th AUN/SEED- Net Regional Conference on Chemical Engineering, Paper id: MOD2 l, 9- 1 0 Feb 2012, Malaysia **(SCOPUS-Cited Publication)**

5. **Azwar,** M. A. Hussain, and A. K. Abdul Wahab,2011, Study on the hydrogen gas production process from wastewater via the electrochemical method in a batch reactor: A preliminary study, Book of Abstracts, Green Process Engineering (GPE) 20ll, paper id: 179, pg. 222-223,Seri Pasific Hotel, Kuala Lumpur,6-8 Dec 2011.**(SCOPUS-Cited Publication)**